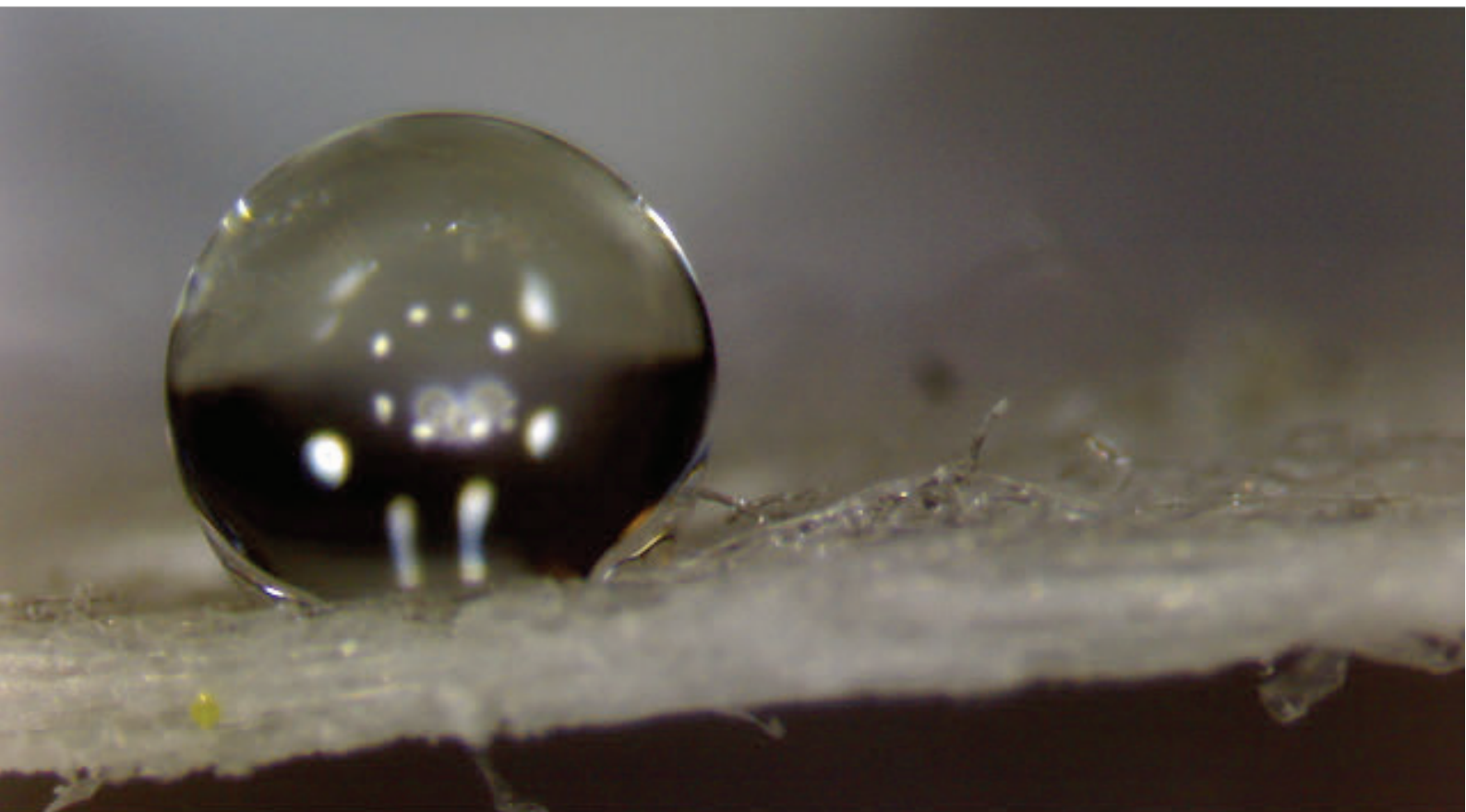


Department of Precision and Microsystems Engineering

Dosing of femto (10^{-15}) liter volumes using hollow atomic force microscope cantilever

Rick Bob Theodorus de Gruiter

Report no : MNE 2015.026
Coach : Dr. M. K. Ghatkesar
Professor : Prof. Dr. U. Staufer
Specialisation : Micro and Nano Engineering
Type of report : Master of Science Thesis
Date : October 15, 2015



This thesis has been performed as a partial fulfillment of the requirements for the degree of Masters of Science in Mechanical Engineering at Delft University of Technology

October 2015

The thesis has been carried out at Delft University of Technology



Title: Dosing of femto (10^{-15}) liter volumes using hollow atomic force microscope cantilever

Author: R. B. T. de Gruiter

Date: October 15, 2015

Student number: 4022041

Institute: Delft University of Technology
Department of Precision and Microsystems Engineering
Research group Micro and Nano Engineering
Mekelweg 2, 2628CD Delft, The Netherlands

Board of examiners: Prof. Dr. U. Staufer
Micro and Nano Engineering, 3mE, TU Delft
Prof. Dr. Ir. J. Lötters
Transducers Science and Technology, EEMCS, U Twente
R. van Oorschot MSc.
MA3 Solutions
Dr. M. K. Ghatkesar
Micro and Nano Engineering, 3mE, TUDelft

An electronic version of this thesis is available at: <http://repository.tudelft.nl>

Contents

| | |
|--|-----------|
| 1. Literature review on small volume fluid dispensing | 9 |
| 1.1. Introduction | 9 |
| 1.2. Usage of hollow cantilever AFM | 12 |
| 1.2.1. Single cell manipulation | 13 |
| 1.2.2. DNA micro array | 13 |
| 1.2.3. Gluing graphene | 14 |
| 1.3. Different dosage techniques | 14 |
| 1.3.1. Predefined volume | 14 |
| 1.3.2. Flow measurement and controlling valves | 17 |
| 1.3.3. Contact printing | 17 |
| 1.4. Dosing parameters | 17 |
| 1.4.1. Contact time | 18 |
| 1.4.2. Pressure | 19 |
| 1.5. Weighing using hollow cantilever AFM | 20 |
| 1.6. Conclusion | 21 |
| 1.7. Goal of the thesis | 21 |
| 1.8. Organization of the thesis | 22 |
| 2. Receding contact angle set-up | 23 |
| 2.1. Introduction | 23 |
| 2.1.1. Theory | 24 |
| 2.1.2. Volume calculation | 24 |
| 2.2. Methods and materials | 26 |
| 2.2.1. Experimental setup | 26 |
| 2.2.2. Substrate preparation | 28 |
| 2.2.3. Software | 29 |
| 2.2.4. Measurements | 30 |
| 2.3. Results and discussion | 31 |
| 2.4. Conclusion | 33 |
| 3. Humidity control for femto liter droplets | 34 |
| 3.1. Introduction | 34 |
| 3.1.1. Theory | 34 |
| 3.1.2. Visualization of liquid bridge | 37 |
| 3.2. Methods and materials | 37 |
| 3.2.1. Stiffness calculation | 37 |
| 3.3. Results and discussion | 39 |
| 3.3.1. AFM measurements | 39 |
| 3.4. Conclusion | 39 |
| 4. Microfluidic interface for hollow cantilever AFM | 41 |
| 4.1. Introduction | 41 |

| | | |
|--------------------|---|-----------|
| 4.2. | Methods and materials | 41 |
| 4.2.1. | Design and considerations | 41 |
| 4.2.2. | Gluing | 42 |
| 4.3. | Results and discussion | 44 |
| 4.4. | Conclusion | 45 |
| 5. | Dosing by varying contact time | 46 |
| 5.1. | Introduction | 46 |
| 5.2. | Methods and materials | 46 |
| 5.3. | Measurements and result | 48 |
| 5.3.1. | Mass weighing based on eigenfrequency shift | 48 |
| 5.3.2. | Force distance curve analysis | 49 |
| 5.3.3. | Dispensing diethyl carbonate | 49 |
| 5.3.4. | Dispensing of water | 52 |
| 5.3.5. | Dependency on previous approaches | 53 |
| 5.3.6. | Step size variation | 53 |
| 5.3.7. | Contact time variation | 55 |
| 5.4. | Discussion | 56 |
| 5.4.1. | Volume calculation | 56 |
| 5.4.2. | Force distance curves | 57 |
| 5.4.3. | Clogging | 58 |
| 5.4.4. | Weighing | 58 |
| 5.4.5. | Light interference | 58 |
| 5.4.6. | Liquid properties | 58 |
| 5.5. | Conclusion | 59 |
| 6. | Dosing by varying applied pressure | 60 |
| 6.1. | Introduction | 60 |
| 6.1.1. | Theory | 60 |
| 6.2. | Methods and materials | 61 |
| 6.2.1. | Liquids | 61 |
| 6.2.2. | Substrate | 61 |
| 6.2.3. | Calculation | 61 |
| 6.2.4. | Pressure control | 61 |
| 6.3. | Results | 62 |
| 6.3.1. | Dispensing with negative pressure | 62 |
| 6.3.2. | Startup behavior | 62 |
| 6.3.3. | Dispensing functionalized surface | 63 |
| 6.4. | Discussion | 63 |
| 6.5. | Conclusion | 65 |
| 7. | Conclusion | 66 |
| Appendix A. | System description | 69 |
| A.0.1. | General description of the AFM system | 69 |
| A.0.2. | Pressure control | 69 |
| A.0.3. | Humidity control | 69 |
| A.0.4. | Operation | 70 |
| A.0.5. | Specifications | 73 |
| Appendix B. | Software steps | 74 |

| | |
|--|------------|
| Appendix C. Visualization of capillary condensation | 77 |
| C.1. Methods and materials | 77 |
| C.2. Discussion | 77 |
| Appendix D. Gluing steps | 80 |
| Appendix E. Cantilever details | 83 |
| Appendix F. Volume data | 84 |
| Appendix G. Force distance curves | 87 |
| Appendix H. Contact angle | 90 |
| Appendix I. Matlab code force distance curves | 94 |
| I.1. Read data from CSV | 94 |
| I.2. Force distance curves | 95 |
| I.3. Save breakup height | 99 |
| I.4. Breakup height with dispensing | 100 |
| I.5. Calculate volume | 101 |
| Appendix J. Stiffness | 104 |
| J.1. Frequency sweep | 106 |
| J.2. Frequency shift | 107 |
| Appendix K. Relative humidity | 109 |

Preface

Micro- and Nano Engineering is a quickly evolving field with lots of challenges and interesting subjects, and fluid handling at the small scale is one of them. When working at a smaller scale, different forces become dominant over the forces that normally influence the process at a large scale. For example: when pouring water out of a glass this is a gravity dominated process, but when the glass becomes small enough the water will adhere to the side and will not leave the glass, as is the case in a capillary where water even moves against gravity. This indicates that in small scale fluid handling surface forces are dominant over the gravitational forces.

This thesis describes the investigation on the parameters influencing the dispensing of droplets in the femto-liter range on a surface. First a literature study is conducted, where it is investigated what studies already have been performed and what parameters influence droplet volumes. Also several applications are explained, indicating the importance of fluid handling at the small scale. For the experiments an atomic force microscope is used which is adapted for fluid dispensing. As part of this thesis an experiment is performed to investigate the influence of the environment on the behavior of the system. For this experiment a semi-open climate chamber is created around the tip and the substrate. Furthermore several experiments are conducted to investigate the relation between the different parameters and their influence on the droplet size. Additionally it is studied how these parameters can be changed to dispense a desired droplet volume.

This thesis is written in order to obtain the Masters degree in Mechanical Engineering at Delft University of Technology. The research is performed in the Micro and Nano engineering group at the department of Precision and Microsystems engineering.

It is assumed the reader has some interest in dispensing small droplets and micro engineering. Some previous technical knowledge is useful but most of the principles are explained briefly for easy understanding. This thesis helps to understand how different sizes of droplets can be dispensed using a fluidic AFM system. Furthermore it provides the reader with knowledge of surface forces and fluid interaction with surfaces.

Acknowledgments

The thesis is carried out within the department of Precision and Microsystems engineering in the group Micro and Nano engineering, a well motivated group of highly skilled and enthusiastic people. Where I had the privilege to collaborate with, I had the opportunity to work on a high end system which is able to dispense liquid droplets in the femto liter range. During this project I was given the freedom to try different kinds of experiments and experience several aspects of research. As a result I have learned a lot, not only educational but also on the personal field.

This thesis could not be carried out without the help of many people, therefore, in the first place, I would like to express my gratitude to my graduation committee: Prof Dr. Urs Stauer the chair of the committee, Prof. Dr. Ir. Joost Lötters from the Universtiy of Twente and Bronkhorst BV, Ralph van Oorschot from MA3 solutions and my daily supervisor and coach Dr. Murali Ghatkesar for their assistance and being critical about the work. Especially Murali and Ralph for the fruitful discussions, the patience and teaching me how to operate the system.

Furthermore, I would like to thank the people in the office: Jeroen Buter, Jan-Willem Feitsma, Michiel Dondorp, Tijn van Omme, Adrián Estrada and Jana Ilieva, for the motivation, the coffee and occasionally a good beer. They have provided me with fun and interesting discussions about a lot of different projects and subjects.

Also I would like to thank the rest of the PME staff which I had the pleasure to meet: Gaby Offermans, Corinne duBurck, Marli Guffens, Eveline Matroos, Birgit Rademakers, Marianne Stolker, Jan Neve, Marcel Tichem and Guido Jansen. Especially I would like to show my gratitude to Rob Lutjeboer, Patrick van Holst, Harry Jansen and Hozanna Miro for their help and the support in the cleanroom. Also many thanks to the PhD candidates: Jaap Kokorian, Alkisti Gkouzou, Tjitte Jelte Peters, Yueting Liu, Enrique Trinidad, Kai Wu, Cristina Varone and Eleonor Verlinden for their helpful suggestions for this project and keeping the group meetings light and enjoyable.

Special thanks to my family, my mum and dad for the support and keeping faith in me. My deepest appreciation goes to my lovely girlfriend Anja Fethke who kept me from going crazy and giving me the power to keep on going.

And of course finally, I would like to thank Dr. Murali Ghatkesar for his guidance, patience and motivation during the project. For giving me the opportunity to work and show my results on this interesting field of research. For the long discussions about what experiments could and needed to be done and the long days in the cleanroom to obtain the results. I wish you luck in all your upcoming projects and all the best. It was a great pleasure working with you.

Rick de Gruiter
Delft, The Netherlands
October, 2015

1 — Literature review on small volume fluid dispensing

1.1 Introduction

Nanotechnology is considered to be the next big step in the development of humanity. In 1959 the American physicist Richard Feynman introduced the first concepts of nanotechnology. In his lecture 'There is plenty of room at the bottom' he describes the direct manipulation of individual atoms and the ability to see individual atoms. These technologies are later developed with the scanning tunneling microscope (STM) and the atomic force microscope (AFM). The world has traveled far from what Feynman already observed but there are more opportunities and challenges at small scale. As an example fluid handling is one of many existing challenges at nanoscale.

The handling of fluids is important in a lot of fields, such as in the microbiology, chemistry and food industries. The words, 'dosing' or 'metering' used in this thesis in combination with 'fluid handling' are referred to as delivering a predefined volume of liquid to a specific location. There are different ways to deliver fluids and every order of magnitude a specific technique of dispensing exists (see figure 1.1). For dosing fluids in the range of liters and milliliters usually beaker glasses and syringes are used. At smaller scale the most common tool to dispense or aspirate fluids of accurate amounts is the micro pipette. This device is able to deliver fluids typically in the range of microliters. With a mechanical piston a partial vacuum is created in the tip to aspirate the fluid. The volume is then controlled by adjusting the range the piston can move [1].

At even smaller scale several other techniques are used for the delivery of fluids. For dispensing and aspirating fluids in the range of femtolitres (10^{-15} l) syringe pumps with very accurate stepper motors are used. For fast dispensing in the picoliter (10^{-12} l) and femtoliter (10^{-15} l) range ink-jet techniques are used. [2] Ink-jet technique uses a piezoelectric technique to pressurize the fluid and by controlling the pressure on the liquid printers are able to dose ink. Ink-jet techniques are mainly used to print on paper but can also be used for printing polymers and proteins [3]. A disadvantage of the ink-jet technique is that it is not able to aspirate fluid.

When dispensing in the range of femtoliter (10^{-15} l) upto zeptoliter (10^{-21} l) electrospray techniques are used, in this technique a high potential is applied between the substrate and the glass capillary containing the fluid [4]. Depending on the ratio of the electric field applied and surface tension of the liquid certain volumes can be dispensed. This technique has the same disadvantage as the ink-jet techniques, electrospray is not able to aspirate the liquid.

For controlled dispensing and aspirating of volumes around femtoliters (10^{-15} l) to zeptoliter (10^{-21} l) range, scanning probe microscope (SPM) based techniques can be used. Scanning probes are micro fabricated cantilevers used for measuring roughness of surfaces at high resolution

An example of a SPM is an atomic force microscope (AFM), an AFM is able to visualize surfaces with atomic resolution which is almost 1000x better than an optical microscope. The

concept of AFM was introduced in 1985 by Gerd K. Binnig [5][6]. The working principle can be compared to a vinyl player (see figure 1.2). A sharp needle moving over a surface to scan the topography. The height of the needle of an AFM is in the range of $20\ \mu\text{m}$. This needle is fixed to a cantilever with a length ranging from $100\ \mu\text{m}$ to $500\ \mu\text{m}$. When the needle approaches a substrate the cantilever bends. This bending can be detected using the reflection of a laser on the cantilever. The movement is subsequently detected by a light sensitive detector. The movement is made detectable by geometrical amplification.

AFM is normally used for imaging, this operation is usually described in one of the three modes corresponding to the tip movement [7]; contact mode, non-contact mode or tapping mode. In the first mode (contact mode) the needle is in contact with the substrate and the needle is dragged over the surface. The contours of the substrate correspond directly the deflection of the cantilever. Using the feedback of the detector the deflection of the cantilever is kept constant. A major disadvantage, due to the contact of tip and substrate is that the tip can wear out over time resulting in lower quality images. The second mode, the non-contact mode, the cantilever is driven at its resonance frequency with a low amplitude. When brought close to the substrate by the surface forces the resonance frequency and the amplitude are decreased [7]. The system remains a constant frequency or amplitude by using the feedback signal from the photo detector. A large advantage is that the wear of the tip is almost reduced to zero. A disadvantage is that there is only a small regime where the tip is influenced by the short range van der Waals forces and not abruptly captured by the surface forces [8]. In the last mode, the tapping mode the cantilever is vibrating with a fairly large amplitude close or at its resonance frequency. The tip is slowly brought closer to a substrate and when close to the substrate the amplitude starts to decrease because of the increase in surface forces. The laser oscillates vertically across the detector as a consequence of the vibrating cantilever. The signal is rectified and low passed filtered into a DC-voltage. The magnitude is proportional to the amount of cantilever deflection. The system uses the amplitude and a set point voltage to control the cantilever such that the tip only touches at the lowest point of oscillation. The tapping mode also has less damage of the tip and the substrate compared to contact mode because of the absence of frictional forces [9].

Another major function of the AFM is the measurement of adhesion forces between the tip and sample [10]. This is done by the force-distance curves (see figure 1.3). When the tip is brought close to the surface, at a certain moment when the surface forces are too strong for the cantilever, snap-in occurs. The tip is pressed into the substrate and the cantilever will deflect more. Next the tip is retracted, but the tip stays longer at the surface, because a small liquid bridge is formed between the tip and the sample which needs to break and subsequently snap-out is observed.

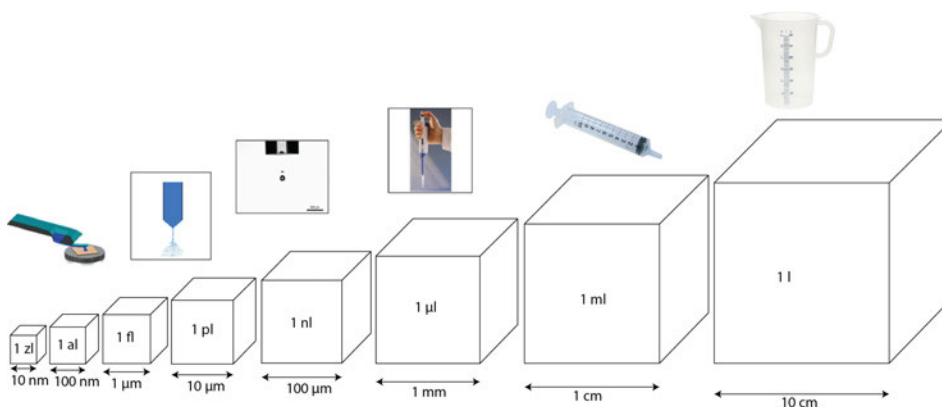


Figure 1.1.: Range of dosing and tools typically used for dispensing

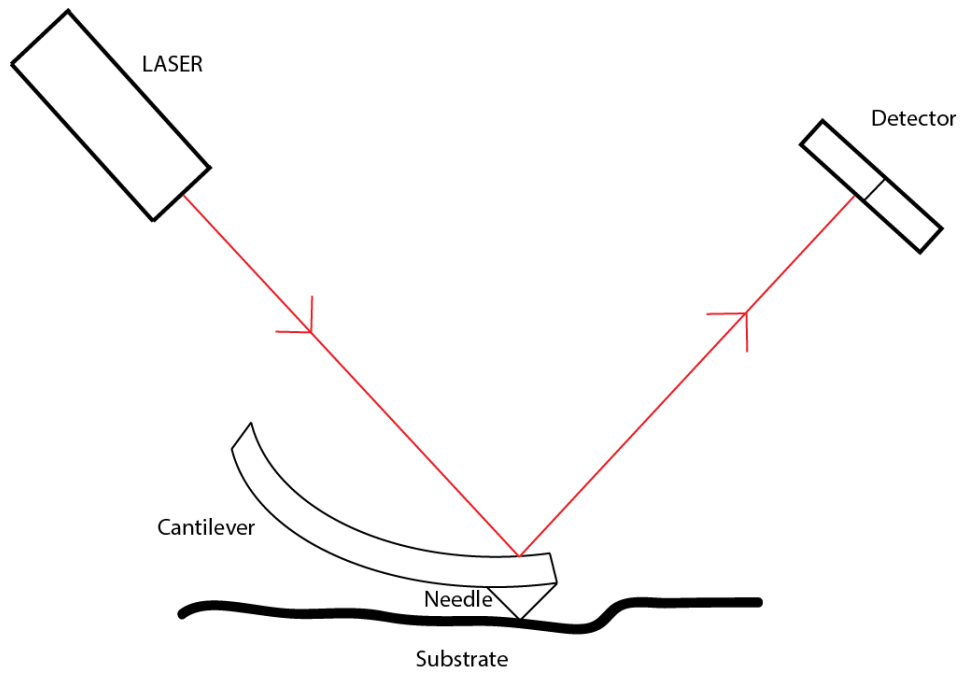


Figure 1.2.: Working principle of atomic force microscope (AFM) in contact mode

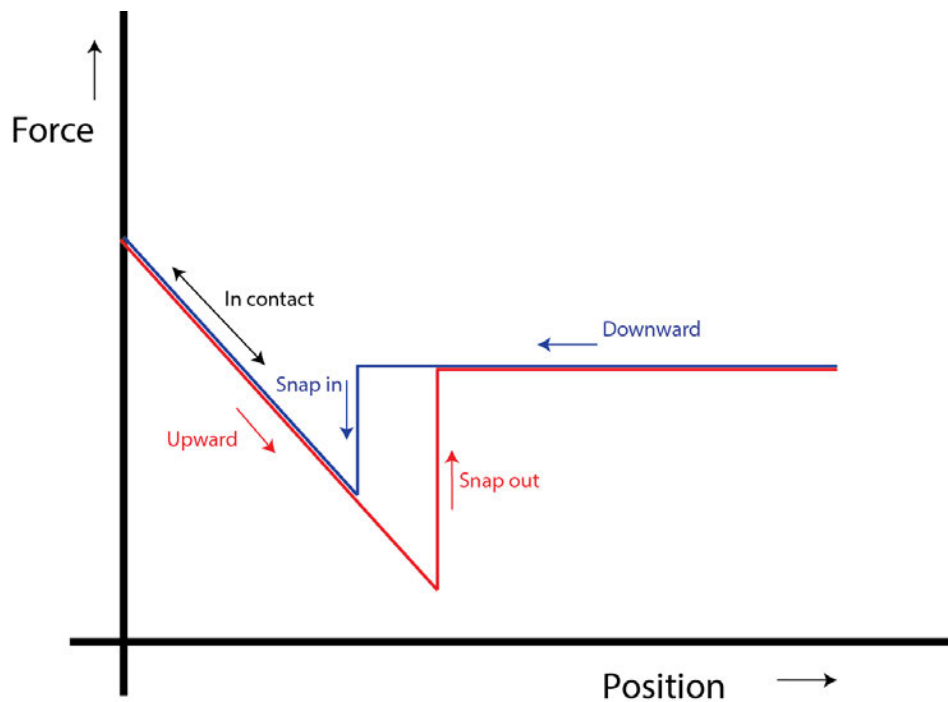


Figure 1.3.: Typical force distance curves obtained from an atomic force microscope (AFM)

Another ability of some AFM equipment is the dispensing of fluids. There are different probes used for dispensing using AFM techniques [11]. In general three categories can be distinguished, a chip with a reservoir which can store liquid and the liquid is transported via the cantilever to the tip (hollow cantilever AFM), cantilevers with a reservoir where liquid is loaded on the cantilever (hollow tip) [12], and chips without reservoir (dip pen)(see figure 1.4)[13]. The cantilevers without storage have the working principle of an ancient quill. First the tip of the cantilever is dipped into a relative large puddle of liquid. The tip is then coated with a thick layer of fluid. The cantilever is moved to the desired location where then the liquid is transferred from the tip to the sample.

Fluidic AFM chips with the ability to store have a hollow cantilever connecting the tip to a reservoir (see figure 1.5). The AFM systems using hollow cantilevers can be again subdivided into two categories, first where only surface forces are used for dispensing and second those which uses an external source to dispense the liquid. In this thesis only pressure is discussed as external source however other sources such as electric field can be used [14]. Dispensing with only surface forces require contact of tip and sample. Pressurizing the liquid enables the dispensing of liquids beyond the surface forces. A comparison of different dispensing techniques using AFM is made by M. K. Ghatkesar et al. [11].

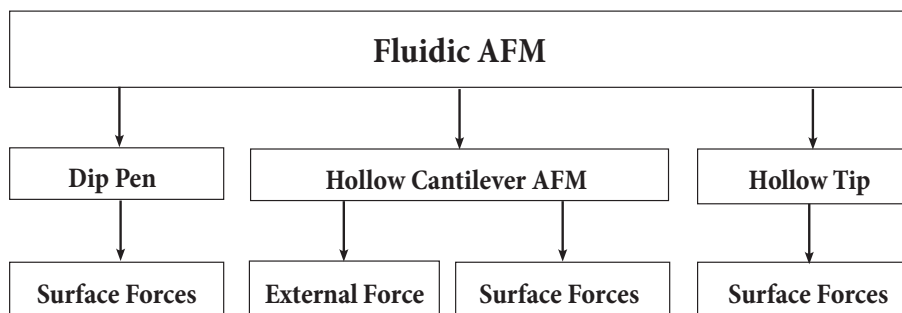


Figure 1.4.: Categorizing different fluidic AFM's

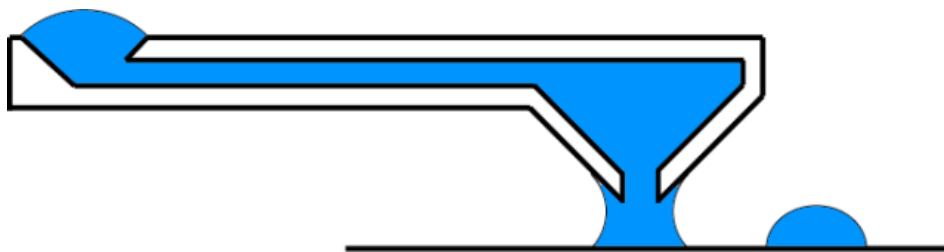


Figure 1.5.: Schematic design of a hollow cantilever AFM

The hereafter following sub chapters will provide a more detailed insight of the different applications of the hollow cantilever AFM, various dosing techniques that are already applied, the parameters that play an important role in the dosing and other applications where the hollow cantilever can be used. The goal of this chapter is to provide sufficient background for the experiments conducted in the later chapters and to help the theoretical understanding of the subjects investigated.

Most importantly, the discussion of the subjects in this chapter should lead to the formulation of a goal that will be answered in this thesis. Additionally the strategy to achieve this goal will be defined.

1.2 Usage of hollow cantilever AFM

There are different reasons as to why dispensing or aspirating with a hollow cantilever AFM is useful. There are several possible applications [15][16] to think of but in this chapter three examples of applications are explained. These examples also demonstrate the importance of this research about dosing and why the hollow cantilever AFM is useful. The three applications which are discussed are single cell manipulation, a micro array and the fixation of graphene to a MEMS tensile device.

1.2.1. Single cell manipulation

Single cell manipulation here defined as performing surgical actions on one cell. There is a great demand for single cell manipulation because it becomes more and more important to investigate how molecules control the functions of a cell. Single cell injection with proteins, peptides or genetic material is widely practiced using microcapillaries [17] [18]. This is used to transplant nuclei or to track the protein expression. Difficulties are found because small cells can be fatally damaged by the inaccuracy in the displacement or by the shape of the microcapillary [19]. A hollow cantilever AFM can help to overcome these difficulties because the sharp tip is less invasive and the controllability of dispensing is better (see figure 1.6). Using the force feedback the situation of the cantilever is known whether the cantilever is touching the cell, indenting or penetrating. This makes the AFM a superior tool for single cell manipulation over the conventional techniques. It should be noted that the length of the tip of an AFM cantilever must be higher than the height of a living cell which is around $3\ \mu\text{m}$. Otherwise the base of the tip comes in contact with the cell wall and disturbs the force measurement. Hollow AFM techniques have been already successfully used to inject a cell with a coloring dye. The cell survived and the neighboring cells were not affected by the dye [20][21][22].

When an under pressure is applied to the hollow cantilever AFM some components of a living cell can be aspirated. These components can later be imaged to gain more knowledge about cells and how a previously injected molecule interacts with a cell. Extraction of mRNA has been previously reported by Uehara et al. [23] which shows the importance to be able to extract features of a cell.

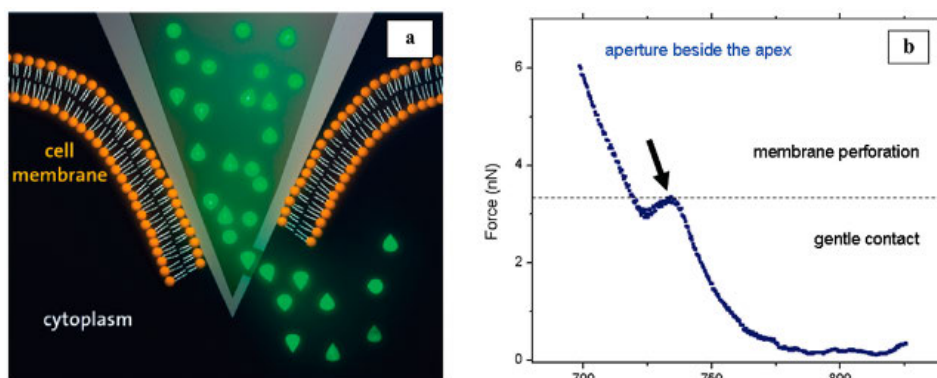


Figure 1.6.: Schematic representation of injecting a cell with molecules [20]

1.2.2. DNA micro array

For patterning biological molecules on a surface, direct writing technique is very useful. Patterning is used in detection of small proteins. The DNA micro array is a micro fluidic chip with spots on it. Each spot contains a known specific DNA sequence. These spots are normally placed by ink-jet techniques [24]. With conventional robotic techniques several thousand known sequences can be spotted on to an array of only a few square centimeters [25]. When using AFM techniques, the spots could be made even smaller it has already been shown that reproducible spots of 10 nm are possible. Because an array exists of thousands of spots the experiment can be executed in parallel reducing the processing time.

An experiment to measure for example gene expression associated with inflammation can be carried out using a micro array (see figure 1.7). The experiment can be executed as follows. mRNA is extracted from normal and inflamed tissue. The normal mRNA acts as control and is labeled green and the inflamed as test which is labeled red. Both samples are mixed together

and applied on the micro array. Under controlled conditions the DNA will hybridize with the corresponding arrayed DNAs. The arrayed spots will become fluorescent. The color of the spot will be red or green depending on which DNA is more strongly represented. When equally represented the spot is orange (green/red). Automated laser and imaging procedures are used to record the fluorescence signal and to identify the differently expressed genes.

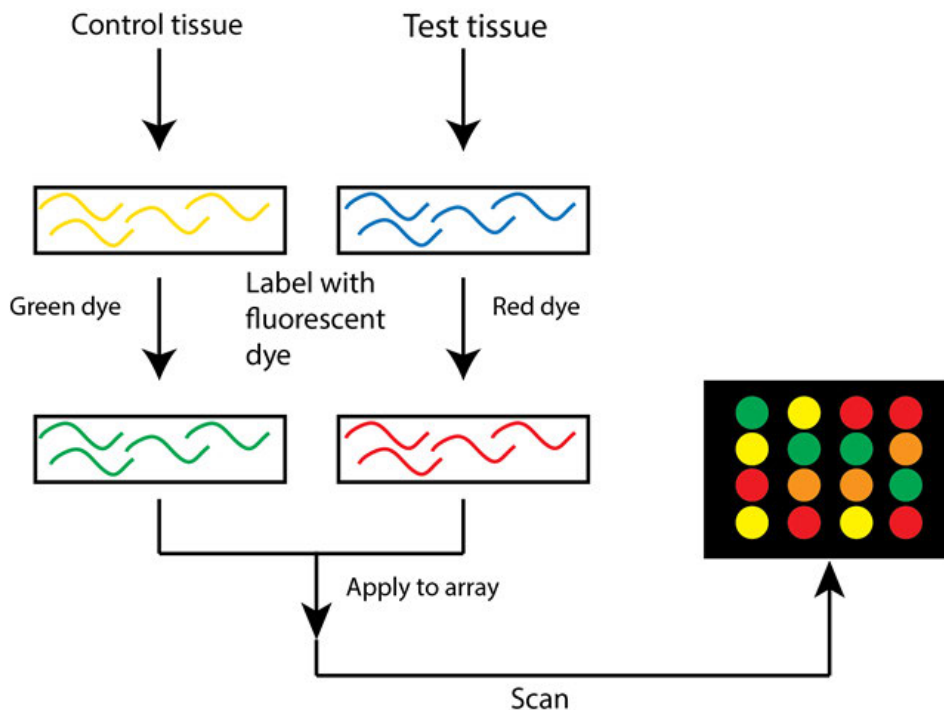


Figure 1.7.: Schematic representation of a gene expression experiment using a micro array

1.2.3. Gluing graphene

Stretching graphene is a challenging topic nowadays, because it is predicted that stretched graphene can safely store hydrogen which can be used as alternative fuel for in example, cars. Most studies performed are mathematical models predicting the percentage strain. The strain is a measure for the amount of hydrogen which can be stored. Using fluidic AFM technology graphene is glued to a MEMS tensile device (see figure 1.8). Stretches of more than 10% are reported [26]. As graphene flakes are too small for ordinary gluing AFM techniques are necessary to be able to clamp the graphene to the tensile device.

1.3 Different dosage techniques

There are various techniques which give a possibility to deliver precise amounts of liquid. The basic techniques can be separated in three fields (see figure 1.9). One way to dose is have a predefined volume which is filled and dispensed on a desired location, another way is to measure a flow and control timing of the valves to deliver a certain amount of fluid. The last method is a contact method where a pin is dipped into the liquid and with surface energies the liquid can be transferred to a substrate.

1.3.1. Predefined volume

A pipette uses a variable predefined volume to measure a certain volume. The liquid can then be transferred to the location. The same technique is used in a syringe. On the smaller scale

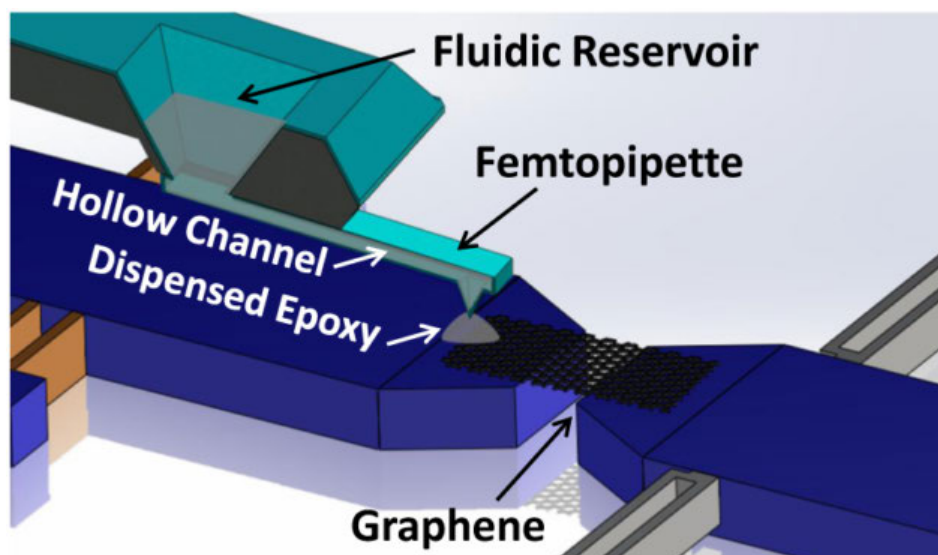


Figure 1.8.: Schematic method of gluing graphene using a hollow cantilever AFM [27]

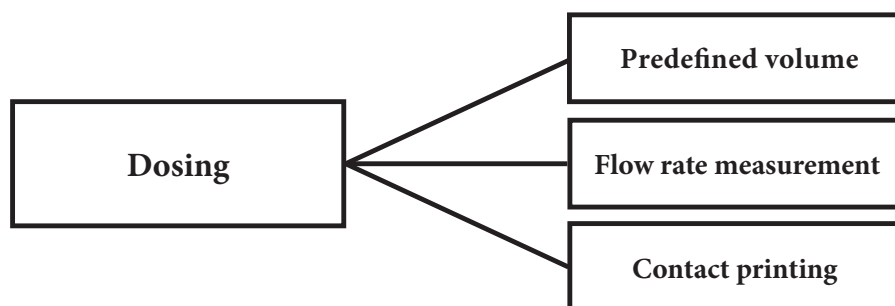


Figure 1.9.: Schematic representation of different dosing methods

these techniques are not often used but the idea of having a defined volume can be used. Using a cartridge system with several rooms with known volumes, predefined volumes can be delivered. This idea is used in [28] where based on the length of the microfluidic channel the amount of drug is determined.

For aliquoting, a large sample needs to be divided in several equal smaller amounts. On a disc a PDMS structure [29] is created (see figure 1.10) with one main channel and several side channels. When the disc is spun around by the centrifugal forces the rectangular chambers are filled. By controlling the turning speed the filling of the chambers is determined. The filling is checked using a stroboscopic images and the volume is calculated afterwards. These defined volumes can be later used for experiments.

Another option used for metering flow is a positive displacement pump [30]. A microfluidic system is created in an elastomer. By controlling valves in a certain sequence a known amount of fluid is pushed into a chamber each time (see figure 1.11). The valves are made out of elastomer and controlled by applying pressure on it. The volumes which are delivered are in the nanoliter range.

The system described in [31] uses pipette tips with a small pocket inside to deliver nanoliter volumes. The pipette tip with pocket are referred to as pockettips. A pockettip has the same dimensions as a normal pipette tip, but it contains a small pocket with known dimensions able to release nanoliter volumes. Operating is in the same way as normal pipette operating. Filling the pocket by aspirating from a source and dispensing the remaining fluid back into the source. A small amount of fluid will remain in the pocket. Finally aspirate a target fluid well above

the pocket so that the liquids can mix. Added volumes of 50 nl are reported.

The disadvantages of dosing using predefined volumes is that it is not possible to dispense less than the chamber size and small chambers can be tricky to fabricate. Also it is hard to be sure chambers are completely emptied or fluids are fully mixed.

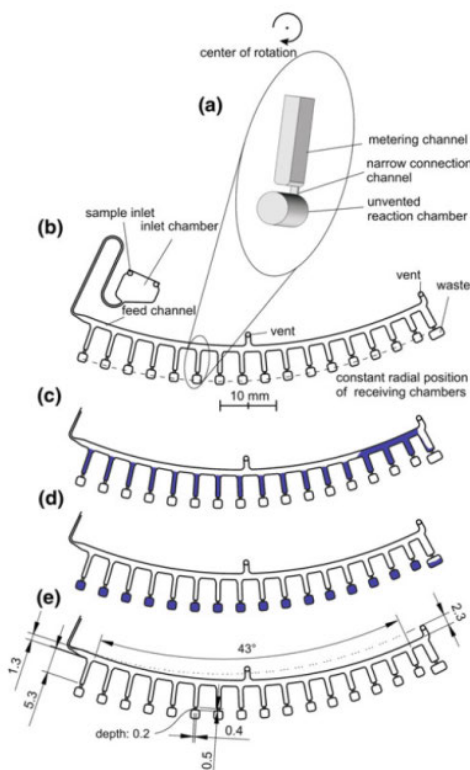


Figure 1.10.: Schematic representation of aliquoting on a microfluidic disc [29]

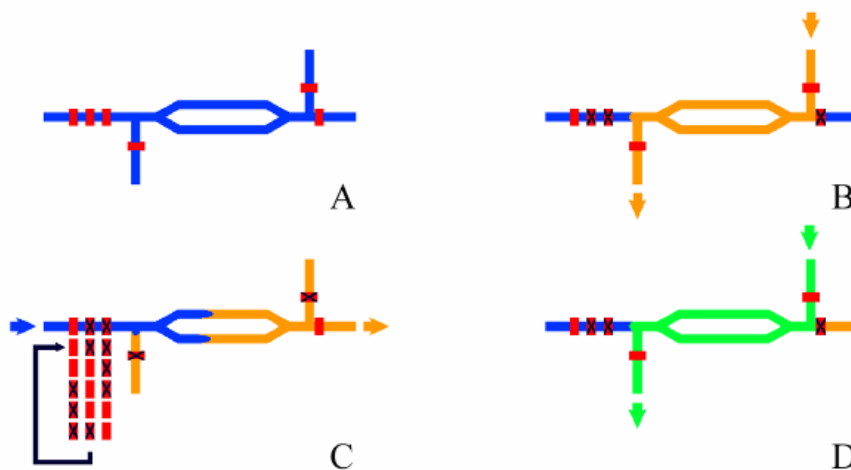


Figure 1.11.: Schematic representation of the working principle of a micro fluidic positive displacement pump (red squares are valves). A. the original state of the chamber. B. The chamber is flushed with orange liquid. C. The sequence of valve switching is shown and blue liquid is pushed into the chamber. D. The chamber is finally flushed with green liquid. [30]

1.3.2. Flow measurement and controlling valves

A possibility to dose a liquid is measuring the flow rate and controlling valves. With timing of valves volumes of nanoliters can be achieved. A system using this principle is described in [32]. The liquid is pushed out by a pressurized reservoir and subsequently the flow is measured using a micro flow sensor (see figure 1.12). The flow sensor is a piezo-resistive low pressure sensor. The pressure at low Reynolds number is directly proportional to the flow. A solenoid valve is utilized to control the droplet sizes, the achieved minimum droplet sizes are 5 nl. Advantage is that it is able to dispense in non contact mode but an extra part is needed.

The resistance of a small hole or an hydrophobic channel can act as a kind of valve and by controlling the pressure also the volume can be precisely controlled. A pdms channel is created [33] and the liquid is pressurized by an compressed air system.

Other ways of dispensing are also reported for example using electrical fields to pull the droplet from a reservoir [34]. The flow rate can be controlled by the strength of the electric field and the size by the duration of the pulse. Droplet sizes of 12 μ l are reported with this technique.

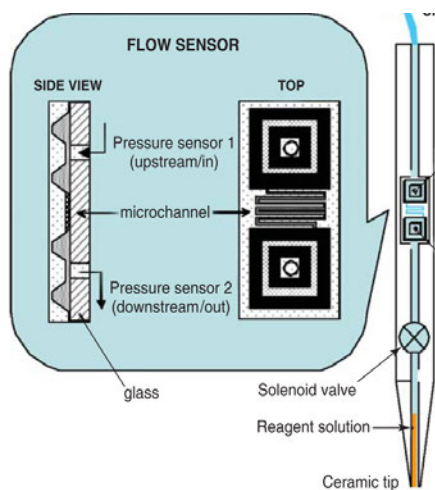


Figure 1.12.: Working principle of dosing using flow measurement [32]

1.3.3. Contact printing

Dosing in contact printing is based on contact time and on the surface energies. A needle is dipped into a source liquid, the liquid will adhere to the needle by surface energy. The needle is transferred to a location and makes contact with the substrate. The surface energy of a substrate pulls the liquid on the sample. It takes time for the droplet to spread on the surface so by controlling the contact time, the amount of liquid can be controlled. This principle is also used to transfer droplets using AFM [13]. At a certain moment the surface forces reach an equilibrium. Using this equilibrium constant amount of liquid can be dispensed.

1.4 Dosing parameters

For dosing it is necessary to know the exact behavior of a droplet on the tip. A lot of parameters play a role in the size of the droplet. In this chapter the dominant parameters of the droplet size are explained. With knowledge and the ability to control these parameters the droplet sizes can be controlled. Dispensing can be executed in several ways first the parameters

for contact printing are explained later the parameters for dispensing with an external pressure source are explained.

1.4.1. Contact time

Spreading of a sessile droplet is depending on several parameters. The force balance is pictured in figure 1.13. If the droplet is smaller than the capillary length (see equation 1.1) the volume can be described by spherical cap equation (see equation 1.2) [35]. The capillary length is given by equation 1.1 where γ is the surface energy ρ the density and g the gravitational constant. The volume of a spherical cap is given by equation 1.2 where r is the radius and h the height of the droplet. For water the capillary length is around 2.7 mm which is much larger than the radius of the droplets produced with AFM, these are around 1 μm .

$$l_c = \sqrt{\gamma/\rho g} \quad (1.1)$$

$$V = \frac{\pi}{6}(3r^2 + h^3) \quad (1.2)$$

Depending on the wetting state a droplet has a certain behavior when it comes into contact with a surface [36]. The wetting state is dependent on the surface tension of the liquid with the substrate γ_{ls} , the surface tension of the liquid γ_l and of the surface tension of the solid γ_s . The so called wetting parameter S describes the wetting properties of a liquid and a solid (see equation 1.3). A positive S indicates complete wetting scenario and a negative S indicates a scenario where the droplet stays together.

$$S = \gamma_s - \gamma_l - \gamma_{ls} \quad (1.3)$$

There are different regimes in droplet spreading depending on the droplet size. Droplets in the order of a volume of 10^{-7}cm^3 follow Tanner's law [27]. This is a power law relating the contact angle to time $\Theta \sim t^{-3}$. When considering smaller droplets in the order of 10^{-8}cm^3 and smaller, long range van der Waals forces start to play a role. The spreading is no longer described by a power law but with linear relation $R(t) = R_0 + v_t t$.

Spreading of a droplet is basically a force balance of three forces, gravitational trying to spread the droplet, capillary forces trying to pull the droplet on the substrate (F_{surface}) and viscous forces (F_{vis}) trying to keep the droplet together. The gravitational force is described by 1.4 but it is neglected as it is an order of magnitude smaller than the viscous forces and the droplets are much smaller than the capillary length. The capillary force is described by 1.5 and finally the viscous friction is described by 1.6 [35]. Where: ρ is the density, g the gravitational constant, V the volume, r the radius of the droplet, γ the surface tension, σ the contact angle and η the viscosity.

$$F_g = \frac{4\rho g V^2}{3\pi r^3} \quad (1.4)$$

$$F_{\text{surface}} = 2\pi r \gamma_l \cos(\theta) - 2\pi r (\gamma_{sl} - \gamma_s) \quad (1.5)$$

$$F_{\text{vis}} \sim \frac{\eta \dot{r} r^6}{V^2} \quad (1.6)$$

When the liquid has large affinity with the surface the liquid is pulled on to the surface. With the surface force the liquid spreads and wets the surface. The viscous force is keeping the droplet together and with this force more water is pulled from the cantilever. With time the droplet increases until a equilibrium is formed between the viscous friction, the spreading force and the surface force. The process of spreading can be interrupted and the volume of the droplet can be controlled.

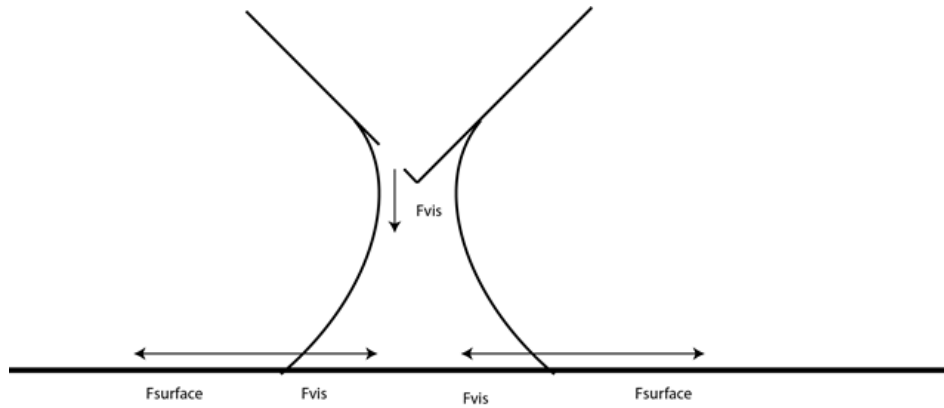


Figure 1.13.: Force balance of spreading a droplet

1.4.2. Pressure

When dispensing beyond the capillary forces pressure is needed. Droplets can be made larger and dispensing inside liquid is possible. With controlling the pressure and the amount of time pressure is applied the droplet size can be controlled. Pressure can be applied using a syringe pump or using a pressure source such as compressed air.

A syringe pump uses a syringe and a linear controlled motion to control the volume. Volumes are relatively easy to control by knowing the syringe diameter. Also the working range can easily be changed by changing the syringe. A syringe pump has several disadvantages. As a constant volume is pressed out, the liquid pressurizes the tubing and at the moment liquid comes out it will keep on coming out. This is dependent on the compliance of the fluidic system [37]. Also due stepwise behavior of the electrical motor it is possible that pulses are created in the flow. These disadvantages make a syringe pump hard to control for dispensing with the AFM. A pressure source with controllable valves can also pressurize the liquid. Pressure pumps create a pulseless flow and have faster response times [38]. Also the less influence of the compliance of the tubes makes a pressure based system a better option to control the dispensing.

Both systems can have the ability to aspirate liquid. The pressure pump can use the Venturi effect to create a partial vacuum, which can be used to aspirate liquid. A syringe pump can aspirate liquid by reversing the motion of the motor so that the syringe is pulled and a vacuum is created.

The behavior of the fluidic system can be described by the electrical analogy. The resistance in the system is comparable with the electrical resistance. The compliance of the tubes is comparable with the electrical capacitance and the pressure source with a voltage source. The schematic of the fluidic system is given in figure 1.14. To calculate the flow rate Q the applied pressure ΔP is divided by the hydrodynamic resistance R_{hyd} (see equation 1.7) [39]. The hydrodynamic resistance for a square channel is given by equation 1.8 where L is the length of the channel, η the dynamic viscosity of the liquid, h the height of the channel and w the width of the channel. Incorporating the compliance of the tubes in the flowrate, the compliance is multiplied by the difference in the applied pressure (see equation 1.9). The compliance of the tubing and the syringe can be calculated by equation 1.10. Where E the Young's modulus and V the volume of the tube [40][41].

$$Q_R = \frac{\Delta P}{R_{\text{hyd}}} \quad (1.7)$$

$$\text{Where: } R_{\text{hyd}} = \frac{12\eta L}{h^3(w - 0.63h)} \quad (1.8)$$

$$Q_C = C_h \frac{d\Delta P}{dt} \quad (1.9)$$

$$\text{Where: } C_h = \frac{V}{E} \quad (1.10)$$

$$Q_T = Q_R + Q_C = \frac{1}{R_{\text{hyd}}} \Delta P + C_h \frac{d\Delta P}{dt} \quad (1.11)$$

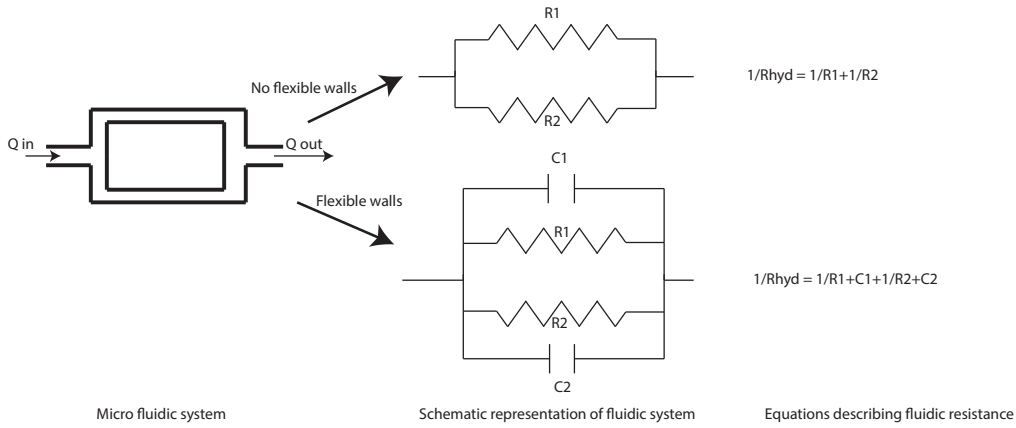


Figure 1.14.: Electrical analogy of the resistance in the fluidic system

1.5 Weighing using hollow cantilever AFM

A hollow cantilever can be used in several applications. One of the applications is the weighing of fluids or particles suspended in the fluid. Weighing can be used for identifying the molecules in a fluid. Ultimately the nanomechanical resonators can be used as mass spectrometry [42]. Hollow cantilevers can be used for weighing of small masses such as single nanoparticles and single cells. Nanomechanical resonators are able to detect masses as small as 7 zepto grams [43]. Masses are detected using the frequency shift. When a cantilever is excited in its eigenfrequency a large deflection is observed. When the cantilever is filled mass is added and the eigenfrequency is decreased. This is described by equation 1.12, where m^* is the effective mass of the cantilever and α the localization factor of the added mass Δm . In [43] a frequency change of 9.1 kHz is observed between a cantilever filled with air and a cantilever filled with water. In [44] (see figure 1.15) a frequency shift of 135 Hz is observed corresponding to an added mass of 3.4 pg. The volume of the hollow cantilever is 2.62 pL for water this corresponds to a mass of 2.62 pg. The difference is explained by the uncertainty of the volume of the cantilever calculation.

$$f = \frac{1}{2\pi} \sqrt{\frac{k}{m^* + \alpha \Delta m}} \quad (1.12)$$

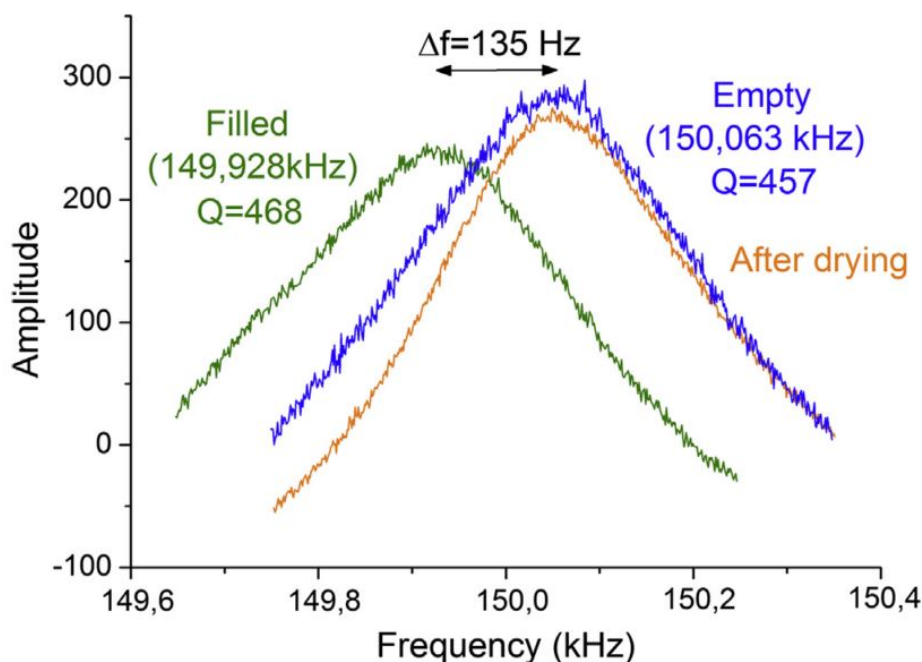


Figure 1.15.: Frequency shift in a filled cantilever, lower resonance is due to increased distributed mass of the liquid[44]

1.6 Conclusion

This goal of this literature study was to give an overview of the several applications of the hollow cantilever AFM, and dosing technique and the dosing parameters that are important when working with the AFM. Three different applications are described, single cell manipulation, DNA micro array and gluing graphene.

AFM is normally used for imaging. Dispensing droplets using AFM probes is shown by dip pen techniques. A disadvantage is that the fluid runs out fairly quickly. By introducing hollow cantilever AFM the ability of dispensing for longer times is shown.

For dosing different techniques exist these can be separated in three categories, dosing with a predefined volume, controlling flow rate and contact printing. For dispensing with AFM the last two categories are important.

Dispensing in AFM can be divided in two categories, dispensing using the surface forces and dispensing using a pressurized liquid reservoir. With dispensing using the surface forces the dominant parameter is the surface energy between the substrate and the liquid. Spreading of the droplet takes time and therefore controlling the contact time different droplet sizes could be dispensed. For proper control of the droplet sizes characterization of the surface energy should be done. The surface energy is characterized by its contact angle.

Pressure is needed for dispensing beyond the surface forces. Dosing with pressure gives two extra parameters to control. The applied pressure and the time the pressure is applied. For dispensing with pressure the fluidic system can be modeled using the electrical analogy.

With a hollow cantilever AFM it is possible to weigh substances. When a cantilever is filled with mass the eigenfrequency will decrease and subsequently the added mass can be calculated.

1.7 Goal of the thesis

The evaluation of the data presented in this thesis and research involving several articles concluded that the ability of dispensing fluids using the AFM is possible, however there were no

methods found whereby the volumes of the dispensed droplets can be controlled.

Therefore the goal of this thesis is to control the dispensing of liquids on small scale. This will be achieved by finding out which parameters influence the size of the droplets and how these parameters can be manipulated to control the droplet size.

1.8 Organization of the thesis

The intention of this thesis is to be able to understand how the dispensing of liquids on a small scale can be controlled. Therefore, first a literature study was performed to gain a better understanding of the background and to see what kind of experiments already have been performed in this field. Also the theory is studied to know which parameters influence the dispensing of droplets and how these parameters can be manipulated.

In the next chapter a method is proposed to calculate volume of a droplet using the contact angle and the break up height. A system is build to measure the contact angle. The contact angle is later used to calculate the volume.

The third chapter discusses the design and fabrication of an interface that is used to connect the AFM chip to an external liquid reservoir. This enables the controlled dispensing of fluids.

In the following chapter, experiments are conducted to investigate the influence of the relative humidity on the breakup height, which is used to calculate the volume. The experiment was executed using the climate controller available at the AFM system.

The final two chapters will show methods of controlled dispensing of liquids using the hollow cantilever AFM. In Chapter 5 dispensing using only the surface forces are shown. Chapter 6 will demonstrate dispensing by applying pressure to the liquid reservoir.

2 — Receding contact angle set-up

2.1 Introduction

Consider a droplet of liquid laying on a flat surface (see figure 2.1 B). For small droplets they will form a sphere or a part of a sphere to minimize the surface energy. The contact angle is then formed by the intersection of the liquid-solid and the liquid-vapor interface [45]. The contact is defined by drawing a tangent to the droplet at that point. The contact angle gives information about the affinity of the liquid with the substrate. When a liquid has a large affinity with the surface, the surface energy is high and the liquid will spread on the surface resulting in a small contact angle (smaller than 90°). In the case of water, the surface is called hydrophilic. When a liquid has low affinity with a surface the liquid will try to form a sphere resulting in a high contact angle (higher than 90°). For water the surface is than called hydrophobic.

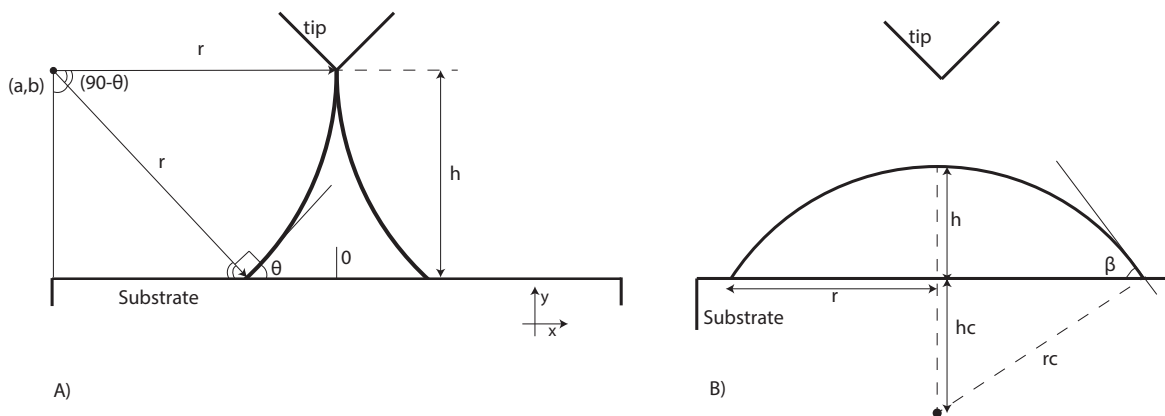


Figure 2.1.: Schematic representation of A) a receding droplet and B) a sessile droplet

The contact angle can be interpreted in different ways, one way is to measure the contact angle of a dispensed droplet at rest, the sessile drop technique [46]. Another method is to measure the contact angle when retracting the dispensing needle or aspirating the droplet, the receding contact angle (see figure 2.1 C)[47]. The receding angle is defined as the angle at the moment the baseline of the droplet starts moving. The receding contact angle is necessary to determine the dispensed droplet volume from the breakup height obtained with the AFM system.

The purpose of this experiment is to create a setup for measuring receding contact angle and sessile contact angle. To simulate the process of liquid bridge breaking in AFM correctly, the setup uses a retracting needle. Droplets need to be as small as possible because it will simulate the AFM process more precisely.

2.1.1. Theory

The receding contact angle is used to determine the volume of a liquid bridge during break up. The input parameters to determine the volume (see figure 2.1) are the contact angle of a fluid with the substrate θ_1 , and the breakup height of the liquid bridge h . From these parameters the curvature r and subsequently the volume of the liquid bridge v is determined. Figure 2.1 gives the assumed shape of the liquid bridge. It is assumed that the bridge forms a point during breakup and that the volume is not dependent on the contact angle of the tip. It is also assumed that the droplet is axial symmetric. The breakup height in AFM measurements is obtained from the force distance curves.

2.1.2. Volume calculation

Calculation for the volume of a liquid bridge. The shape assumed is given in figure 2.1. There are two input parameters the contact angle θ and the height h . The curvature r can be determined by equation 2.1.

$$r = \frac{h}{\cos(\theta)} \quad (2.1)$$

The curvature of one side of the liquid bridge, only looking in plane describe a part of a circle. Formulas for a circle are given in equation 2.3 and 2.4. Here t is a parametric variable. When rearranging equations 2.3 and 2.4 an expression for x is obtained which results in equation 2.4. x describes the radius of the liquid bridge for a given y position.

$$x = a + r \cos(t) \quad (2.2)$$

$$y = b + r \sin(t) \quad (2.3)$$

$$x = a + r \cos(\sin^{-1}(\frac{y-b}{r})) \quad (2.4)$$

The volume of the liquid bridge can be determined by integrating the area of the cross section of the liquid bridge over the height of the liquid bridge (see equation 2.5 [48]). The cross section of the liquid bridge is described by a circle and the area of a circle is described by equation 2.6. Where x is the radius of the circle described by equation 2.4.

$$V = \int_0^h A(y) dy \quad (2.5)$$

$$A(y) = \pi x^2 \quad (2.6)$$

$$V = \frac{2\pi h^3}{\cos(\theta)^2} - \frac{\pi h^3}{3} - \frac{\sqrt{\pi h^3(1 - \cos(\theta)^2)}}{\cos(\theta)^2} - \frac{\pi h^2 \sinh(h\sqrt{\frac{-\cos(\theta)^2}{h^2}})}{\sqrt{\cos(\theta)^2 \frac{\cos(\theta)^2}{h^2}}} \quad (2.7)$$

Using Matlab to integrate the area over the height, an expression for the volume of the bridge V is found dependent on the receding contact angle and the break up height (see equation 2.7). As a test sample a droplet with a height of 1 m and a contact angle of 15 degrees a volume of 0.25 m³ is found and figure 2.2 is obtained. Which describes the desired shape. When calculating the volume of a cone with equation 2.8 where A_{base} is the area of the base and h is

the height a volume of 0.6 m^3 is obtained. This is in the same order of magnitude as obtained with equation from Matlab and therefore it is assumed to be correct. As a second check the shape is recreated in Solid Works (see figure 2.3) and a volume of 0.25 m^3 is obtained which is the same as obtained with the function created in Matlab.

$$V_{\text{cone}} = \frac{1}{3} A_{\text{base}} h \quad (2.8)$$

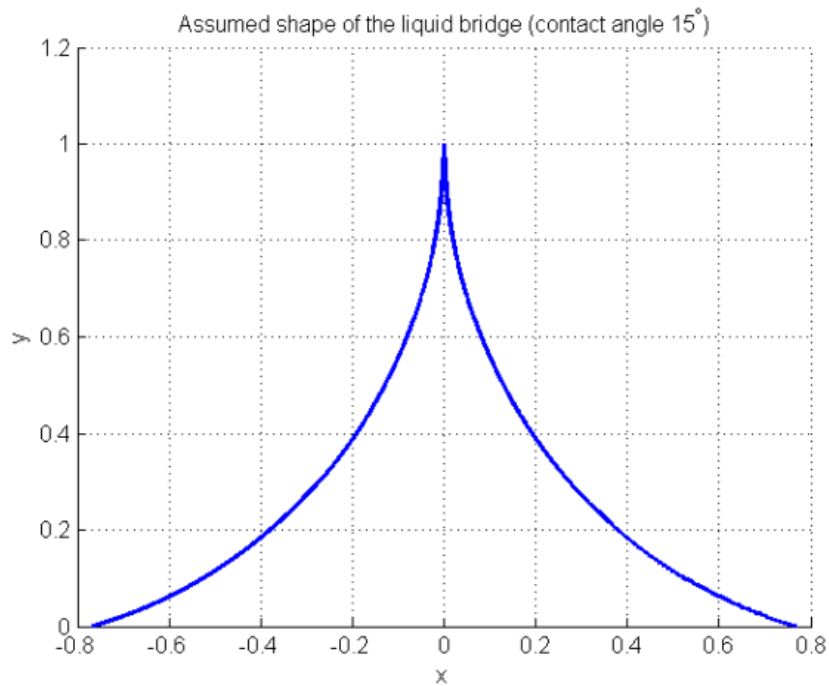


Figure 2.2.: Obtained figure with Matlab for a liquid bridge

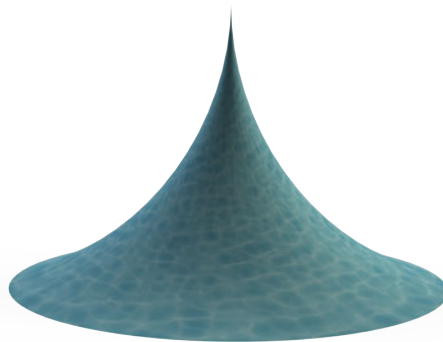


Figure 2.3.: Recreated droplet shape in Solid works

2.2 Methods and materials

2.2.1. Experimental setup

A setup for measurement of the receding contact angle is made using standard parts of Thorlabs and some 3D printed parts. The bridge need to be visualized and subsequently the contact angle can be measured using image processing software. The droplets will be dispensed on a surface with a gradient in the surface energy. Different surface energies result in different contact angles. Eventually the break up height can be obtained from the force distance curves from the AFM measurement. On the large scale the breakup height can be obtained from the image taken with the microscope.

Materials

For this experiment the following materials are needed.

- Camera (Digital Viewer III 2.0M)
- Camera fixing unit
- Dispensing pump (MA3 Solutions)
- Height varying dispenser holder (Thorlabs)
- Water
- Microscope glass
- functionalized silicon (Octyltrichlorosilane Sigma Aldrich)

Droplets of water are dispensed on the substrate and then a picture is taken. The camera needs to be stable to make a sharp image, therefore the camera is placed in a 3D printed holder. The syringe used for dispensing is fixed in a 3D printed holder (see figure 2.4). The holder can move up and down using a micro screw. With this set up the following picture can be obtained for the receding droplet (see figure 2.5a) and for the sessile droplet (see figure 2.5b).

Under influence of gravity it is possible the contact angle changes. The radius of the droplet must be much smaller than the capillary length [35] see equation 2.9 because than the gravitation can be neglected and is the shape only dominated by the surface forces. The capillary length of water is 2.7 mm. The goal is to dispense droplets with a radius of 1 mm. This is smaller and therefore the gravitation is neglected. It is assumed that droplets dispensed with the AFM have the same contact angle as dispensed with this setup.

$$l_c = \sqrt{\frac{\gamma}{\rho g}} \quad (2.9)$$

where:

- γ : surface tension (0.07199 N/m)
- ρ : density (998 kg/m³)
- g : gravitational constant (9.81 m/s²)

The volume predicted from the breakup height should match the volume when imaging the droplet and calculating the volume from the spherical cap equation 2.10. With imaging the diameter of the dispensed droplet is obtained. With a known sessile contact angle the volume can be determined (see figure 2.1 A). The droplet height can be obtained from the geometry (see equation 2.11). Where r is the droplet radius, h the droplet height and β the sessile contact angle.

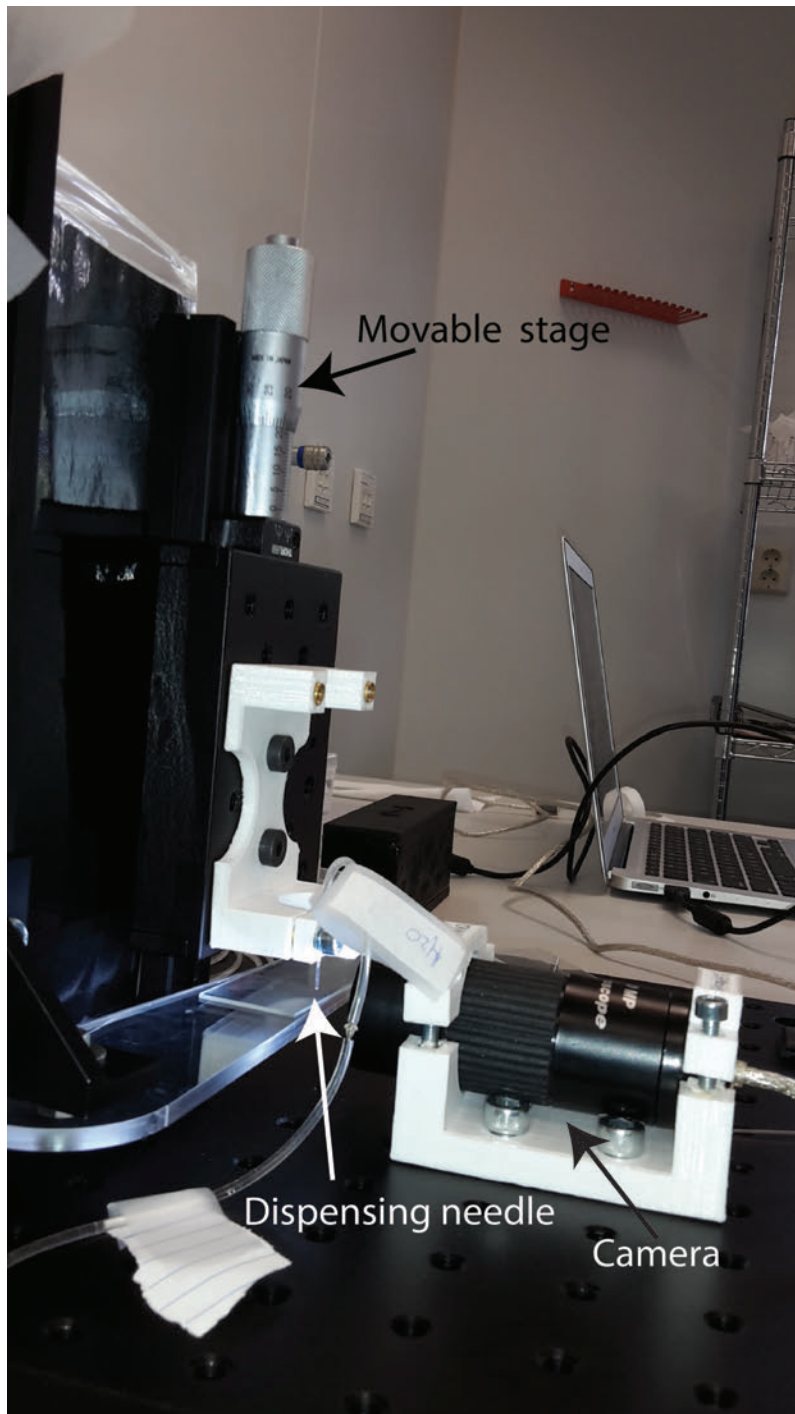


Figure 2.4.: Experimental setup for receding contact angle measurement

$$V_d = \frac{\pi h}{6} (3r^2 + h^2) \quad (2.10)$$

$$\text{with: } h = rc - hc \quad (2.11)$$

$$\text{where: } rc = \frac{r}{\sin(\beta)} \quad (2.12)$$

$$hc = r \tan(90 - \beta) \quad (2.13)$$

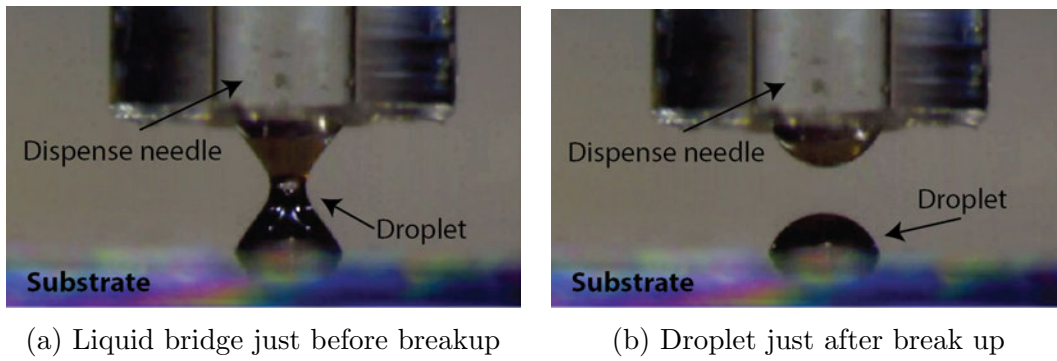


Figure 2.5.: Droplets for contact angle measurement

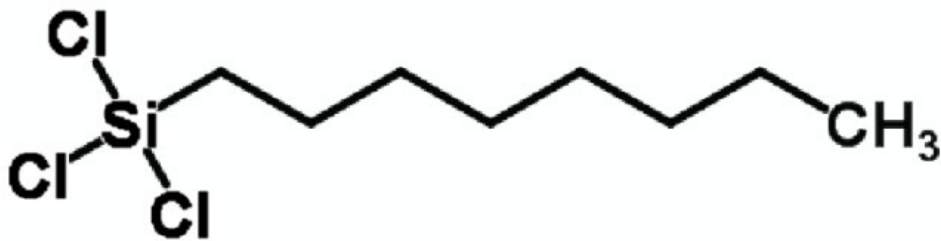


Figure 2.6.: Octyltrichlorosilane

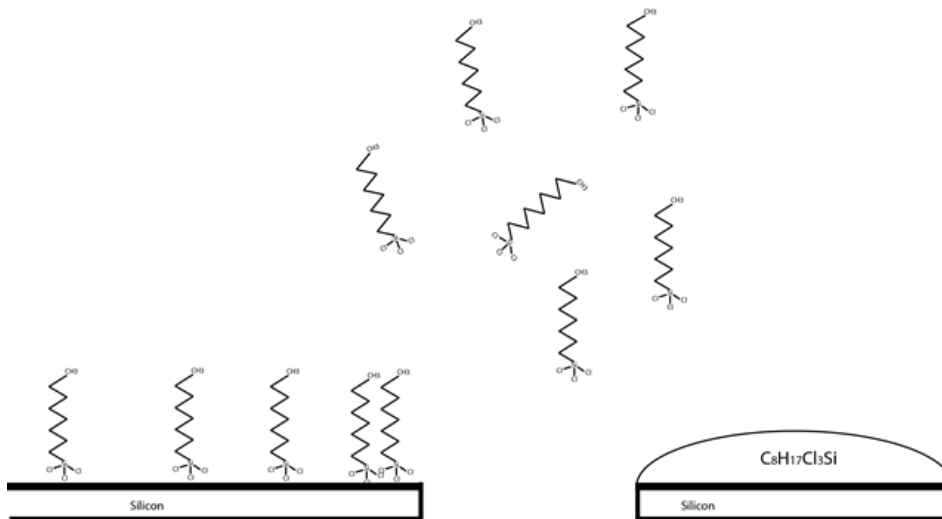


Figure 2.7.: Schematically given the setup and the working principle

2.2.2. Substrate preparation

For the functionalization of the substrates a fresh silicon wafer is scribed into pieces of 10x15 mm. These silicon pieces are functionalized using octyltrichlorosilane ($C_8H_{17}Cl_3Si$) (Sigma Aldrich) the structural formula is schematically given in figure 2.6. These surfactants adhere to the substrate to form a monolayer. The more surfactants on the surface the more hydrophobic the surface becomes. The setup and the working principle is schematically given in figure 2.7 [49]. Two pieces of silicon are placed 10 mm apart in a polystyrene Petri dish and then a droplet of 40-50 μ L octyltrichlorosilane is dispensed on one of the silicon pieces then the Petri dish is closed of and left for 2 minutes and 30 seconds. The chemical starts to evaporate and the further away from the source the less chemical will adhere to the other silicon substrate. This is described by the formula for the diffusion length C (see equation 2.14) which is a generalization of Fick's law [39] page 82, where D is the diffusion coefficient and t the time.

Finally the the piece without the droplet is removed and tested whether a gradient of surface energy is achieved. This is tested by dispensing a droplet of water using a syringe and visually checking the contact angle. The expected result is given in figure 2.8. The side with a a large amount of surfactants will result in a droplet with a large contact angle and the side with less surfactants will have a small contact angle.

$$C = \sqrt{Dt} \quad (2.14)$$

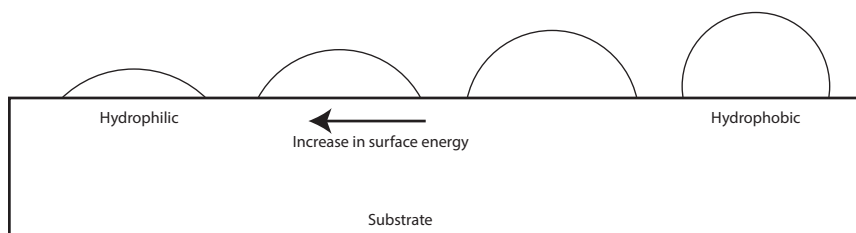


Figure 2.8.: Expected result of the functionalization, with on the right side large contact angle indicating lower surface energy and on the left high surface energy and small contact angle

2.2.3. Software

Using the image processing tool from Matlab (see appendix H), a program is written to analyze the contact angle of the liquid bridge and the sessile droplet. The program is based on a method described by [50]. The advantage of using Matlab to detect the contact angle is that the reproducibility of the measured contact angle is higher. The program is able to analyze sessile drops and receding contact angles, this is useful to relate the sessile drop contact angle to the receding contact angle. The basic idea is that the sessile drop can be described by a part of a sphere. In a two dimensional picture this sphere becomes a circle, also the walls of a receding droplet can be described by a circle. Using this knowledge a circle is fitted around the edge of the droplet and this in combination with some user inputs can be used to determine the contact angle. Subsequently the volume of the liquid bridge or the dispensed droplet can be determined.

See appendix B, first the image is loaded and a matrix is created containing the color values of the pixel and the position in the matrix corresponding to the pixel location. Now a user input is required to reduce the processing time. The image needs to be cropped, this is done by dragging a window around the droplet discarding information unnecessary for the analysis of the contact angle.

For better distinction between the background and the droplet the image is converted to a gray scale image. Now another user input is necessary to define the substrate this is done by clicking around the substrate a couple of times. Matlab determines an average line between those points. This line is used to find later the triple point of the droplet and to reduce the error of rotation in the picture.

Next a filter is applied to find the edge of the droplet it turned out the "Canny" filter gives the best results. After filtering edge detect software is used. The software also detects some edges on the background. To make sure that the correct points are used for the fitting of the circle another user input is acquired. Clicking close to the detected white line the rest of detected edges are not used for fitting. The number of clicks gives the number of data points

for the circle fitting. The function for the fitting of the circle returns the center point and the radius. This can be used to calculate the intersection with the substrate which results in the triple point of the droplet this also gives the width of the contact area of the droplet. Using the radius and the width of the droplet the contact angle can be calculated. There are 4 cases (see figure 2.9) 1. sessile drop on hydrophilic surface, 2. sessile drop on hydrophobic surface 3. receding angle on hydrophilic surface and 4. receding angle on hydrophobic surface. Each case corresponds to a different contact angle equation described in equations 2.15 to 2.18.

The obtained data is saved to a text file and can be used later to display the varying contact angle of the substrate or to calculate the volume of dispensed droplet.

$$Ca_1 = 90 + \cos^{-1}\left(\frac{w}{2r}\right) \quad (2.15)$$

$$Ca_2 = 90 - \cos^{-1}\left(\frac{w}{2r}\right) \quad (2.16)$$

$$Ca_3 = 90 - \cos^{-1}\left(\frac{w}{2r}\right) \quad (2.17)$$

$$Ca_4 = 90 + \cos^{-1}\left(\frac{w}{2r}\right) \quad (2.18)$$

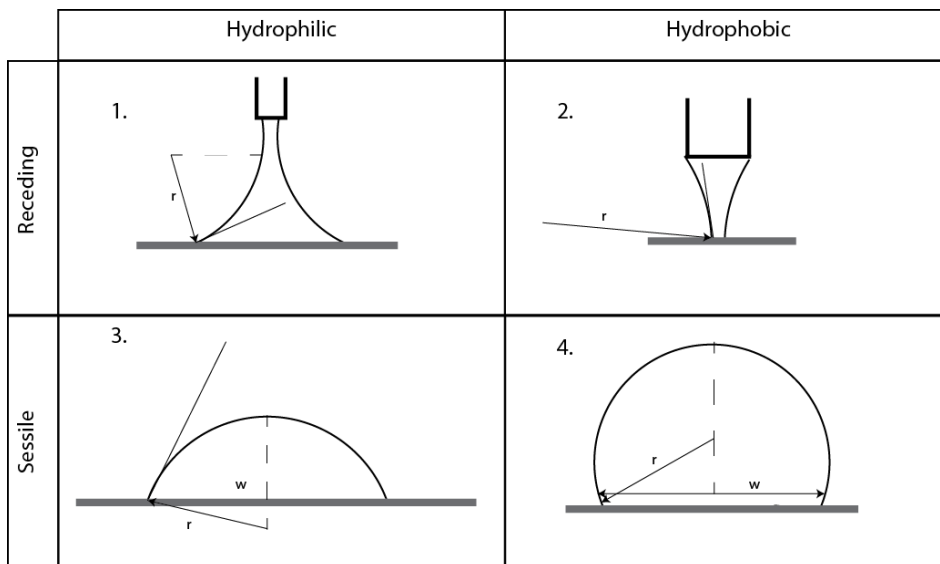


Figure 2.9.: Schematic overview the four possibilities of the dispensed droplet 1. Receding droplet hydrophilic surface, 2. Receding droplet hydrophobic surface 3. Sessile droplet hydrophilic surface, 4. Sessile droplet hydrophobic surface,

2.2.4. Measurements

At different locations on the substrate a droplet is dispensed. First a droplet hanging on the needle is created using a computer controlled pressure source. The needle is also silanized to prevent the droplet spreading on the needle. The needle is brought down by the microscrew to dispense the droplet. During the dispensing a movie is made using the software provided with the microscope (Digital viewer III 2.0M). A frame rate of 30 frames per seconds and a resolution of 1600x1200 is used. With free movie maker software (Videopad video editor) the frame before the breakup is selected for the receding contact angle and the frame after the breakup for the sessile contact angle. The frames are saved and analyzed using the Matlab software.

2.3 Results and discussion

Using the substrate as described earlier a gradient of surface energy is obtained (see figure 2.10). This figure is created by combining a sequence of pictures corresponding to a different position on the substrate. In this figure it can be seen that the droplet on the left got a large contact angle corresponding to a low surface energy. The contact angle is 94° in the sessile case and 90° in the receding case. The droplet on the right got a lower contact angle corresponding to a high surface energy. The contact angles were 61° for the sessile case and 43° for the receding droplet. This means that the left side is hydrophobic and the right side is hydrophilic. The hydrophilic side contact angle is more than measured in Chaudhury et al. but the contact angle at the hydrophobic side is in the same order [49]. Probably cleaning of the silicon will result in more hydrophilic surfaces because hydrocarbons from the air will adhere to the silicon.

The variation of contact angle versus the position of the substrate is given in figure 2.11. The square root trend is visible which is expected. Especially in the sessile case the contact angle could be measured well. As expected the receding contact angle is smaller than the sessile droplet because pulling on the droplet reduces the contact angle. The contact angle is still dependent on a user input in Matlab, because the surface is too dark to detect automatically. By enough clicking around the substrate an accurate enough determination of the substrate location can be made. Filtering can increase the sharpness of the picture making probably the edge of the substrate detectable. For 5 experiments on the same picture on average a receding angle of $15.6 \pm 2.8^\circ$ and sessile angle of $54.6 \pm 2.3^\circ$ is obtained. For confirmation of the assumed shape of the liquid bridge experiments with a high speed camera should be conducted. A high speed camera can take a picture closer to the breakup as the breakup happens fast. Also larger magnification and higher resolution can help increasing the accuracy of the measurement.

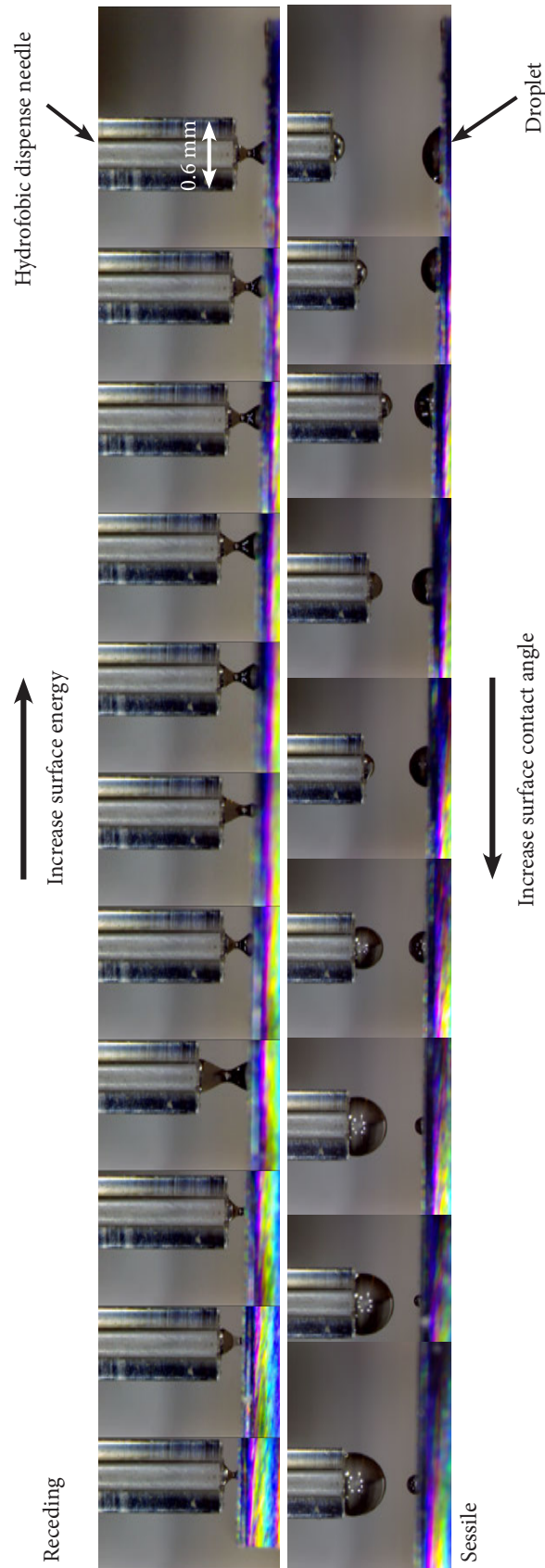


Figure 2.10.: Compilation of different pictures, showing gradient of surface energy, from right to left increasing contact angle, top row receding droplets, bottom row sessile droplets

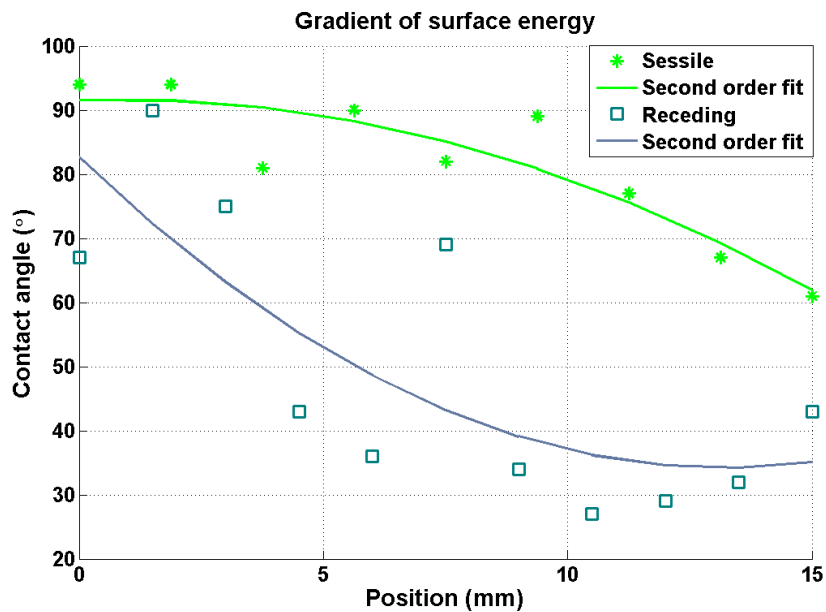


Figure 2.11.: Plot of the varying contact angle versus the position on the substrate

2.4 Conclusion

The system build is capable of measuring the receding and the sessile contact angle of a droplet with a contact diameter of around 0.5 mm. With the supplementary software, created in Matlab, the ability to detect the droplet edges is created. Using the detected edges the contact angle is calculated both for the receding and sessile case with a standard deviation of 3°. Functionalized substrates are made and perform as expected. A gradient of surface energy is obtained this is reflected in the contact angle of the water droplet. The contact angle changes smoothly over the substrate especially in the sessile case. The square root relation created by the diffusion process is visible in the measured contact angle. Especially in the sessile case is the expected relation well visible. The method proposed of measuring the contact angle is used in later experiments to determine the volume from AFM measurements, because droplets are small the contact angle is only dominated by surface energy therefore gravity is neglected and the measurement can be used in AFM measurements.

3 — Humidity control for femto liter droplets

3.1 Introduction

AFM is used to measure adhesion force between tip and a substrate [51]. Several researches show a relation between relative humidity and breakup force [52][53][54]. When dispensing femto liter water droplets they will evaporate almost immediately [62]. To increase the lifetime of a droplet the humidity can be increased, therefore a climate controller is added to the AFM system. For proper characterization of the system the influence of the relative humidity on the breakup height is investigated. The breakup height is later used as identification of the dispensed droplet. The goal of this experiment is to find the relation between the breakup force of the capillary bridge and the relative humidity. Theoretical calculations are performed on the adhesion force of an AFM tip and a substrate, also an experiment is conducted where the breakup force is measured in relation to the relative humidity. An experiment to try to visualize the liquid bridge formed by capillary condensation is executed. The liquid bridge formed by capillary condensation plays an important role in dispensing with an AFM as it is the initial driving force to pull out liquid from the tip.

3.1.1. Theory

Capillary condensation is the spontaneous formation of a water bridge when two objects come in close contact. It is the initial driving force for dispensing a droplet and the main reason for stiction of a cantilever to a substrate. The water bridge is formed by condensation of water molecules from the air below the saturated vapor pressure of the pure liquid. Due to the increased van der Waals forces it is more energy favorable for the water to condense rather than stay in gaseous form. The bridge is under deeply negative pressure [55]. Pressures of -160 MPa are reported. This pressure will pull water from the cantilever on the substrate. Negative pressure is compared to water in an enclosed cylinder with tensile force on it. Because the liquid bridge is close the critical cavitation radius no gas bubbles will be created in the bridge [56]. The cavitation radius is given in equation 3.1, where γ_{lv} is the surface tension between liquid and vapor, P_{sat} the saturated vapor pressure and P the actual pressure. When taking for $\gamma_{lv} = 0.072$ N/m and $P_{sat} - P = 10^5$ Pa the critical cavitation radius becomes 1.4 μm [51]. When the thickness of the liquid-vapor interface reaches the critical cavitation a lower energy path for nucleation is taken to connect the liquid to the vapor phase.

$$R_c = \frac{2\gamma_{lv}}{P_{sat} - P} \quad (3.1)$$

Several forces are responsible for adhesion of a cantilever to a substrate [57]. The adhesion force consists of the capillary force (F_c), van der Waals forces (F_{vdW}), electrostatic forces (F_e) and the chemical bonding forces (F_b) (see equation 3.2). Electrical forces can be neglected

because the cantilever is left in air for long time therefore no net charges remain. Chemical forces are neglected because the tip is inert in respect to the substrate. The capillary force the only force left and is divided in two parts, one the Laplace force (see equation 3.4) acting on the wetted area (πl^2) and two the line tension force (see equation 3.6) acting on the circumference of the wetted area πl [53]. Where, l is the azimuthal radius of the droplet, r is the meridional radius and γ is the surface tension. The Laplace pressure can be estimated by the relative humidity using the Kelvin equation (see equation 3.10). Where, $\frac{1}{r_k} = \frac{1}{l} + \frac{1}{r}$, $RH = \frac{P_{vap}}{P_{sat}}$, R is the universal gas constant, T absolute temperature and V_m molar volume of water. The capillary force is calculated by adding the Laplace pressure and the line tension force. Figure 3.1 describes the breakup force for different opening angles of the tip versus the relative humidity based on continuum formulas (see equation 3.7).

The radius b is varied and subsequently l and r are calculated, later the relative humidity is calculated with the kelvin equation (see equation 3.10). The contact angles θ_1 and θ_2 are kept constant at 10° . D is the interatomic spacing and is considered to be 0.17 nm, this value is often used in literature. The continuum equation do not describe the measured behavior very well because atomic level is approached [58]. The equation 3.3 gives a good idea of what is happening in the process. With increasing humidity an increase in breakup force is expected.

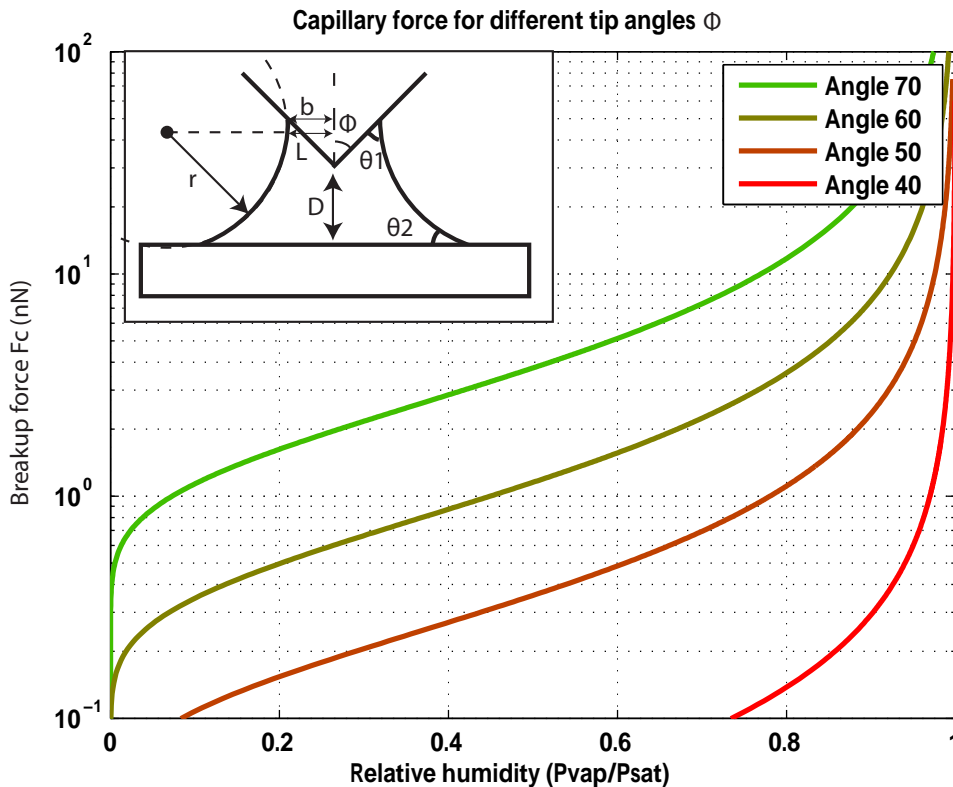


Figure 3.1.: Relative humidity related to the capillary force

$$F_{\text{ad}} = F_c + F_{\text{vdw}} + F_E + F_b \quad (3.2)$$

$$\text{with: } F_c = F_{\text{Laplace}} + F_1 \quad (3.3)$$

$$F_{\text{Laplace}} = \pi l^2 \Delta P \quad (3.4)$$

$$\text{with: } \Delta P = \gamma \left(\frac{l}{r} + \frac{1}{r} \right) \quad (3.5)$$

$$F_1 = 2\pi\gamma l \quad (3.6)$$

$$F_c = \pi\gamma b \left(2 \cos(\phi - \theta_1) + b \left(\frac{1}{r} - \frac{1}{l} \right) \right) \quad (3.7)$$

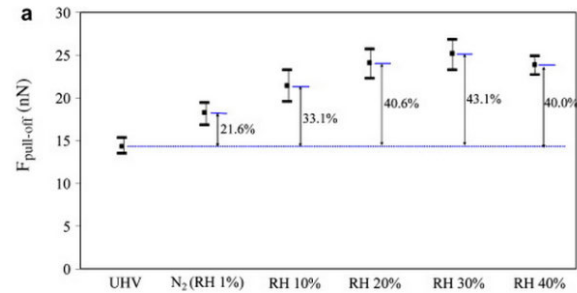
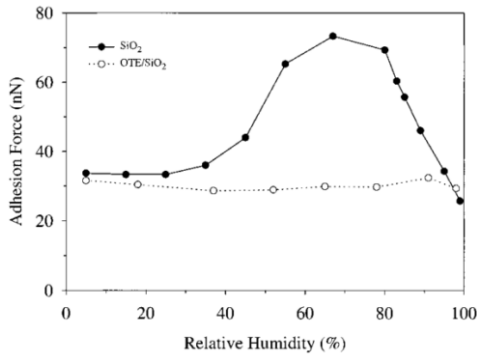
$$\text{with: } r = \frac{\frac{b}{\tan(\phi)} + D}{\sin(\phi - \theta_1) + \cos(\theta_2)} \quad (3.8)$$

$$l = b - r(1 - \cos(\phi - \theta_1)) \quad (3.9)$$

$$\frac{1}{r_k} = \frac{RT}{\gamma V_m} \text{Ln} \left(\frac{P_{\text{vap}}}{P_{\text{sat}}} \right) \quad (3.10)$$

The capillary force on a hydrophilic surface is strongly dependent on the relative humidity. This can be observed in figure 3.2a and 3.2b, where the breakup force is plotted versus the relative humidity. On a hydrophilic surface (SiO₂) at intermediate humidity an increase in breakup height is found due to the increase in capillary force. The decrease at high humidity is explained by changing tip shape or that the thermodynamic equilibrium is not reached. The straight line indicate the breakup force on a hydrophobic surface (contact angle 108°), the observed breakup force is constant, this suggests that capillary force is suppressed because the water bridge cannot exert any force on the substrate and therefore only van der Waals forces remain.

Another research shows the same behavior but the relative humidity is not increased to 100%, where an increase in breakup force was found in relation with an increase in humidity (see figure 3.2b). This research suppresses the capillary condensation by using ultra high vacuum because then there is no water to condense. The force obtained at ultra high vacuum is subtracted from the force in air to obtain the capillary force. When the capillary force is divided by the wetted area the pressure inside the bridge is obtained.



- (a) Relative humidity up to 100% no influence of capillary condensation by force measured on a hydrophobic surface [57] (b) Relative humidity up to 40% no capillary condensation using ultra high vacuum [55]

Figure 3.2.: Breakup force related to the relative humidity

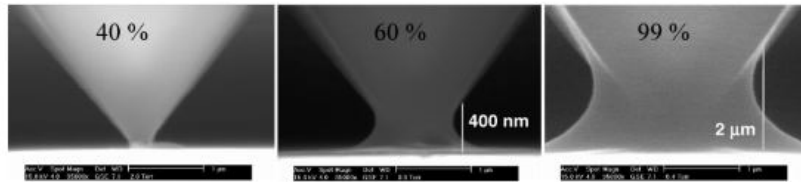


Figure 1. Sequence of images collected at various relative humidity. All images were collected at 5 °C, 15.0 kV accelerating voltage, at 35 000 \times . The humidity was varied by decreasing the pressure of the water vapor from 6.4 Torr down to 1 Torr: 40% rh, 2 Torr; 60% rh, 3.2 Torr; 99% rh 6.4 Torr.

Figure 3.3.: Relative humidity related to the liquid bridge size [59]

3.1.2. Visualization of liquid bridge

The visualization of a capillary condensed liquid bridge (see figure 3.3) is possible as shown in several researches [59][60][61]. These researches show also the dependency of relative humidity on the liquid bridge size. It is concluded by Honschoten et. all.[60] that the liquid bridge is much larger than estimated by the Kelvin equation. For a relative humidity of 0.98 a liquid bridge with a radius of 27 nm is expected and a radius of 200 nm is measured. Electrostatic charging by the electron gun is suggested as one of the reasons for the discrepancy between the measured and the predicted result.

The dependency of relative humidity on the liquid bridge is one nice thing to show with the visualization of the liquid bridge. It can also be used for confirmation of contact angle at the smaller scale. For the visualization an environmental SEM (ESEM) is needed. Normal SEMs operate at high vacuum but by going to low vacuum foreign molecules such as water molecules are allowed in the chamber. These water molecules can condense and form the water bridge. The ESEM used in weeks et. all [59] varies the pressure from 1 Torr (15% RH) to 6.3 Torr (99% RH). To force the water to condense also a decrease in temperature is used. This is created by using a Peltier element. A constant temperature of 5 °C is maintained during the experiments. An attempt has been made to visualize the capillary bridge for experimental details see appendix C.

3.2 Methods and materials

An AFM system from AFM workshop is used for the experiments. The AFM system is adapted for fluidic dispensing of droplets in the femto liter range. Typically, droplets in the range of 10 fl or smaller will evaporate within a second [62]. To extend the lifetime of the droplet a controlled climate, with an increased humidity is created. The system is described in appendix A. For proper characterization of the system the influence of the increased humidity on the breakup height is investigated.

3.2.1. Stiffness calculation

To properly compare different results from the literature and the breakup height obtained from the AFM experiments, the breakup height must be translated to a breakup force. This is done via Hooks' law, the stiffness k of the cantilever, multiplied with the breakup height ΔZ (see equation 3.11) this gives the breakup force. The breakup height is obtained from distance distance curves. It is the difference between the z-position of snap out and snap in, as defined in figure fig: force distance.

The stiffness of a cantilever can be obtained in several ways. One way is to model the cantilever in a finite element program. With known dimensions from SEM images a 3D model is created. Using Comsol multiphysics the eigenfrequency is simulated (see figure 3.4). The eigenfrequency is also checked by analytical calculations (see equation 3.12) [63]. Where α_n is

a constant, E the Young's modulus (179 GPa), $I = \frac{wh^3}{12}$ the moment of inertia ($w = 41.1 \mu\text{m}$ and $h = 3.6 \mu\text{m}$), ρ the density (2330 kgm^3), A the area of the cross section and l the length of the cantilever ($132 \mu\text{m}$). The analytical answer (333 kHz) is in the same order of magnitude as the measurement (338 kHz) and the finite element analysis.

To match the eigenfrequency of the measurement exactly with the simulation (see figure 3.5), a parametric sweep over the thickness of the cantilever is executed. With this thickness the stiffness is calculated by applying a force to the tip of this cantilever and subsequently calculating the deflection. Resulting in 47.43 N m^{-1} .

The eigenfrequency is measured by applying a frequency sweep to the cantilever. A laser is focused on the cantilever to measure the deflection. Using geometrical amplification the deflection is measured by a photo detector. When the eigenfrequency is reached a peak in deflection is observed.

Another method to calculate the stiffness of a cantilever is the Cleveland method [64][65]. Based on the dimensions and the measured eigenfrequency ω_m the stiffness is calculated (see equation 3.16). Resulting in a stiffness of 60.2 N m^{-1} which is deviating from the parametric sweep result, probably because of the variance in Young's modulus and the density. Also the geometrical shape is different. In the Cleveland method is a rectangular beam is assumed whereas in the FEM model the actual shape is used.

$$F_{\text{break}} = k\Delta Z \quad (3.11)$$

$$\omega_n = (\alpha_n)^2 \sqrt{\frac{EI}{\rho A l^4}} \quad (3.12)$$

$$\text{with: } \alpha_1 = 1.875 \quad (3.13)$$

$$\alpha_2 = 4.694 \quad (3.14)$$

$$\alpha_3 = 7.855 \quad (3.15)$$

$$k_{\text{cl}} = 2w(\pi l \omega_m)^3 \sqrt{\frac{\rho}{E}} \quad (3.16)$$

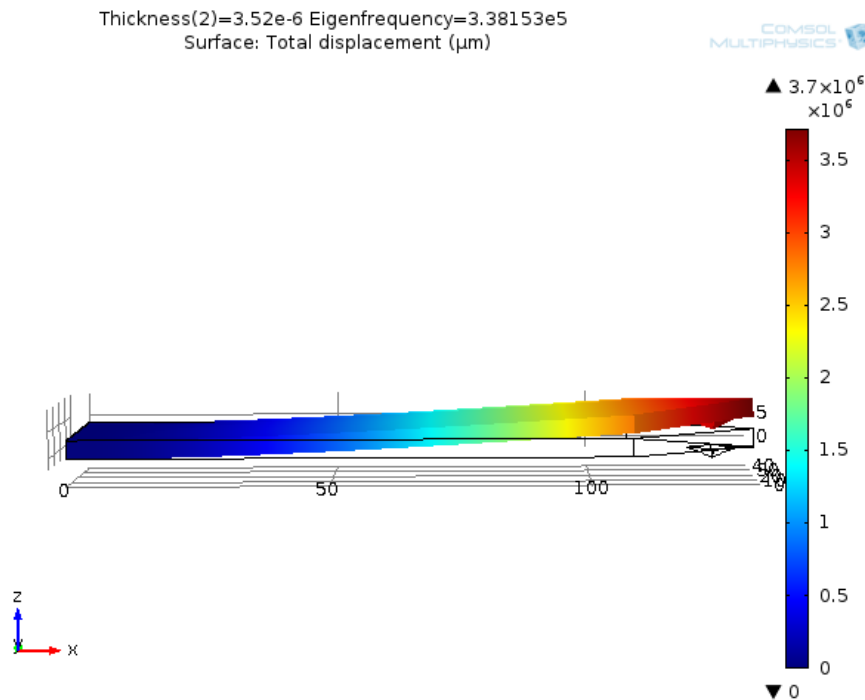


Figure 3.4.: Eigenfrequency analysis, first modeshape of an AFM cantilever

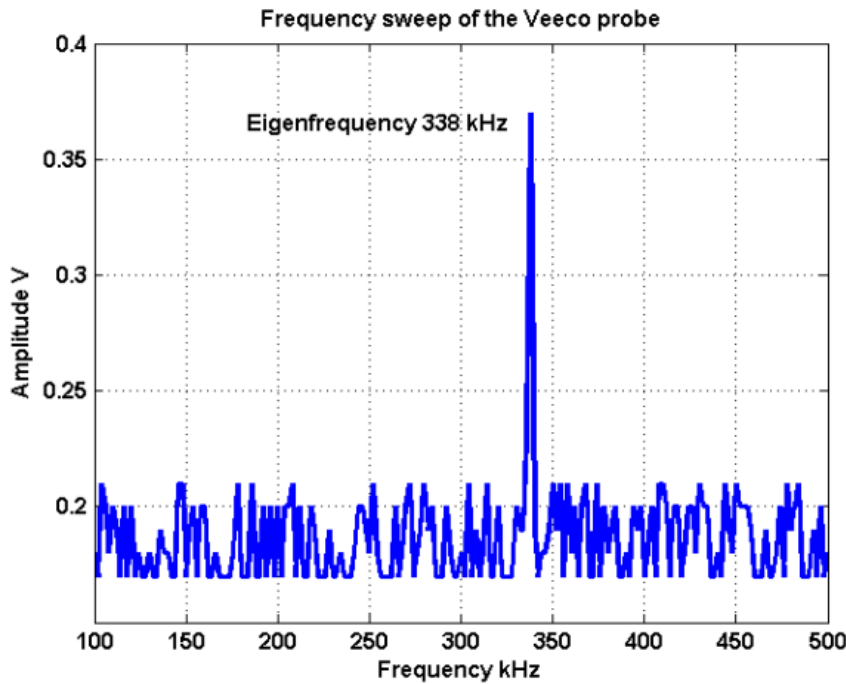


Figure 3.5.: Eigenfrequency analysis experimental result

3.3 Results and discussion

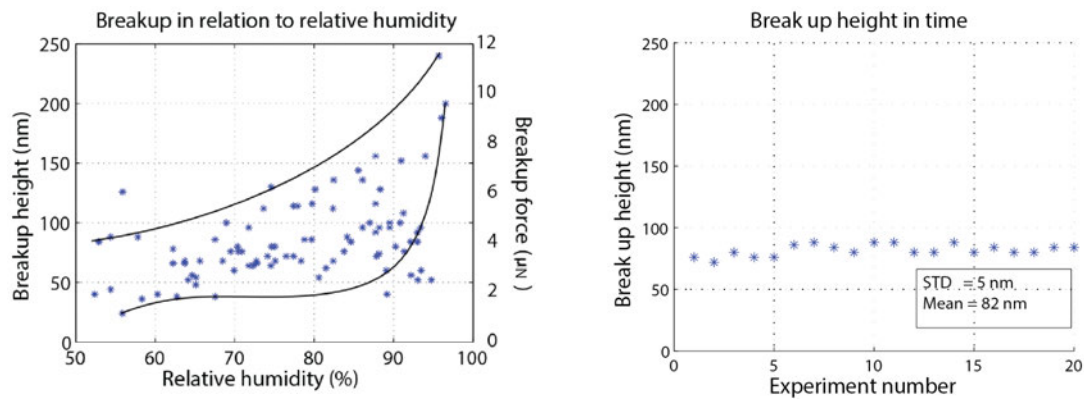
3.3.1. AFM measurements

AFM measurements are used to identify the influence of relative humidity on breakup height (see figure 3.6a). An increase in breakup height is observed as expected. The large spread is probably due to in process parameters because large spread is also observed in [58]. Also the climate controller is not constant which makes it difficult to relate the relative humidity to the breakup height. When measuring breakup height, without climate controller the spread is significantly reduced (see figure 3.6b). This indicates the climate is responsible for the spread in breakup height. Figure 3.7 shows a selection of force distance curves. For higher humidities larger snap out is observed.

For good comparison the breakup height is converted to break up force using Hooks' law using a stiffness for the cantilever of 47.43 N m^{-1} (see figure 3.6a). It is observed the breakup force is in the order of micro Newtons whereas forces in the literature are around tens of nano Newton. This might be related to the hysteresis in the piezo actuator. Ideally the approach and the retract line have the same position. In the experiment this is not the case as the retract line is always behind the approach line. The software used can be found in appendix I and appendix K. To reduce the spread the experiment can be repeated using a box to cover the AFM system. Because of the presence of people in the cleanroom it is possible that some turbulence in the air is induced causing the climate around the tip to vary which is not measured directly. Also the PID parameters of the climate controller need to be tuned, it is observed the climate controller varies with +5 and -9% from the set point.

3.4 Conclusion

Capillary condensation is the initial driving force for dispensing it is driven by the relative humidity. Experiments show an increase in breakup height as the humidity increases. Unfortunately large spread is found in the measurements. Future experiments should be executed with



(a) Breakup height related to relative humidity (b) Variability of breakup height without climate controller

Figure 3.6.: Breakup height

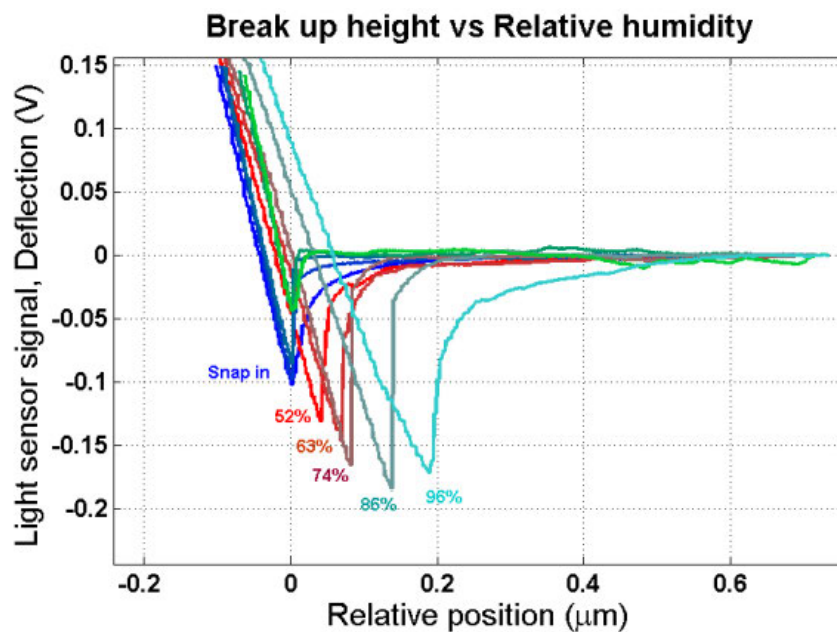


Figure 3.7.: Increase in breakup height with increasing relative humidity

a closed system to prevent turbulence of air around the tip. The force related to the breakup height is a factor 100 larger as found in the literature probably because no correction is used for the hysteresis in the piezo stage. To observe the trend of breakup height in relation to relative humidity no correction is needed because the hysteresis is constant [66].

Visualization of the capillary condensation can be used in two ways, one is that the contact angle stays constant even at the small scale. The second place to use the information is when dispensing with the AFM system, because, the initial liquid bridge pulls more liquid from the reservoir onto the substrate. Experiments are conducted to visualize the the capillary bridge. Using an ESEM with an increased humidity it is tried to visualize the liquid bridge. The liquid bridge was not visible because the temperature could not be reduced and the vacuum was too high. .

4 — Microfluidic interface for hollow cantilever AFM

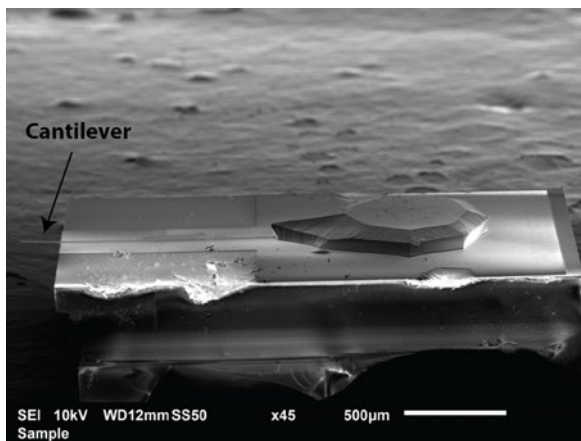
4.1 Introduction

The main goal of this thesis is to control droplet dispensing in the femto liter range. In order to achieve the dispensing, a connection between the reservoir and the chip is required, therefore a special interface is created. An interface is necessary because side access to the chip is needed because the clamp holding the AFM probe is blocking the top access. This chapter is about the design of the interface for connection of an AFM chip to the pressure and fluidic system. The designed interface is glued to the AFM chips. The steps in the gluing process are explained, additionally the considerations in the design and how the interfaces performs are described.

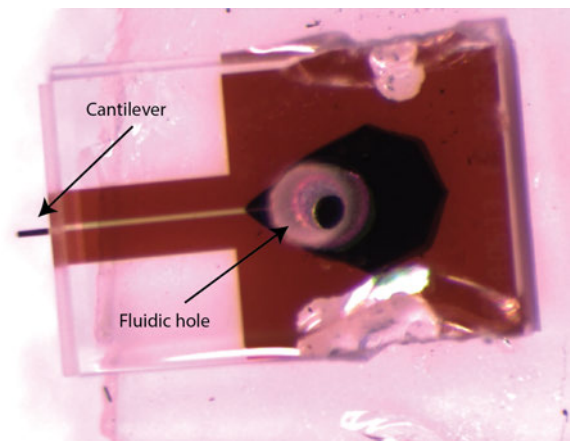
4.2 Methods and materials

4.2.1. Design and considerations

For proper connection of the AFM chip (see figure 4.1a and figure 4.1b) to the pump system an interface is designed using CAD software (Solidworks) (see figure 4.2a). In figure 4.2b the interface is mounted on the chip. The design is based on a design reported earlier [67] and is a 3D printed plastic part which is glued to the chip. The interface consists of a channel for a syringe needle and hole to transport the fluid from the reservoir to the cantilever. A syringe needle is glued to the interface for tube connection to the pressure system. For easy alignment of the hole of the chip to the hole of the interface an alignment marker is created. In the previous design two alignment markers are used but the second alignment marker for the side is omitted due to the lack of design space. The interface has to fit in the AFM holder (see figure 4.3). The channel for the stainless tube is therefore located at a specific height (0.2 mm) so the stainless tube does not make contact with the holder. The interface is trade off between hole size and glue space. The hole in the interface is as large as possible because sideways alignment has to be done by eye. On the contrary there has also to be enough glue space to assure a leak free connection of the chip and the interface. To prevent blockage of the laser the topside of the interface is slanted. The interface is finally 3D printed by Mareco prototyping. The material used for printing is HTM140 [68], a high temperature resistant polymer. The process used to make the interfaces is a digital light processing system, the polymer is cured using light. It is therefore advised to store the interfaces in a dark place because failure can occur under influence of uv light. Cleaning with ethanol, isopropanol or acetone is not advised because breakage of the interfaces can occur. The final 3D printed interface is shown in figure 4.4a and a complete assembly of interface, tube and chip is shown in figure 4.4b.

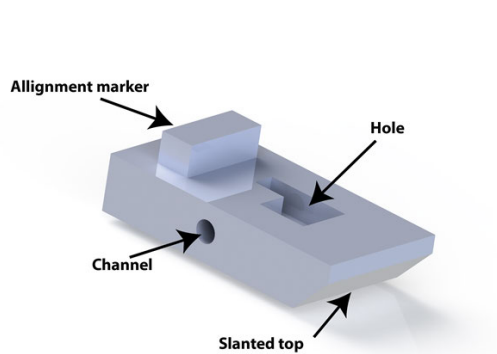


(a) Side view of fluidic chip

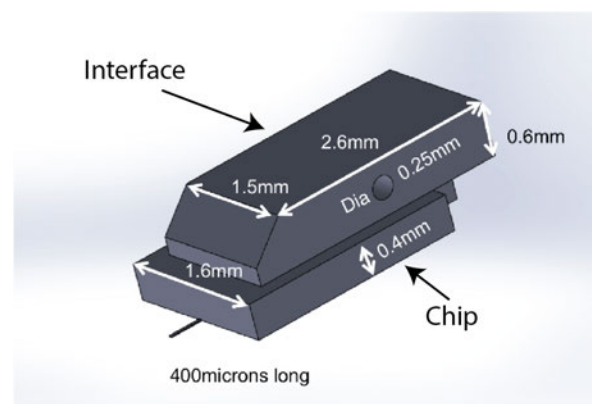


(b) Top view of fluidic chip

Figure 4.1.: Fluidic AFM chip



(a) Solidworks design of the interface



(b) Design of the interface with chip

Figure 4.2.: Solidworks interface design

4.2.2. Gluing

For gluing of chips several steps are needed (see table in appendix D). The steps are described below. Always be careful when gluing chips, cantilevers are fragile and can easily break. The cantilever is located at the top side of the chip. Work as clean as possible to prevent later clogging of the chips.

First step is the removal of the chips. Place a small piece of double sided tape under the right bottom corner of the chip to prevent flying away of chips during cutting. Use a scalpel to cut the chips from the array. Place the blade in between the chips, there is a small notch. Apply little pressure on the handle to cut the chip. Now using a small tweezers remove chip from the double sided tape and store the chip in a gel box. It is possible that gel boxes contaminate the chips if that is the case plasma cleaning can be used to clean the chips.

Step two is the gluing of the stainless tube to the interface block. The glue used for the process is Loctite Hysol 9492 from a glue gun. First prepare some glue on a microscope glass. The mixing ratio is 2:1, 2 parts of white resin and 1 part gray harder. Mix thoroughly using a syringe needle (blue 23 Ga). The glue has a high viscosity to prevent glue flowing inside the stainless tube. The glue is cured at 80°C for 10 minutes. All parts survive this temperature.

Holding the interface block at the side between tweezers the stainless tube can be inserted in the hole on the side. Place the syringe tip with interface block on the holder. Pick up a small droplet of glue using a syringe needle (brown 26 Ga) or scalpel. Under a microscope apply some glue to the interface and stainless tube. Start on the backside of the interface then turn

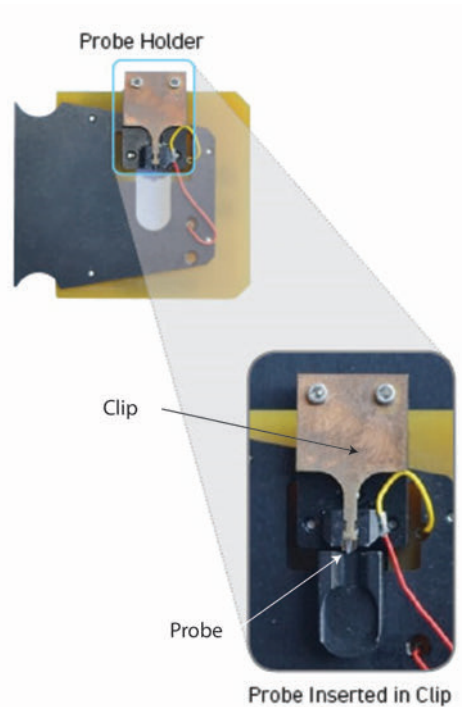


Figure 4.3.: Probe holder where the interface has to fit in

the syringe tip on the holder and apply glue on the front side (side with square hole). Create a small meniscus of glue to assure sealing but pay attention to only put glue on the side. Cure the glued interface on a hotplate at 80°C for 10 minutes, under a glass Petri dish. The Petri dish prevents heat loss. After curing the glued interfaces can be stored on a microscope glass with double sided tape.

The third step is the gluing of a chip to the interface. Before gluing clean off excess dirt on the interfaces with compressed nitrogen or air. Mount a syringe tip on the holder with the square hole facing up. Apply using a syringe needle or scalpel a small continuous line of glue around the hole. Make it as thin as possible. This helps to make sure the chip is mounted flat on the interface and that no glue enters into the hole.

Now using small tweezers mount the chip to the interface. Use the alignment marker to align the holes and make sure the chip is centered on the interface. Prevent a lot of sliding around with the chip, this may cause later clogging of the chips.

Cure the mounted chips on the hotplate for 10 minutes at 80°C. Pay attention that the chip is facing upwards to prevent the cantilever touching the hotplate and be careful that the syringe tip does not turn this can also cause breakage of the cantilever.

Final step of gluing is sealing the chip and interface. Mount the syringe tip on the holder for easy access to all sides. Using the syringe needle or scalpel, apply glue on the side between the interface and the chip to prevent leaking when in operation. Also apply some glue between the alignment marker and on the front. Pay attention to apply as little glue as possible on the front to prevent laser blockage later. Make sure no glue is on the backside of the chip this can result in unstable clamping.

Before use the complete assembly must be removed from the syringe tip. Using a small wire cutter the assembly can be removed. Place the wire cutter just below the edge of the yellow tip. Apply some pressure to the handle and the assembly will pop out. Now using large tweezers the glued chip can be mounted in the holder of the AFM. As well the Tygon tubing can now be connected to the chip.

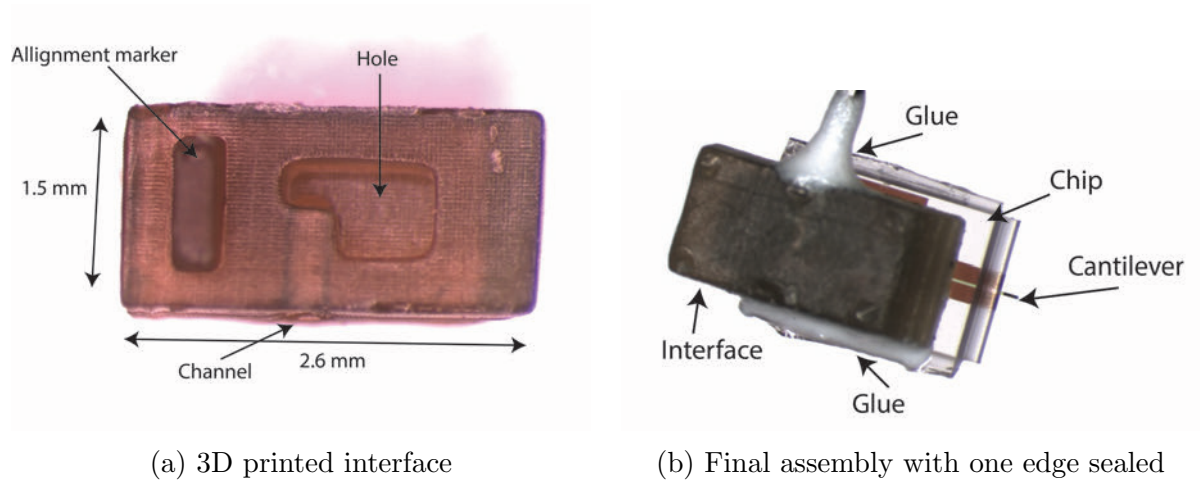


Figure 4.4.: Produced result

4.3 Results and discussion

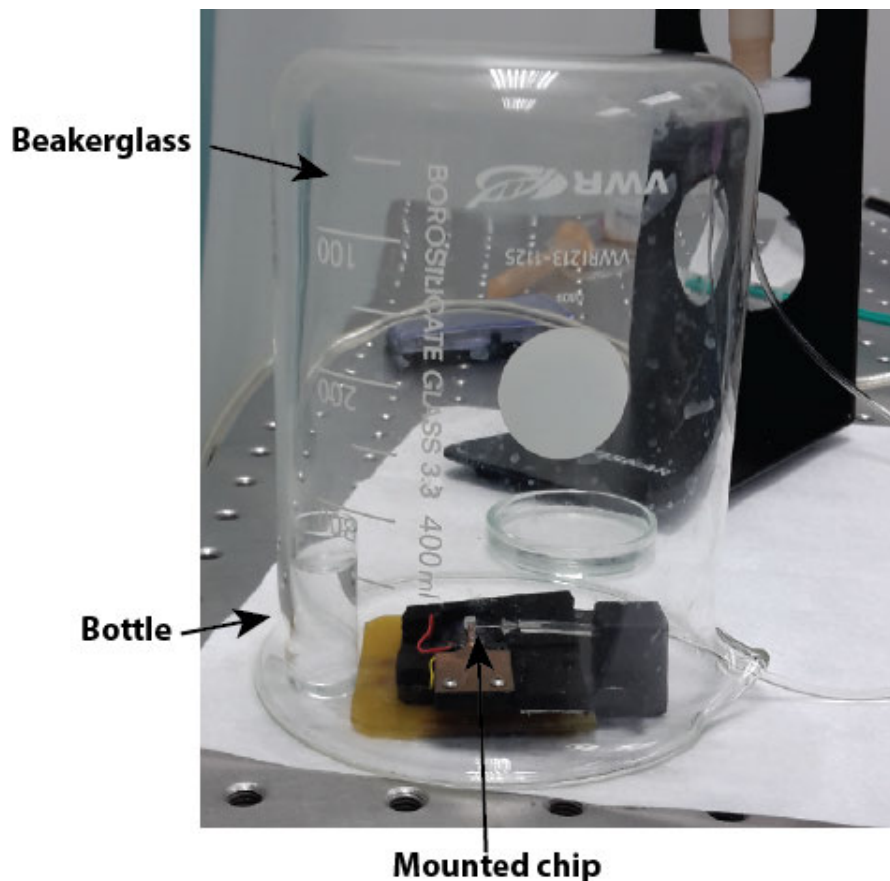


Figure 4.5.: Storing of the chip for later experiments

An interface is designed to connect an AFM cantilever to the pressure pump. For easy gluing a holder is created. The syringe tip can be turned around without change of breaking the cantilever. The process does not lead to 100% yield of working chips. Chips are easily clogged or damaged. Possible causes of clogging are, no clean water, gluing leaves particles or fabrication steps result. When testing a chip, a syringe filled with air is used to apply pressure to the chip when no pressure is build up in the syringe the chip is open.

The water can evaporate at the tip hole and some residue can clog the chip. Residue is also

observed when dispensing on silicon according to EDS analysis it is organic material. Particles can also come from the interface itself, the chip or the glue. When imaging chips using SEM it was observed the hole was not completely open.

There are also in process parameters which can result in clogging. The tip makes contact with the substrate therefore the tip can pickup particles from the substrate. The water used for dispensing comes from a DI water system and is subsequently filtered using a 0.45 μm or a 0.2 μm syringe filter. The filtering already resulted in longer lifetime of a chip. When the chip is left overnight the chip can clog by evaporation at the tip. This can be prevented by storing the connected chip at high humidity (see figure 4.5). When storing the chip under a beaker glass and supplying water from an open bottle the chip survives for several days up to two weeks. After two weeks the cantilever has some residue on it and high pressure was needed to pump out water. Storing at high humidity may cause on the long term oxidation of some other materials.

4.4 Conclusion

With the design of the interface a leak free connection is established between the interface and the AFM chip. Pressures up to 5 Bar are applied, the maximum of the system. When applying pressure using a syringe, higher pressures are applied and the fluidic system starts to leak at the connection between the Tygon tubing and the stainless needle. The interface allows for easy connection of the AFM chip to the pressure system. To prevent clogging, clean working is advised and little amounts of glue are applied. For dispensing, fresh, clean and filtered liquids are used. Several liquids are used for dispensing: water, diethyl carbonate and a 5% water based glycerol solution. It is observed that diethyl carbonate affects the Tygon tubing. Other liquids that affect the interface are ethanol, isopropanol and acetone and therefore not advised to use in combination with the interface. Little amount of glue should be applied at the slanted edge, to prevent laser blockage. It should be noted that the cantilever is fragile and can be easily broken. The chip is mounted in the front of the holder to assure the cantilever is touching first instead of the clamp of the holder. To use the chip multiple times it is stored at high humidity to reduce the evaporation of water at the tip.

5 — Dosing by varying contact time

5.1 Introduction

Dispensing can be done in several ways, the easiest method is just touching the surface and use the capillary forces to pull the liquid on the substrate. Dispensing small droplets on a surface is interesting in for example DNA spotting [24]. The intention of this experiment is to find the parameters influencing the droplet size. These parameters are manipulated to control the dispensed volume. It also gives a characterization of the systems capabilities and variation in the dispensed droplets. Dispensing is done with three liquids, water, water with 5% glycerol and diethyl carbonate. Water is used because it is an ordinary liquid where a lot of principles are based on. Diethyl carbonate is used because it does not evaporate and has almost the same density as water. Diethyl carbonate behaves a little different then water with respect to surface energies. Therefore also experiments with a 5%, glycerol water based solution are executed. When the cantilever touches a substrate the liquid will be transported via the capillary bridge on the surface, the droplet starts to spread and is pulling more liquid from the cantilever. The process of spreading takes time, therefore experiments with varying contact time on different substrates are performed. On the larger scale when something is pulled fast an additional force is exerted on the object by the inertia of the object. To investigate whether speed of retraction has an influence on the droplet size experiments with varying step size are conducted. Also an experiment using the eigenfrequency shift of the cantilever, used to determine the filling is executed.

5.2 Methods and materials

For dispensing an commercial AFM system (AFM workshop) [69] has been adapted for fluidic applications. The adaption is performed by MA3 solutions. A pressure pump with corresponding software was added. Also a climate controller has been added to increase the lifetime of the droplets. New AFM software was written to incorporate controlled dispensing, further details can be found in appendix A.

Two different AFM chips were used. One with the aperture on the tip of the pyramid and one with the aperture on the side of the pyramid (see figure 5.1 and 5.2). The cantilevers of both chips are the same (see figure 5.3a). The tips depicted show some artifacts, the cantilever in figure 5.1, the hole is fairly big, the tip might be broken off. The tip in figure 5.2 has some residue left around the aperture as a result from the production process. Also on the figure it seems to be the chip is blocked. As these chips were used for imaging a conductive coating is applied and they were not used for dispensing.

As a substrate, a silicon chip from Bioforce Nanoscience was used. The substrate is cleaned in an ultra sonic bath with acetone and rinsed with ethanol, it is finally dried using nitrogen.

To gain information about the dispensing process three different kind of experiments were conducted. The first experiment was approaching with a filled cantilever and only varying the position of dispensing, the second experiment is varying the speed of approach and retracting,

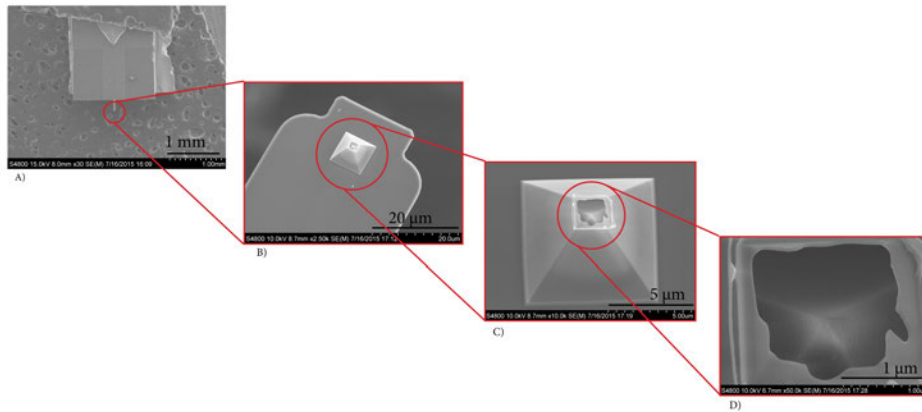


Figure 5.1.: Chip used for dispensing, the hole is on the tip of the pyramid. A) overview , B) detailed view of tip, C) detailed view of the pyramid, D) detailed view of the hole

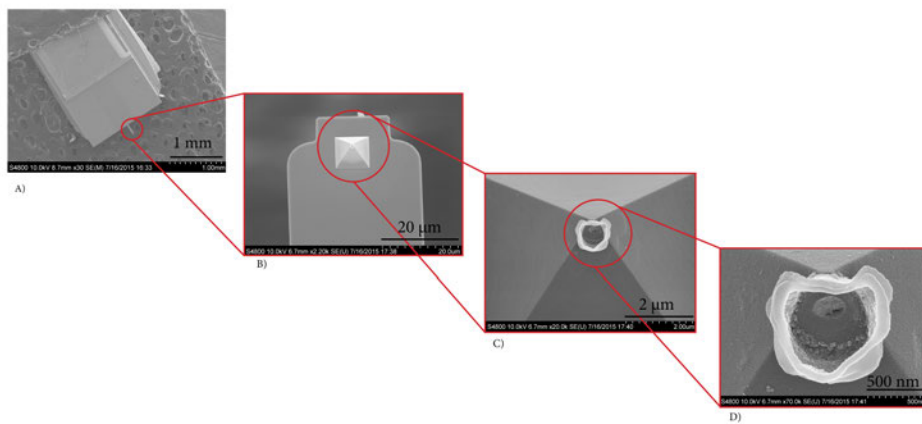


Figure 5.2.: Chip used for dispensing, the hole is on the apex of the pyramid. A) overview , B) detailed view of tip, C) detailed view of the pyramid, D) detailed view of the hole

the third experiment was varying the contact time, because as it takes time for the droplet to spread varying the contact time will create different droplet sizes. For dispensing, two different liquids are used, water and diethylcarbonate. Diethylcarbonate is a liquid with high vapor pressure this increases the life time of the droplet.

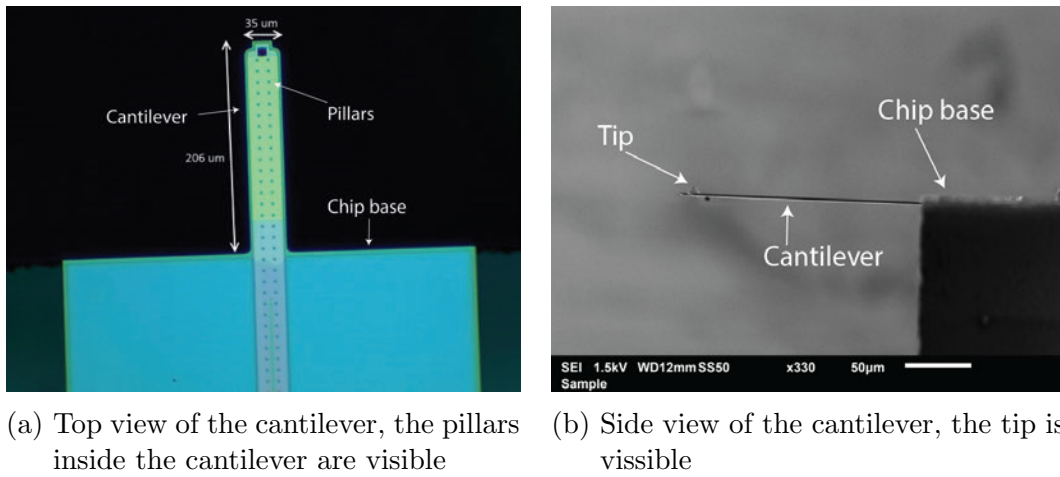


Figure 5.3.: Cantilever used for dispensing

5.3 Measurements and result

5.3.1. Mass weighing based on eigenfrequency shift

To assure the cantilever is filled experiments with the eigenfrequency are conducted (see figure 5.4). When a pressure of 0.07 Bar is applied the eigenfrequency is at 65.5 kHz. When a negative pressure of -0.5 Bar is applied the frequency shifts up to 68 kHz when then again a pressure of 0.07 Bar is applied the eigenfrequency shifts down with 2.5 kHz back to 65.5 kHz again. As expected the added mass of the water will decrease the eigenfrequency. No visible droplet is formed with the applied pressure. At every pressure the eigenfrequency is measured twice and the amplitude is averaged.

A theoretical expression is obtained for a decrease in frequency based on continuum equations (see figure 5.5 and equation 5.1). Where, $\alpha = 1.875$ a constant obtained from the boundary conditions, E is the Young's modulus, $I = I_{\text{solid}} - I_{\text{hollow}}$ moment of inertia, $m_{\text{cantilever}}$ mass of the cantilever and L length of the cantilever. For cantilever details see appendix E. Resulting in a stiffness of 2.26 N m^{-1} which is close to the value given by the supplier of 3 N m^{-1} . The eigenfrequency estimated for an empty cantilever is 86.5 kHz. The measured eigenfrequency for an empty cantilever was 68 kHz. The associated software is given in appendix J Difference can be explained by several reasons. The continuum formulas for solid beams do not describe the behavior of a hollow beam completely, despite the moment of inertia of a hollow beam and the mass of a hollow beam are used. It is also possible the cantilever was not completely emptied by applying negative pressure which would already give a decrease in eigenfrequency. In these calculations also the mass and the added stiffness of the pillars inside the cantilever are not taken into account. Finally there are uncertainties in the measures of the cantilever, because the sizes differ per cantilever because of fabrication process variations and it was not feasible to measure every cantilever.

Based on the channel dimensions (see appendix E) and density of water ($\rho_{\text{liq}} = 1000 \text{ kg/m}^3$) a frequency shift of 6.8 kHz is expected (see equation 5.2 and figure 5.5 b). Where m_{added} is the added mass of the fluid [43]. Based on the continuum formulas for the measured frequency shift an added mass of 1.9 ng is expected (see figure 5.5 c). The added mass based on the channel dimensions is 5.6 ng (see equation 5.3). Inaccuracies are expected due to the uncertainty in the channel dimensions and previous mentioned reasons. The volume of the pillars in the channel is estimated (see figure 5.3a), the diameter used is $2.0 \text{ }\mu\text{m}$ and a height of 950 nm resulting in a volume of $0.1 \text{ pl} = 0.1 \text{ ng}$ for 36 pillars, this is subtracted from the channel based mass so that the calculated mass based on the dimensions of the added water becomes 5.5 ng.

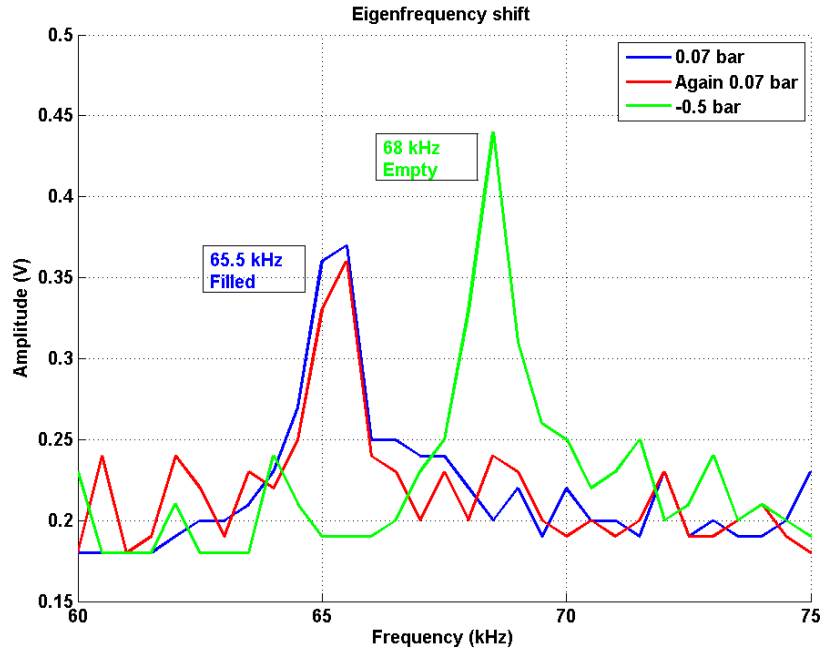


Figure 5.4.: Frequency shift for a filled and empty cantilever

$$\omega_{\text{empty}} = \alpha_1^2 \sqrt{\frac{EI}{m_{\text{cantilever}} L^3}} \quad (5.1)$$

$$\Delta\omega = \alpha_1^2 \left(\sqrt{\frac{EI}{m_{\text{cantilever}} L^3}} - \sqrt{\frac{EI}{(m_{\text{cantilever}} + m_{\text{added}}) L^3}} \right) \quad (5.2)$$

$$\text{Where: } m_{\text{added}} = \rho_{\text{liq}} V_c = \rho_{\text{liq}} AL \quad (5.3)$$

5.3.2. Force distance curve analysis

The breakup height is directly obtained from the force distance curve and this is used as a measure for the volume (see figure 5.7). The curves obtained from dispensing are different compared to curves without dispensing (see figure 5.6). In a dry experiment a vertical line is observed when snapping out whereas in the wet case a more flat curve is obtained. The flat part of the retract curve indicates moving inside the droplet without change in deflection [12]. From these curves the breakup height is determined in the following way: using Matlab the first derivative is determined (see figure 5.8) and I.4. The first time a negative derivative is observed is set as contact and the largest negative derivative is the snap out. The difference between those points gives the breakup height. Which is used in combination with the receding contact angle to calculate the volume of the dispensed droplet (see equation 2.7).

5.3.3. Dispensing diethyl carbonate

Diethyl carbonate is an organic liquid with a lower vapor pressure (1333 Pa) [70] than water (2300 Pa). This assures that the droplets will not evaporate. Diethyl carbonate has a larger affinity with silicon as water, it is observed that the diethyl carbonate has the tendency to spread more. The densities are close for diethyl carbonate (970 kg/m³) and water (997 kg/m³) at 25 °C).

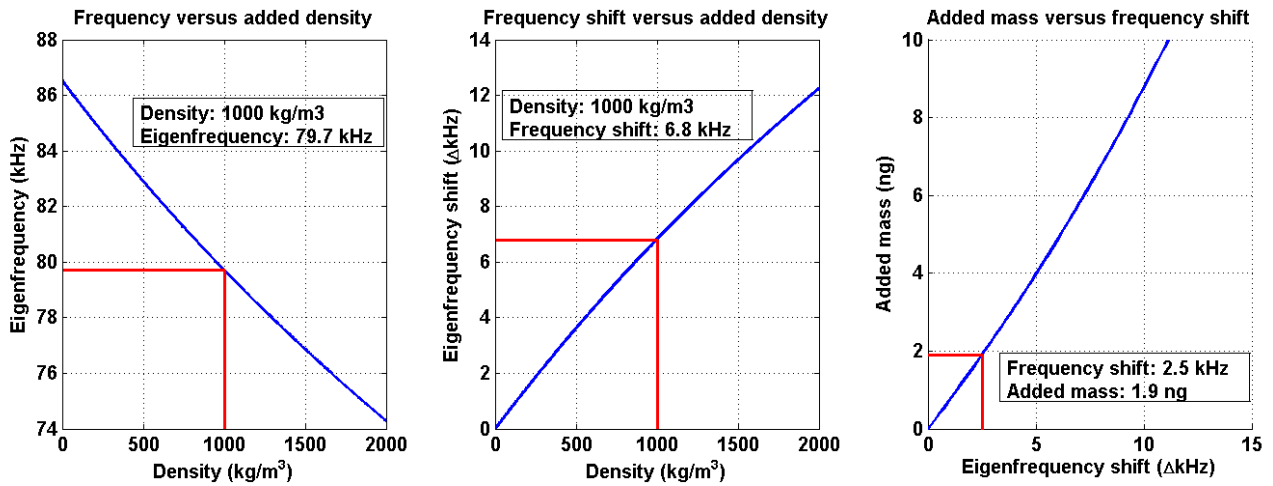


Figure 5.5.: a. Eigenfrequency for different added densities. b. Expected eigenfrequency shift for added densities. c. Added mass for a measured frequency shift

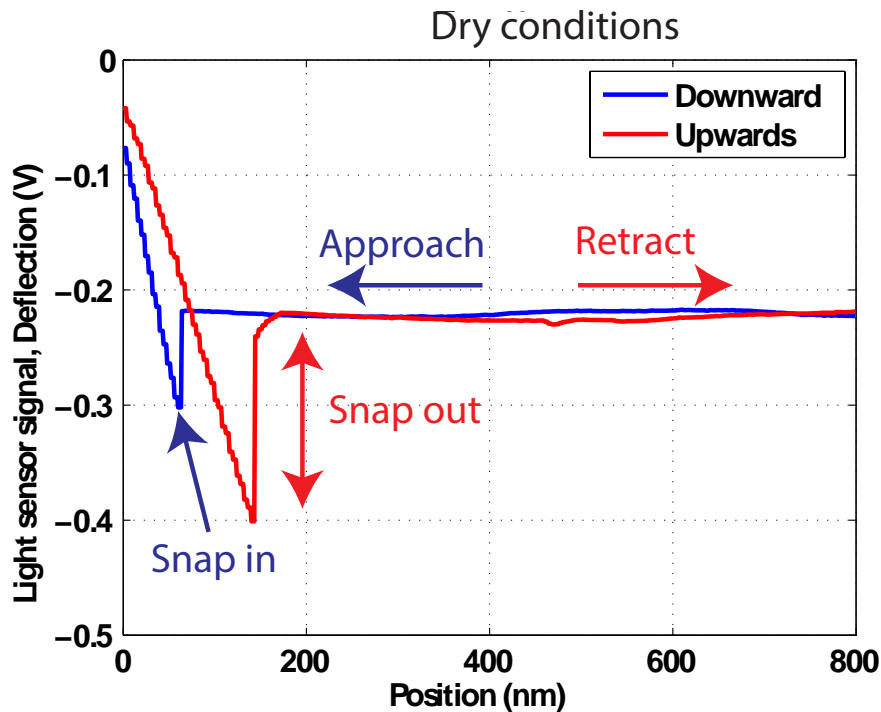


Figure 5.6.: typical force distance curve of a dry experiment

Droplets of diethyl carbonate are dispensed on a silicon substrate. Constant stepsize of 30 nm and no pressure was used for dispensing (see figure 5.9). Droplets form the letters MNE (Micro and Nano Engineering) the department of the research. The spacing between the droplets is 4 μm . Using the breakup height from the force distance curves and the receding contact angle (30.5°) an estimate of the volume is given (see equation 2.7). Using Matlab to count the pixels and with a known pixel to μm ratio the width of the droplets is obtained. The volume is subsequently calculated from the sessile contact angle (30°) and the width of the droplet (see equation 2.10). The results of the top row droplets are given in figure 5.9. In the top row, on average dispensed volume of 0.10 fl with a standard deviation of 0.02 fl is obtained from the breakup height. Using the diameter an average volume of 0.16 fl with a standard deviation of 0.02 fl is obtained.

The volumes of all the droplets are given in figure 5.10. Also a comparison of two different

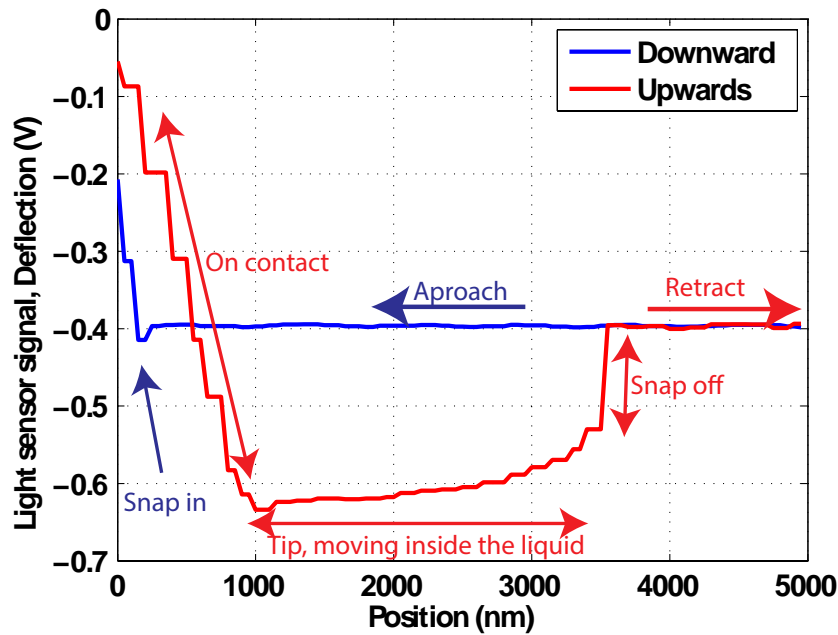


Figure 5.7.: typical force distance curve

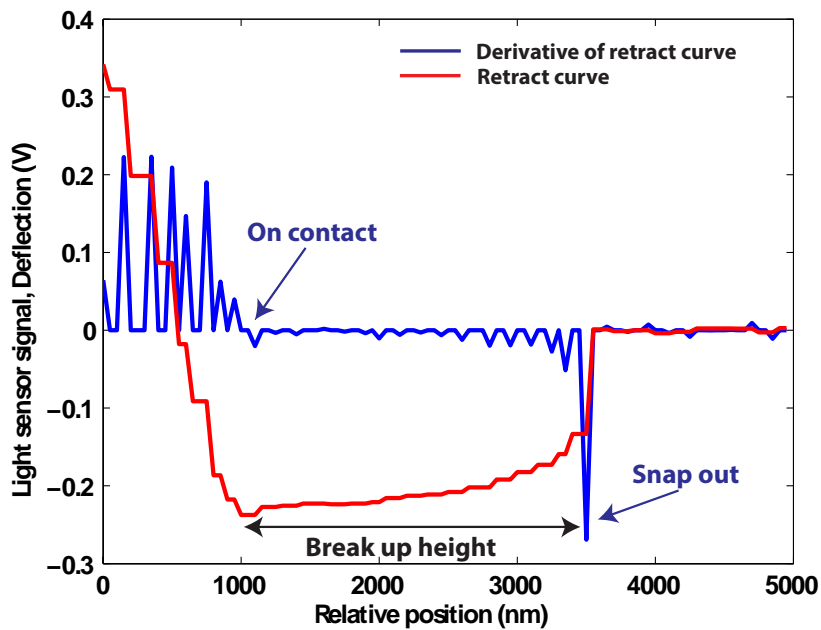


Figure 5.8.: Analysis of force distance curve.

methods of analyzing the volume is given. In blue the volume from the receding contact angle and the breakup height is given and in red the method using a second image analyzing software. The software uses a difference in color to detect the edges and through the detected edges a circle is fitted. The width is calculated from the diameter of the fitted circle. The width is then used in the spherical cap equation to calculate the volumes. From the breakup height the average dispensed volume is 0.085 fl with a standard deviation of 0.028 fl. From the image analyzer an average volume of 0.13 fl with a standard deviation of 0.11 fl is obtained. In this calculation the volume of droplet one is assumed to be an outlier and therefore discarded from the measurement. The volumes obtained from both methods have the same order of magnitude and therefore assumed to be correct.

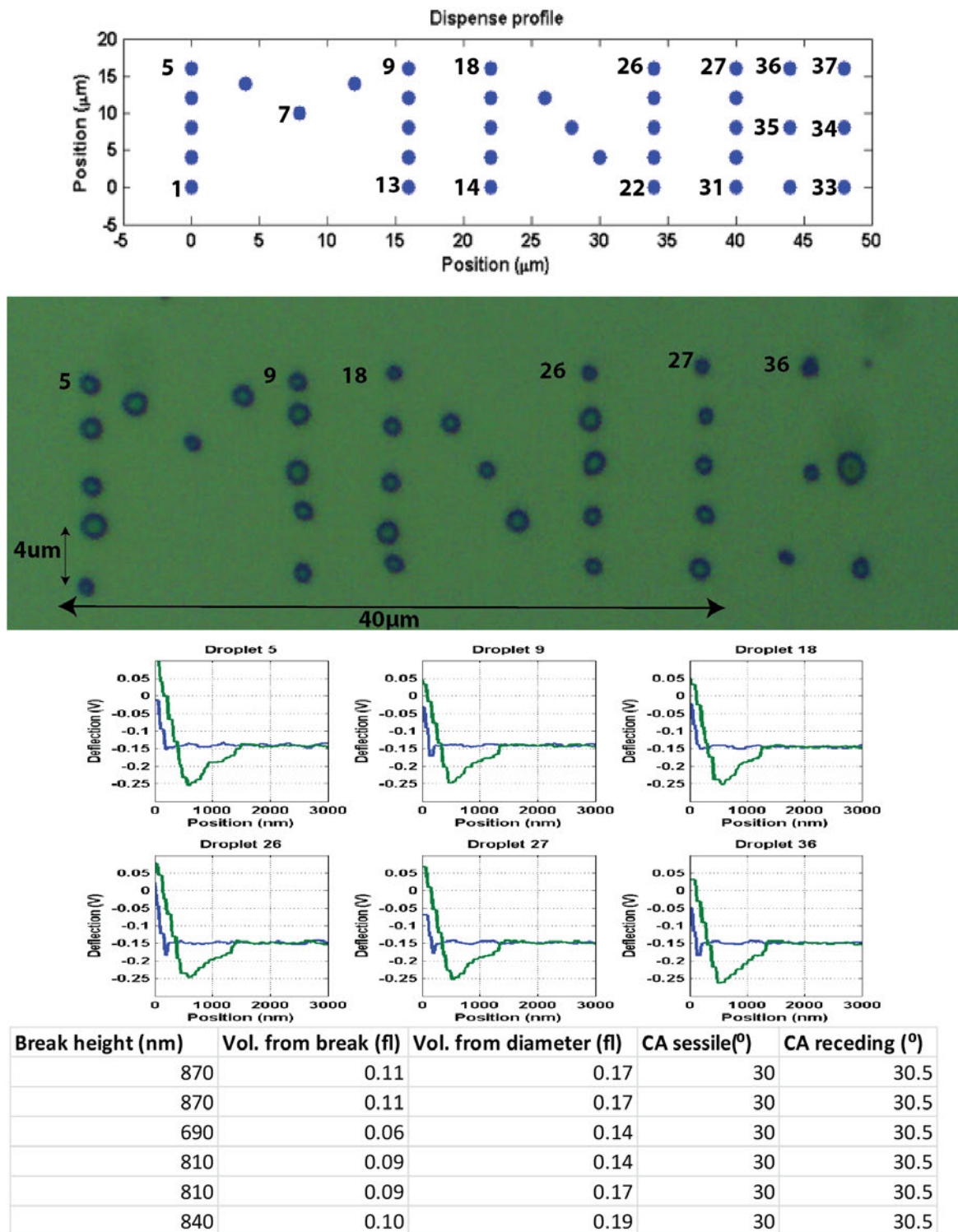


Figure 5.9.: Diethylcarbonate droplets. From top to bottom 1. the profile used for dispensing, the droplets form the letters MNE (Micro and Nano Engineering) 2. The result of the dispense action. 3. Force distance curves of selected droplets. 4. Obtained data from the force distance curves and the optical image.

5.3.4. Dispensing of water

The same experiment is repeated using a different chip for dispensing water (see figure 5.11). Water droplets evaporate almost immediately after dispensing, what is left after dispensing is residue. The residue visible is probably due to the clustering of dirt molecules on the substrate. It is observed that the water droplets have more variation in size than droplets of diethyl

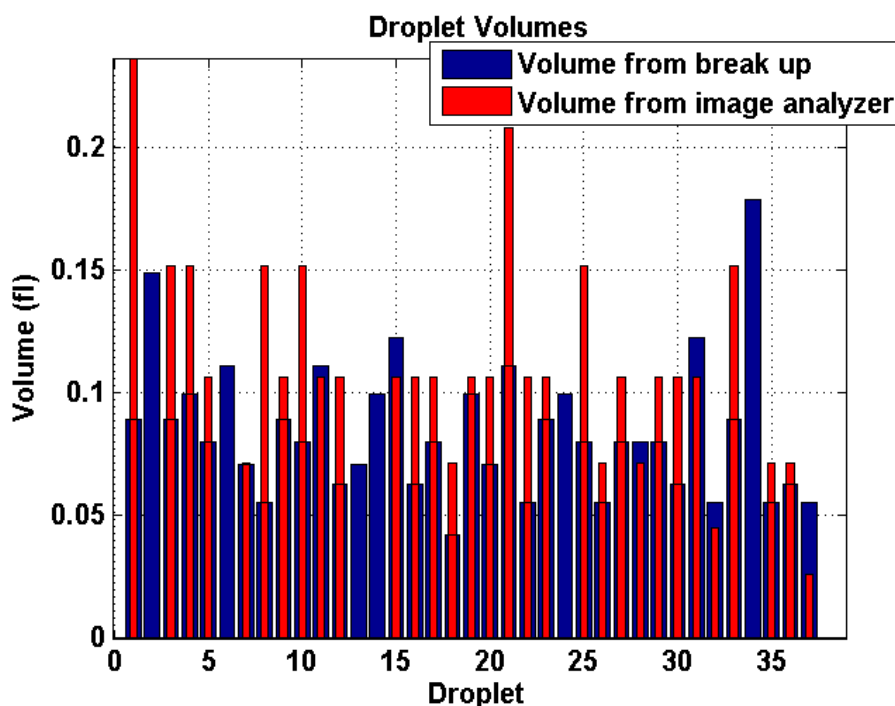


Figure 5.10.: Volumes of dispensed diethylcarbonate droplets comparison between volume from the breakup height and from an image analyzer.

carbonate. The estimated volumes of water from the breakup height are in the same order of magnitude as from the width of the residue. When comparing the values of the sessile volume and the volume from breakup it is observed that the values are better matching than the values from the diethyl carbonate. Probably because water has less tendency to spread the droplets are better defined making it easier to measure the droplets. All the droplet volumes are summarized in figure 5.12. It took about 6 minutes to dispense all the droplets. A step size of 30 nm is used and a settling time of 10 ms.

5.3.5. Dependency on previous approaches

In a different experiment, water is dispensed and the breakup height is plotted over time (see figure 5.13). A step size of 30 nm is used. After several experiments the substrate was out of range. Presumably the substrate is slightly slanted and when approaching at the lower side the substrate is further away. Subsequently a calibration step was executed to find the substrate again. During operation a contact time of 10 ms is used the minimum of the system, during calibration the tip makes a longer contact with the substrate. Presumably the surface forces then create a droplet on the tip. During the next steps each time the tip touches some liquid is released but the contact time is not long enough for the surface forces to replenish the droplet on the tip. To be able to properly dose a droplet it should be known what happened previous with the cantilever.

5.3.6. Step size variation

To see whether speed of approaching and retracting has influence on the droplet size the step size is varied so the tip is retracted faster. When pulling with larger speed the moment of inertia can cause a change in droplet size. In the first experiment the step size is varied in an decreasing manner making it slower and in the second experiment in an increasing manner making it faster (see figure 5.14). Both experiments use diethyl carbonate for dispensing. Despite the

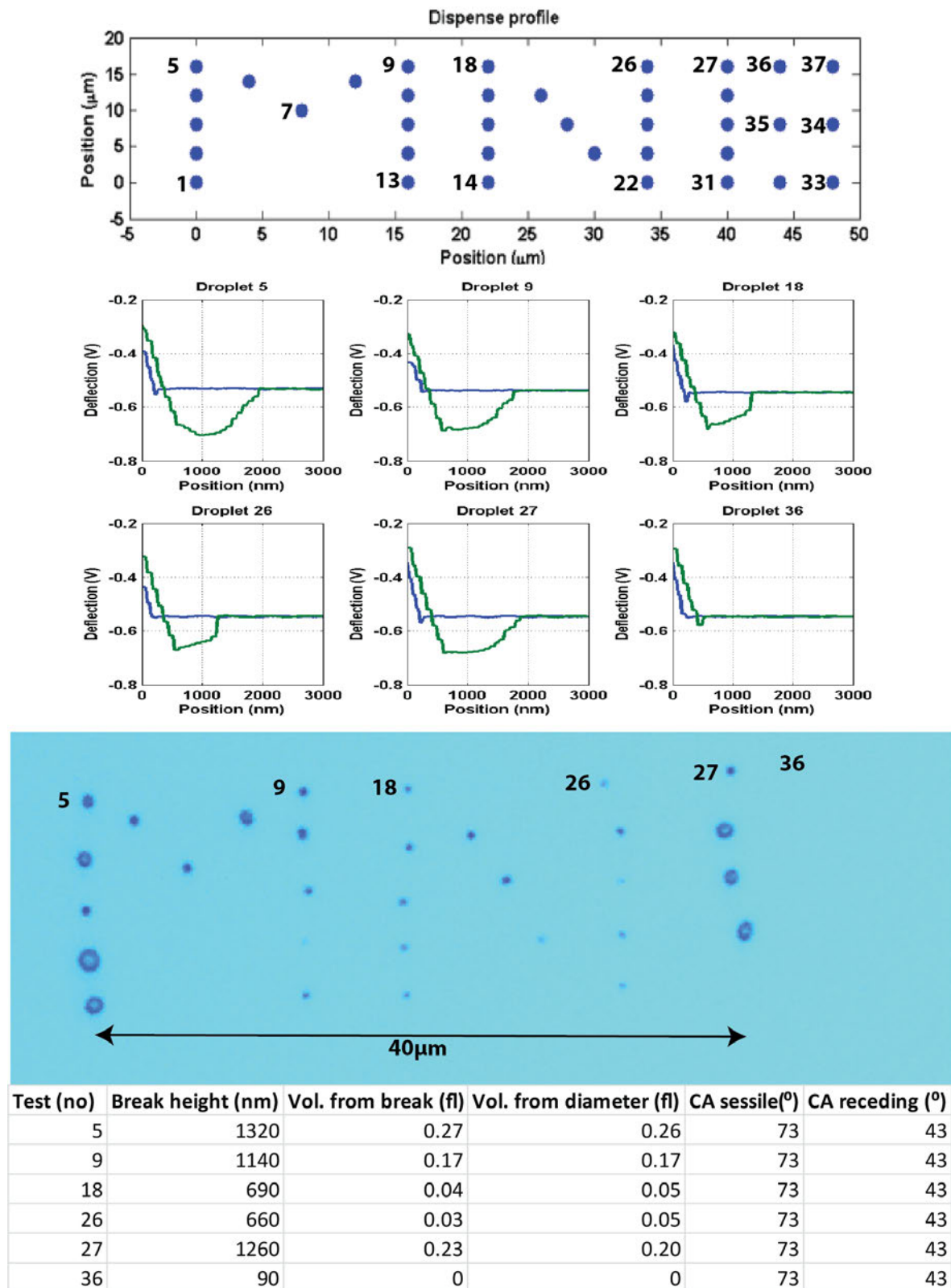


Figure 5.11.: Residue of dispensing water. From top to bottom 1. the profile used for dispensing, the droplets form the letters MNE (Micro and Nano Engineering) 2. Force distance curves of selected droplets. 3. The result of the dispense action. 4. Obtained data from the force distance curves and the optical image

large difference (factor 10) in volume observed between the experiments no dependence on the step size is found. Therefore dispensing will be a trade off between speed and resolution of the force distance curve. With increasing step size the resolution goes down.

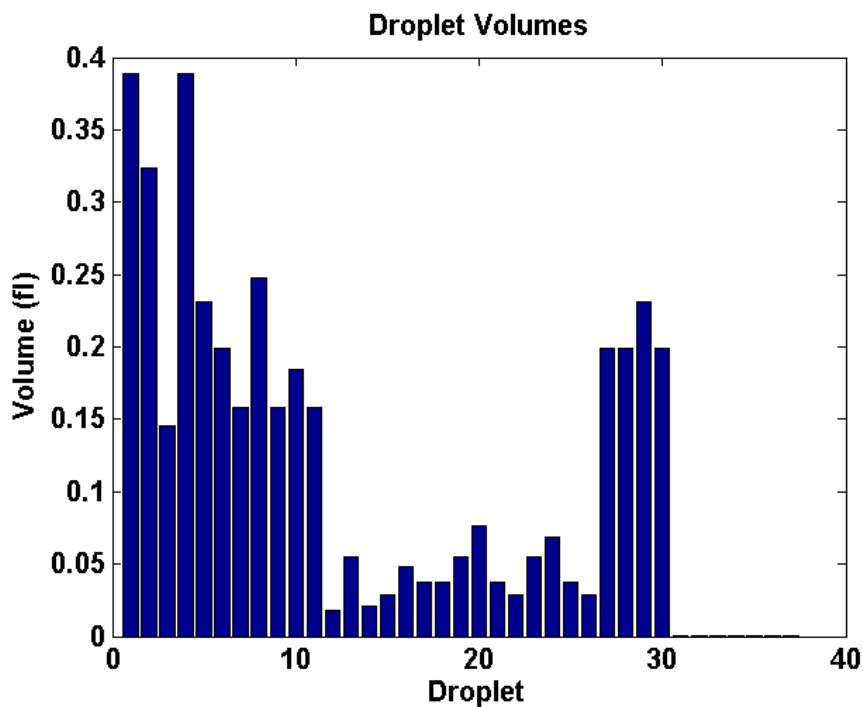


Figure 5.12.: Volumes of dispensed water droplets based on distance distance curves

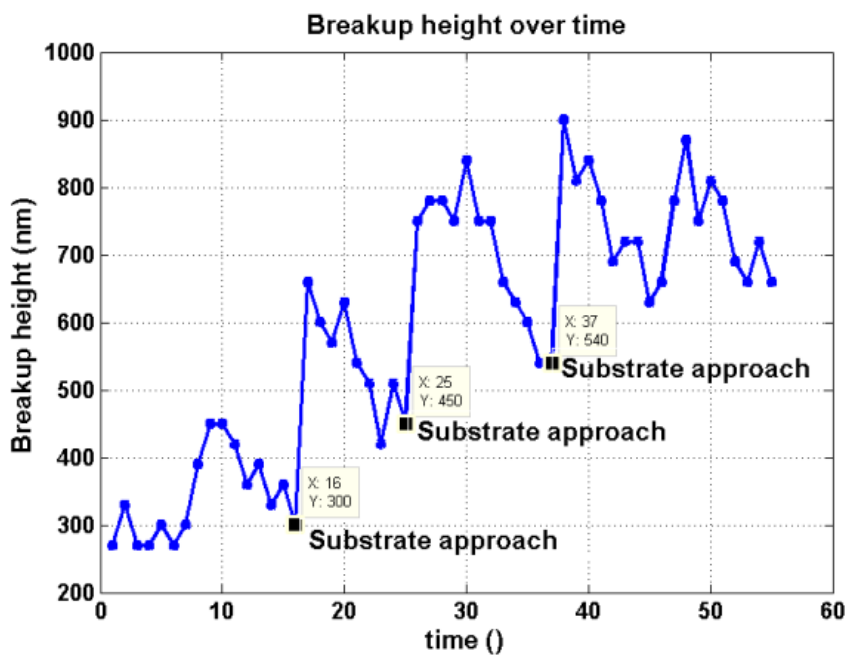


Figure 5.13.: Breakup height over time. After a substrate approach a large breakup is observed which decreases with number of experiments

5.3.7. Contact time variation

To have less influence of the surface forces and the dependency of previous approaches the substrate and the cantilever are silanized to make it more hydrophobic. Functionalization of the cantilever [71] and the substrate is performed the same way as described in section 2.2.2, only now leaving it exposed longer so a homogeneous mono layer is created. This resulted in a receding contact angle of 50.5° . To prevent water from evaporation 5% glycerol is added. An array of 4x4 droplets is created the and the average volumes of each contact time are given

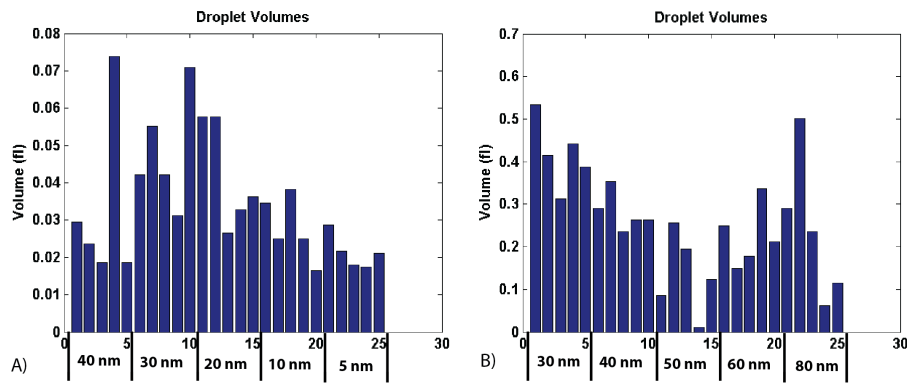
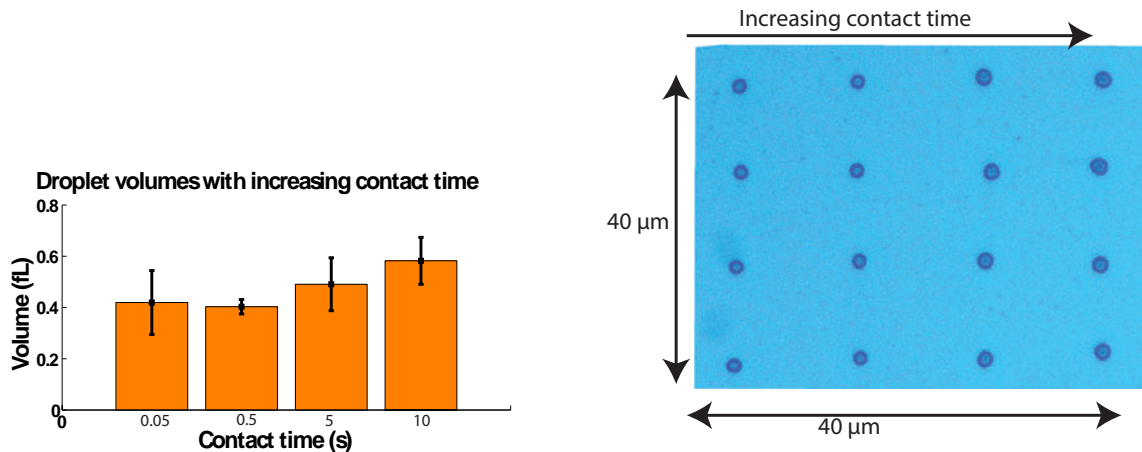


Figure 5.14.: Volumes of the diethyl carbonate droplets for varying step size. Stepsize is given below the figure after 5 experiments the stepsize was varied. A). Decrease in step-size B). Increase in stepsize. Between the experiments there is a large difference in volumes

in figure 5.15a and the dispensed result is given in figure 5.15b. The contact times for the 4x4 grid are 0.05, 0.50, 5.00 and 10.0 seconds and the 6x6 grid 0.02 0.05 0.50 5.00 10.0 and 15.0 seconds. With increasing contact time an increase in droplet size is observed as expected. Droplet volumes increase from around 0.4 fl to 0.6 fl with an average variation of 0.09 fl.

Also an array of 35 droplets is created with varying contact time. The dispensed volumes are given in figure 5.16a and the corresponding dispensed result is given in 5.16b. The droplets are dispensed on a area of 50x50 μm . The spacing in between the droplets is 10 μm . The contact times are 0.02, 0.05, 0.5, 5, 10 and 15 seconds. The droplet volumes are given in appendix F. The trend of increasing droplets is visible but no clear conclusion could be drawn.



(a) Volumes of 5% glycerol droplets in relation to the contact time (b) Dispensed result 5% glycerol on a substrate with contact angle of 50.5°

Figure 5.15.: Result of dispensing a 4x4 grid using varying contact time

5.4 Discussion

5.4.1. Volume calculation

Droplets of water and diethyl carbonate are dispensed. Droplet sizes are not constant and are quite hard to control especially on the more hydrophilic surfaces. Droplets dispensed with only surface forces are large. Often the droplets both from diethyl carbonate and water are so

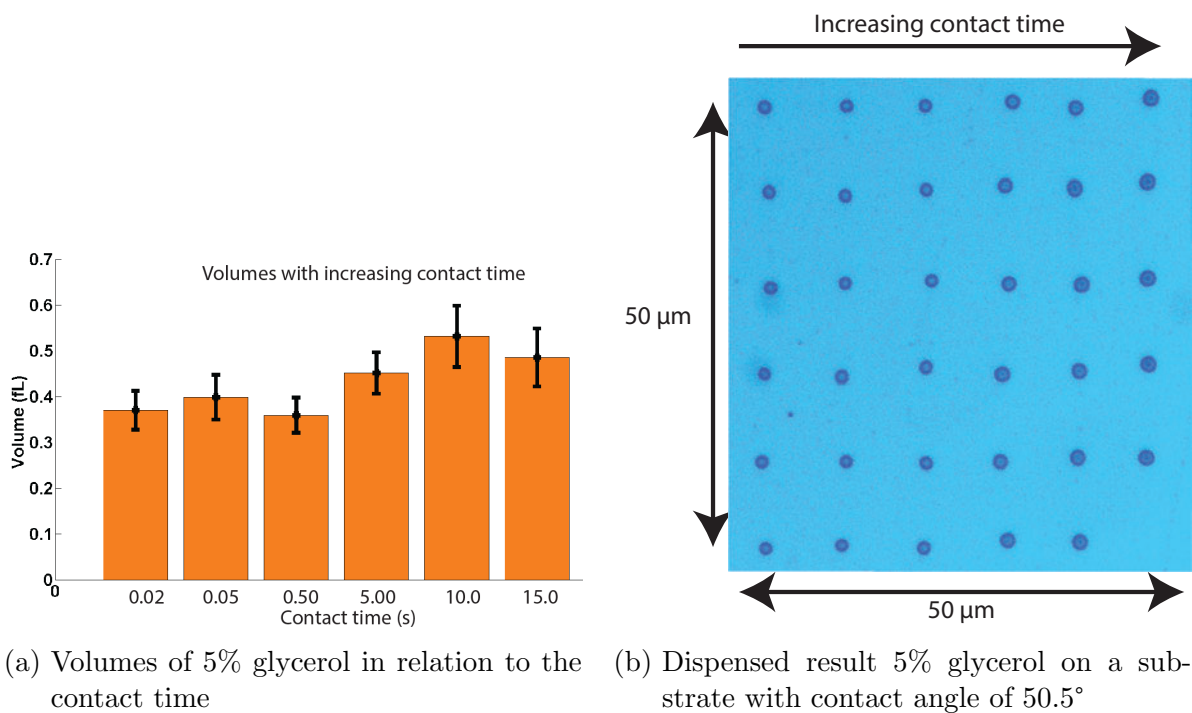


Figure 5.16.: Result of dispensing a 6x6 grid using varying contact time

large no snap out was observed during the measurement. A retract height of 2500 nm is not enough for these droplet sizes. The method used to get better controllability of the dispensing is functionalization of the substrate and the cantilever. The surface energy is reduced and becomes therefore more hydrophobic. The droplets have then less tendency to spread and therefore droplet sizes are more constant. It is also better defined where the liquid is coming from because it does not have the tendency to wet the cantilever.

When snap out did occur a calculation of the volume based on the breakup height and the receding contact angle could be performed. Volume calculation from the breakup height is a relative easy method. The obtained volume is in good comparison with the obtained volumes from the image analyzer. Especially with water where on average 0.01 fl difference is observed whereas with diethyl carbonate an average difference of 0.07 fl is observed.

Dispensing of droplets is dependent on the previous droplet. It was observed after a longer contact the breakup height increased dramatically. To minimize this behavior and reduce the variance in volume, the cantilever and the substrate are functionalized to decrease the surface energy. The average variation in dispensing the 35 grid is 0.05 fl (see figure 5.16b) whereas the variance in the MNE dispensing with water is 0.11 fl (see figure 5.12).

5.4.2. Force distance curves

The force distance curves do not look the same as in experiment without water. In dry measurements there is a clear snap off indicated by a vertical line. Probably because the tip of the cantilever is moving through the droplet, a bathtub shape is observed during the retracting (see figure 5.8).

The cantilevers used have some problems, the tip shown in figure 5.1 and 5.2 show that some kind of residue is left around the aperture. This residue is probably some silicide left from the microfabrication process. A new cleaning procedure should resolve this problem.

5.4.3. Clogging

During the experiments quite a lot of clogging occurred, making the chips unusable. It is observed that dispensing with filtered water less clogging occurred and the chip could be used with proper storing up to a month. The filter is a 0.02 μm syringe filter. Dispensing with diethyl carbonate resulted eventually in clogging even with filtered liquid. Diethyl carbonate reacts with the tubing because tubing becomes hard after staying in contact with the liquid. It is supposed that, this can cause clogging of the cantilevers because particles can be released by the reaction which can travel with the liquid to the aperture.

5.4.4. Weighing

Proper filling can be checked using the eigenfrequency. When a cantilever is filled with a liquid the eigenfrequency is shifted down because mass is added. Successfully a shift is observed when negative pressure was applied to empty the cantilever. The eigenfrequency shifted back to its original position when pressure again was applied. The added mass is calculated based on the eigenfrequency shift and on the dimensions of the cantilever. Based on the dimensions and the density of water a frequency shift of 6.8 kHz is expected whereas an frequency shift of 2.5 kHz is observed. Based on the measured frequency shift an added distributed mass of 1.9 ng is expected whereas based on the dimensions of the channel a mass of 5.5 ng is expected. Inaccuracies are expected because it is not granted that the cantilever was completely emptied with the negative pressure. Also some inaccuracies can come from the modeling, the mass and the stiffness of the pillars inside the cantilever are not taken into account which can result in a lower eigenfrequency by the added weight. The added stiffness would increase the eigenfrequency, also the stiffness of pressurizing of the water are is not taken into account.

5.4.5. Light interference

When observing the images of the droplets (see figure figure 5.15b and 5.16b) a black center dot is observed in the right row whereas in the left row no dark dot is observed. Probably the difference in height gives another interference pattern of the light. The left row of droplets are smaller, having constructive interference and giving a light center dot. The droplets on the right have destructive interference resulting in a dark center dot. Based on the breakup height there is 225 nm height difference which is around half of the wavelength of blue light and therefore different interference patterns are expected.

5.4.6. Liquid properties

The force distance curves of diethyl carbonate and water are compared. For two droplets with approximately the same breakup height resp. for diethyl carbonate 810 nm and for water 780 nm the force distance curves are given in 5.17. It is observed that the slope, of when the cantilever is moving through the droplet, is steeper in the case of diethyl carbonate dispensing. It seems that it is more easy for the cantilever to move through diethyl carbonate than through water. The cantilever is already starting to deflect back to its original state whereas in water the cantilever keeps a more constant deflection throughout the movement. The viscosity of diethyl carbonate (0.749 mPa s) [72] is lower than the viscosity of water (0.894 mPa s). A lower viscosity indicates that it is easier to move through and therefore the cantilever can already start to deflect back.

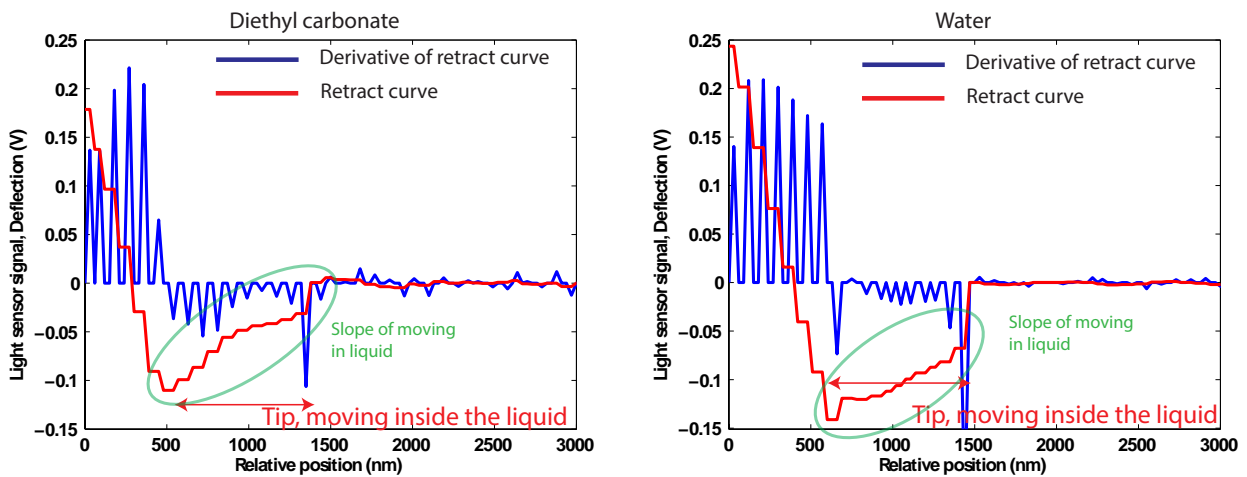


Figure 5.17.: Force distance curves of diethyl carbonate and water, the slope, of when the tip is moving inside the liquid, is steeper for diethyl carbonate

5.5 Conclusion

Different droplets sizes are dispensed using three different kind of liquids. A glycerol solution and diethyl carbonate are used to reduce the influence of evaporation. An experiment of filling the cantilever is conducted. Using negative pressure to empty the cantilever. An added mass of 1.9 pg based on the frequency shift is found. Droplets are dispensed using a commercial available AFM system which is adapted for fluid applications. Droplet sizes are dependent the contact time. As the contact time increases the droplet size increases. It is difficult to predict the droplet size but with calibration and dispensing with a functionalized cantilever it is possible to dispense droplets in the femto liter range with 0.05 fl variance.

Also some behavior, dependent on the previous experiments is found. Especially when dispensing on a more hydrophilic surface, the droplet volumes are variating a lot. The volumes are calculated from the breakup height and the receding contact angle. The volumes obtained from the breakup height match with image analyzing software especially when dispensing with water.

6 — Dosing by varying applied pressure

6.1 Introduction

One of the advantages of the MA3 system compared to the DPN [13] technique is the ability to control droplet sizes with pressure. The liquid reservoir can be pressurized using a pressure source. Advantages of dispensing with pressure is that larger droplets can be created than possible with only surface forces. When a droplet does not like to be on a surface it can be forced onto the surface by using pressure. Also additional pressure is needed when dispensing inside a liquid because the surface forces do not exist. A biological cell is filled with fluid so when dispensing inside a cell also additional pressure is needed [19]. Pressure is applied on the liquid via tubing and the fluidic interface. The pressure comes from a compressed air source and is controlled via valves by the computer. The goal of this experiment is to find a relation between applied pressure and the droplet size. Surfaces with different surface energy are used to dispense water droplets on. With the proposed method of calculating droplet volumes from the breakup height the droplet sizes are investigated. Theory is as well studied to support the experiments.

6.1.1. Theory

Using the electrical analogy the fluidic system can be modeled. For an increase in hydronic resistance the flowrate is reduced. Also when pressure is reduced the flowrate reduces. The flow rate Q is described by equation 6.1. Where R_{hyd} is the hydronic resistance and ΔP the pressure applied on the reservoir. Therefore the time the pressure is applied and the amount of pressure influences the droplet size. The hydronic resistance is dependent on the dimensions of the fluidic system and the dynamic viscosity μ of the liquid (for water $\mu = 8.9 \times 10^{-4} \text{ Pa}\cdot\text{s}$). The resistance of the cantilever is calculated by equation 6.2. Where L is the length of the channel (1706 μm), w the width (30 μm) and h the height (1 μm). Resulting in $6.2 \times 10^{17} \text{ Pa}\cdot\text{s}/\text{m}^3$ which is in the same order of magnitude as calculated by Ghatkeser et. all. [44] where a hydrodynamic resistance is obtained of $3.3 \times 10^{17} \text{ Pa}\cdot\text{s}/\text{m}^3$. The resistance of the tubing is calculated by equation 6.3. Where R is the inner radius of the tube (0.18 mm) and L_t the length of the tubing (40 cm). The resistance of the tubing is $6.5 \times 10^{11} \text{ Pa}\cdot\text{s}/\text{m}^3$ which is 6 order of magnitude smaller than the resistance of the cantilever and is therefore neglected. For a pressure of 0.2 bar and a time of 0.5 seconds the estimated dispensed volume is 0.16 pl.

$$Q_R = \frac{\Delta P}{R_{\text{hyd}}} \quad (6.1)$$

$$R_{\text{hyd rect}} = \frac{12\mu L}{h^3(w - 0.63h)} \quad (6.2)$$

$$R_{\text{hyd circ}} = \frac{8\mu L_t}{\pi R^4} \quad (6.3)$$

6.2 Methods and materials

6.2.1. Liquids

Droplets of water and a mixture of water with 5% glycerol are dispensed. Water is used because a lot of applications use water based liquids. Water has the disadvantage it will almost immediately evaporate when dispensed, diethyl carbonate does not evaporate because it has a low vapor pressure. Diethyl carbonate behaves different on the substrate as it has the tendency to wet the surface. To obtain a liquid which behaves the same as water and also has a lower evaporation rate, glycerol is added to the water. The glycerol reduces the evaporation of the water so the lifetime of the droplets are increased.

6.2.2. Substrate

Two different substrates are used for dispensing the first substrate is bare silicon with a receding contact angle of 41° . The second surface is made more hydrophobic by functionalizing the silicon. For the functionalization octyltrichlorosilane ($C_8H_{17}Cl_3Si$) is used the procedure is described in section 2.2.2 only now they are exposed longer to obtain a uniform mono layer. The functionalization resulted in a receding contact angle of 50.5° . The cantilever is as well functionalized so the water does not wet the cantilever and only comes from the tip.

6.2.3. Calculation

Assuming a certain shape of droplet the volumes are calculated using the contact angle and the breakup height obtained from the force distance curves. The assumed shape is given in figure 2.2. Using the derivative the on contact point can be found as the first negative derivative and the snap out is the largest negative derivative (see figure 5.8). Linking those points to the retract height, the break up height can be obtained automatically using Matlab (see appendix I.4).

6.2.4. Pressure control

The AFM system used is a commercial available AFM from AFM workshop. The system is adapted for fluidic applications. Also a pressure controller is added. The system uses compressed air as pressure source. By controlling valves the applied pressure on the liquid is controlled. Using the Venturi effect an under pressure can be created. Using this under pressure aspiration of droplets is shown, for further details of the system see appendix A.

6.3 Results

6.3.1. Dispensing with negative pressure

Different experiments are executed subsequently (see figure 6.1a and figure 6.1b). First an approach was executed and then from 9 to 11 experiments without pressure were conducted. No snap off occurred indicating large droplets. The force distance curves are given in appendix G Snap off was forced by moving the substrate. Next a negative pressure of -0.8 bar is applied in experiment 12 to 16 and snap off is observed. Droplet sizes of around 0.1 fl were dispensed. Next no pressure was applied and droplets of 2.3 fl were dispensed. With the experiments an increase in droplet size is observed. The droplets became so large (after droplet 26) snap off could no longer be enforced by moving the substrate. The droplet was dragged over the substrate resulting in several small droplets. This indicates that the system is not able to dispense on a hydrophilic surface.

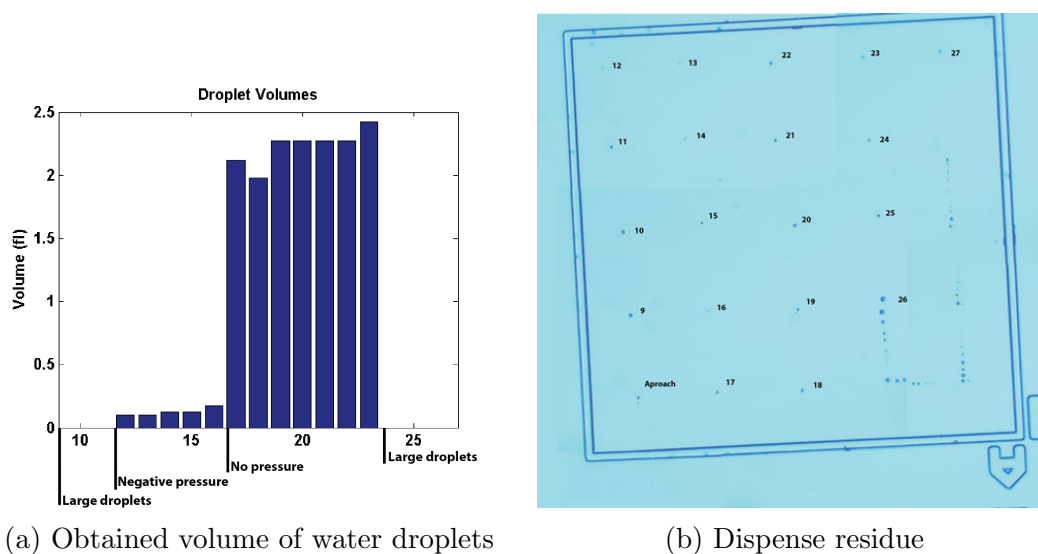
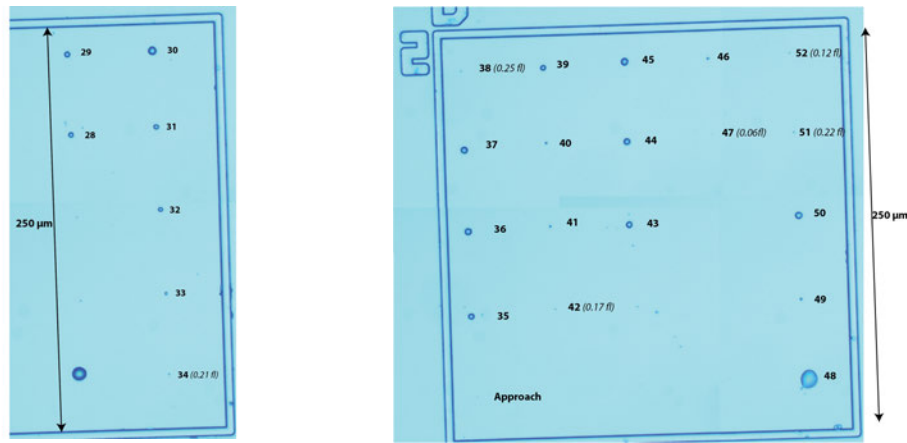


Figure 6.1.: Residue after dispensing water on clean silicon. Experiment 9 to 11 were without pressures but no snap out was observed during force distance curves. Experiment 12 to 16 were performed with constant negative pressure (-0.8 bar) on the fluid and experiment 17 to 26 were performed with no pressure. Between 26 and 27 there was a droplet on the tip and the cantilever was dragged over the surface

6.3.2. Startup behavior

Initially a large droplet of water is created using pressure (see figure 6.2a). If no snap off was observed then it is enforced by moving the substrate after the approach. Subsequently several approaches are made until snap off during the measurement is observed. Snap off is observed when the retracting line is back at the base line. In experiment 28 a droplet is created using 2.4 Bar. No snap off was observed indicating a droplet which was too large for the system. In experiment 29 to 34 a pressure of 0.4 bar is applied. Snap off during the measurement is finally found at experiment 34. Then the volume can be calculated from the force distance curve. The dispensed volume is 0.21 fl. The corresponding force distance curves are given in appendix G.

In experiment 35 to 52 initially a pressure of 2.4 bar is applied and subsequently no pressure is applied (see figure 6.2b). It is observed it takes several steps until snap off can be observed during the measurement. These measurements were taken with a retract height of 2500 nm, When dispensing with arrays the retract height is set to 5000 nm.

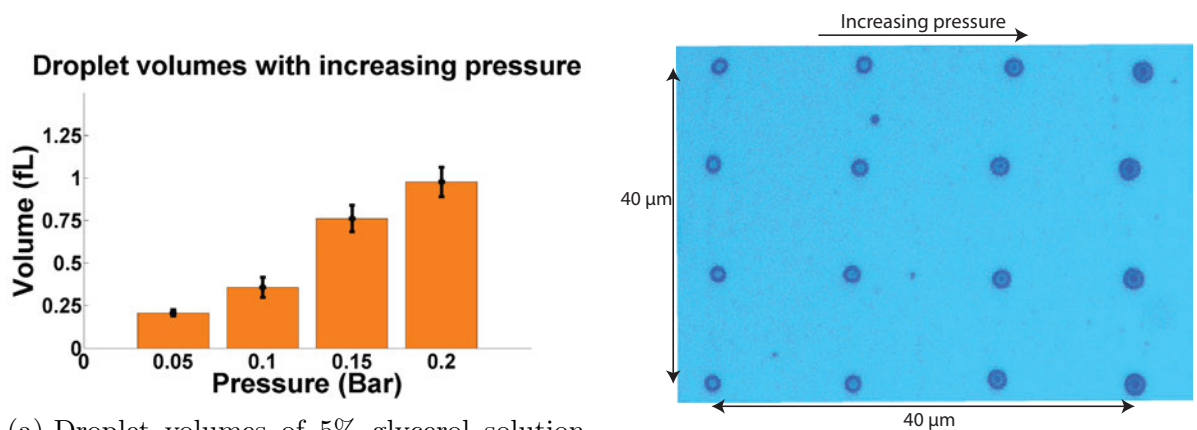


(a) Dispense residue 2.4 bar subsequently 0.4 Bar (b) Dispense residue 2.4 bar subsequently 0 Bar

Figure 6.2.: a. Experiment 28 a large droplet was created using 2.4 bar. Following experiments (29 to 34) a pressure of 0.4 bar is applied. b. Experiment 35 a droplet was created using 2.4 bar next (36 to 37) no pressure is applied. In 39 a droplet is created using 2 bar, next (40 to 42) no pressure is applied. In 43 and 48 droplets are created using 2.4 bar and subsequently no pressure is applied. It is observed the droplet size decreases with number of experiments

6.3.3. Dispensing functionalized surface

A 5% glycerol solution is dispensed on a functionalized surface. With the functionalization less startup behavior is observed. Also the tip is functionalized to reduce the wetting of the cantilever. The pressure is varied between 0.05 Bar and 0.2 Bar. It is observed that with increasing pressure the droplet size increases (see figure: 6.3a and figure 6.3b). Droplet sizes start around 0.2 fl and increase up to 1 fl with an average variation of 0.06 fl. The droplet volumes are given in appendix F.



(a) Droplet volumes of 5% glycerol solution with varying pressure (b) Dispensed result on functionalized surface

Figure 6.3.: Obtained result of dispensing with pressure and 5% glycerol solution

6.4 Discussion

When negative pressure is applied still some droplet could be dispensed. This droplet was much smaller as when dispensing using no pressure. Dispensing with extra pressure is not useful on

the bare silicon substrate as the droplets were already so large no snap off was observed. Additional pressure may be useful for dispensing on substrates with high surface energies. It may also be useful for dispensing inside liquid because there no surface forces exist. When dispensing on bare silicon startup behavior is observed. When a large droplet is created several steps are needed until snap off is observed.

When dispensing on a surface with higher surface energy and using a hydrophobic needle a direct relation is found between the droplet size and the pressure (see figure 6.4). With increasing pressure larger droplets are dispensed. Based on the theory (see equation 6.1) the hydronic resistance of the system is constant therefore a pressure difference is linear related to the flow rate and because time of the applied pressure is constant an increase in pressure would result in a linear increase in volume. During the experiments the contact time is kept constant, therefore the average volumes describe a linear relation. The estimated volume from the theory over estimates the dispensed volume by a around a factor 100 probably because the resistance is under estimated. Only the cantilever resistance is taken into account, the orifice, chip, interface and tubing resistance are not considered as well the pillars inside are not considered. Approximately the same variation is observed as when dispensing with contact forces (0.05 fl) as when using pressure (0.06 fl).

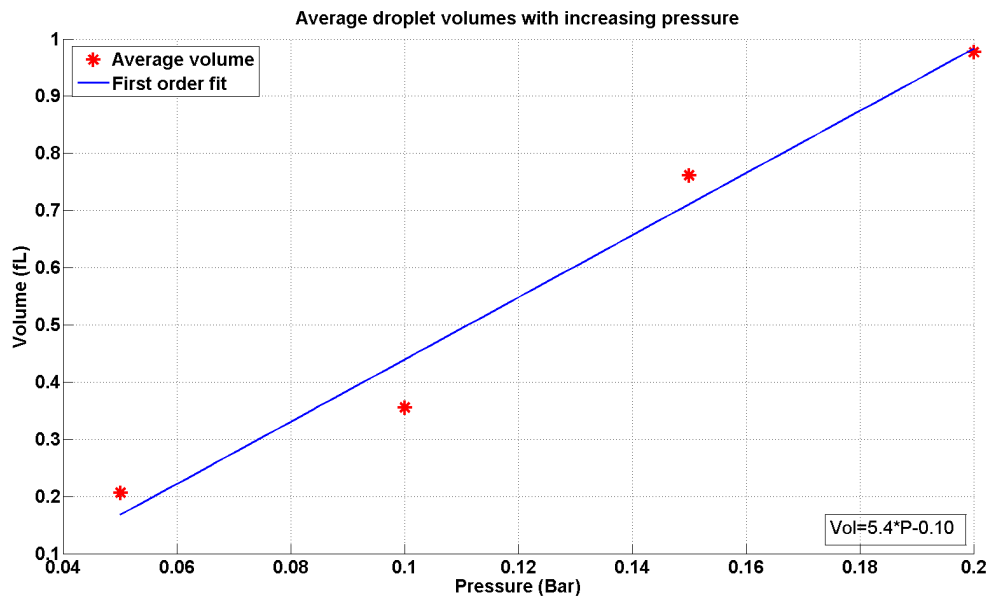


Figure 6.4.: Average volume with first order fit

For proper control of the droplet size a surface needs to be characterized. A hydrophobic surface helps to dispense smaller droplets. When the contact time and the pressure are identified droplets of a defined volume can be dispensed. Using the receding contact angle and the breakup height the volumes can be calculated.

The largest droplet which can be dispensed should be around the 7 fl because the maximum retract height is around 4 μm . The minimum droplet size which are dispensed are around 0.2 fl. Smaller droplets should be possible using a hydrophobic surface and negative pressure. A smaller tip hole can also reduce the droplet size [12]. Disadvantage of smaller droplets is that they are more difficult to see.

For an increase in life time of the droplets the humidity might be increased, then pure water can be dispensed. Still the residue left needs to be identified and removed other wise it is difficult to be sure really water is left, then also experiments to determine the evaporation rate can be conducted.

6.5 Conclusion

The results shown in this chapter demonstrate the relation between the droplet size and the applied pressure. To minimize wetting during dispensing a functionalized surface and needle were used. Using the break up height and the receding contact angle the volumes the droplets can be calculated. With increasing pressure larger droplets are dispensed, as expected from the theory a linear relation between droplet volume and pressure is found. Droplets are dispensed with an average variation 0.06 fl. Nevertheless, further experiments are needed to increase the robustness of the system. For controlled dispensing, several calibration steps are needed until the desired volume is reached, using then the corresponding pressure and contact time the desired droplet sizes can be dispensed.

7 — Conclusion

This thesis contributes to the ability of gaining control on the dispensing and aspiration of droplets in the femto liter range. Therefore, first a literature study was performed to investigate what kind of experiments have been performed in the past and what kind of knowledge was already available. Three applications of dispensing using hollow cantilever AFM are discussed in this chapter: single cell manipulation, DNA spotting and gluing of graphene. Additionally, the different kinds of dosing are categorized in three fields and discussed in this thesis: dosing using a predefined volume, controlling flow rates and contact printing. For AFM dispensing, controlling of the flow rate and contact printing are important as these principles are used to dispense. The parameters influencing the dispensing and how they can be controlled to manipulate the droplet size were investigated. By systematically varying the contact time and the pressure different sizes of droplets can be dispensed.

Receding contact angle set up

The objective of this chapter was to find parameters that are important when calculating the volume of the dispensed droplets. Two parameters have been identified: using the breakup height and the measured contact angle the volume can be calculated.

A contact angle is defined as the angle of the tangent to a droplet at the interface of liquid, vapor and solid. A contact angle can be present in two different forms: a droplet at rest, which is called the sessile contact angle, and the contact angle when a droplet is pulled, also referred to as the receding contact angle. A system was build to measure the receding contact angle using a retracting needle. Additionally supplementary software was created in Matlab to detect the edges of the droplet. The detected edges were then used to calculate the contact angle.

When dispensing with an AFM, a droplet is pulled from the substrate by the AFM tip, then the moment of breakup is detected and the breakup height is obtained. The droplets dispensed with this contact angle measurement system were small enough that gravity does not have an influence and the contact angle is only defined by the surface forces. Therefore the contact angle measurement is considered to remain constant when going to the smaller scale.

Humidity control for femto liter droplets

For understanding the effect of relative humidity on the breakup height experiments are executed. An experiment using the AFM system to measure the breakup height with varying relative humidity is performed. A trend is observed, with increasing humidity an increase in breakup height is obtained. Large spread in breakup height is observed when the climate controller is switched on. When measuring without climate controller an average breakup height of 82 ± 5 nm is obtained. The PID parameters of the climate controller need to be tuned to obtain a more stable climate. To reduce turbulence induced by moving people the system can be covered with a casing.

An attempt is made to visualize the liquid bridge using a environmental scanning electron microscope but no capillary condensation was visible. For visualization the pressure should be

increased or the temperature should be reduced.

Design of a fluidic interface

To enable dispensing with the AFM system, the AFM chip needs to be connected to the liquid reservoir and the pressure system. To ensure a leak free connection a microfluidic interface was designed and fabricated with a 3D printer. The interface was glued to the AFM chip and could withstand 5 bar of pressure, which is the maximum of the system. When more pressure is applied, the connection of the tubing to the stainless tube starts to leak. The interface is compatible with water. Other liquids are also used but may interact with the interface or tubing which can subsequently result in clogging of the AFM chip.

Dispensing with contact time

Dispensing with an AFM can be executed by just touching the substrate with a filled cantilever. The surface forces of the substrate start pulling on the liquid and the fluid will spread until an equilibrium of the surface forces and the viscous forces is obtained. The process of spreading takes time, therefore by controlling the time of contact the process can be interrupted and subsequently the droplet size is controlled.

An experiment was conducted to find the relation between contact time and droplet size. Three different liquids were used: water, diethyl carbonate and a 5% glycerol solution. Additionally two different substrates were used for dispensing: the first substrate was a cleaned piece of bare silicon and the second substrate was functionalized with octyltrichlorosilane to decrease the surface energy. The volume of the droplets were obtained from height of the force distance curves and the receding contact angle measured in previous experiments. During this experiment it was found that droplets of around 0.5 fl could be dispensed with an average variation of 0.05 fl. Additionally the trend of increasing droplet size with contact time was made visible.

Dispensing with pressure

For dispensing beyond the surface forces, for example on an hydrophobic surface or in a liquid, additional pressure is needed. To find a correlation between the applied pressure and droplet size an experiment was performed: on a functionalized surface, droplets of 5% glycerol were dispensed. Then, using the breakup height from the force distance curve and the receding contact angle, the volumes were calculated. As a result droplets with an average variation of 0.06 fl were dispensed. Additionally a linear relation was found between the droplet volume and the applied pressure. This was in line with the expectations because the contact time is kept constant and also the hydronamic resistance of the system is kept constant. Therefore it can be concluded that the pressure is directly related to the flow rate. Additionally it could be concluded that with a constant time of the applied pressure, the dispensed volume is directly related to the pressure.

Recommendations

Dispensing of droplets of around 0.4 fl with a variation of 0.05 fl has been shown. Further experiments should be conducted to reduce the variance in the droplets. Therefore more knowledge should be created of the dispensing process, an investigation of the tip before and after dispensing could result in information about how the tip changes, because this can have influence on the breakup height and therefore on the droplet size. An investigation is possible by imaging

the AFM tip with a scanning electron microscope before and after an experiment. Then also exact measures can be taken of a cantilever for stiffness calculations.

Dispensing inside a dispensed droplet or another liquid and controlling droplet size can be an interesting experiments because then the whole system can be used. The precision stages to find the liquid, the pressure system to deliver the droplet and the humidity control to keep the droplet "alive". If the droplets stay under the height of 4 μm the proposed method of calculating volume from the breakup height can be used.

Already a trend has been seen that with an increasing humidity, an increase in breakup height is observed. A clear conclusion could not be drawn because the climate was not stable and therefore large spread in the breakup height is seen. For future experiments to stabilize the climate, the system can be covered to reduce the turbulence in the air by moving system operators. As well the PID parameters could be optimized for further stabilization.

A nice experiment to conduct is to find the relation of pressure on the stiffness of the cantilever. Think about an inflatable toy animal, deflated there is no stiffness in the toy animal but when inflated it keeps its shape and it even can withstand forces. This also can happen when pressurizing a cantilever. For this experiment a hollow cantilever without tip hole is needed or a way of closing the tip aperture.

For better controllability of the dispensed droplets already an idea for a feedback controller based on the breakup height from the force distance curves exists. The controller will be an automatic learning device to dose the desired volumes. As well a project is started to aspirate something from a cell.

A — System description

A.0.1. General description of the AFM system

The system used for the experiments is a commercially available AFM system from AFM workshop, which is adapted by MA3 solutions to enable fluid dispensing, more details can be found in van Oorscot et al. [67]. The system (see figure A.1) can still be used for AFM imaging. The remaining basic components are a pressure control, a climate control and the positioning stages. The positioning stages can be subdivided into coarse stages and the fine piezoelectric stages. The whole system is controlled by a computer with associated software. The software is a labview based program which is able to handle automatic dispensing tasks.

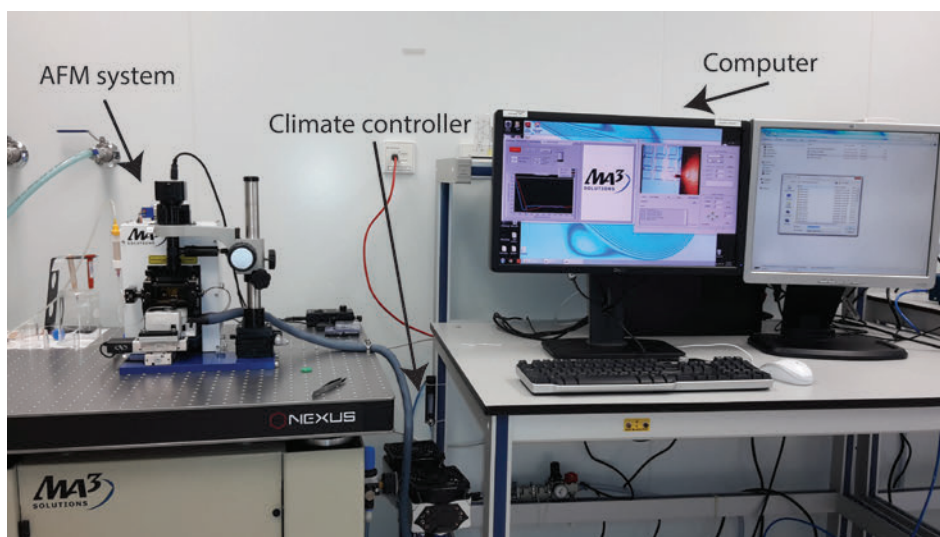


Figure A.1.: Entire system

A.0.2. Pressure control

The schematic of the pressure control is shown in A.2. The system includes two MAC valves, type 35A-ACA-DDAA-1BA, which have a switch time of 2-6 ms to control the pressure. A maximum of 5 bar can be applied with a resolution of 0.01 bar as well an under pressure of -0.85 bars can be utilized. The system is able to dispense and aspirate liquids, this can be controlled via the software application. A 3 cc syringe is used as a fluidic reservoir located on the left of the system (see A.3)

A.0.3. Humidity control

To control the climate around the AFM tip the AFM system is equipped with a semi open climate chamber. The semi open chamber is a 3D printed box with a ring of holes at the top. A humid air curtain is created through the ring of holes. First dry air is passed through a

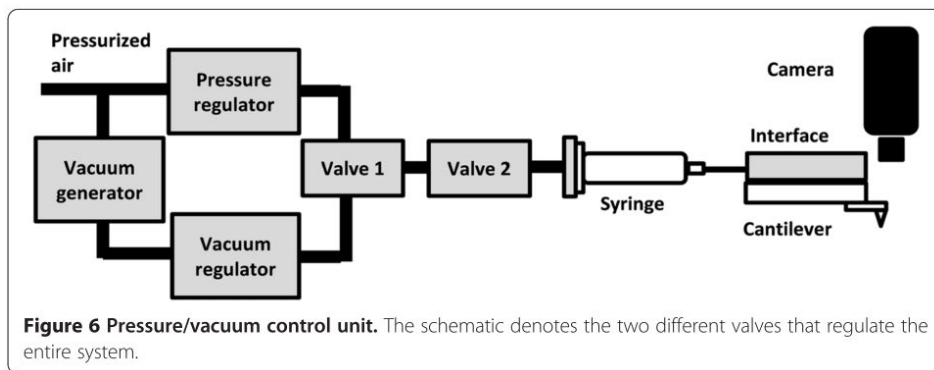


Figure A.2.: Schematic of the pressure control, it denotes two different valves that regulate the entire system

bubbler (water bath). The bubbler assures that saturated vapor is created, by passing the saturated vapor through a heated tube the relative humidity can be decreased. The humidity is measured and with a feedback loop the humidity is controlled by the heated tube. Also the temperature around the chip is measured and controlled, the controlling of air temperature is done by Peltier elements which can increase and decrease the temperature. The Peltier elements heat or cool the water in the bubbler and subsequently the temperature of the climate. A finite element model of the flow is given in figure A.4 and the specifications in figure A.6.

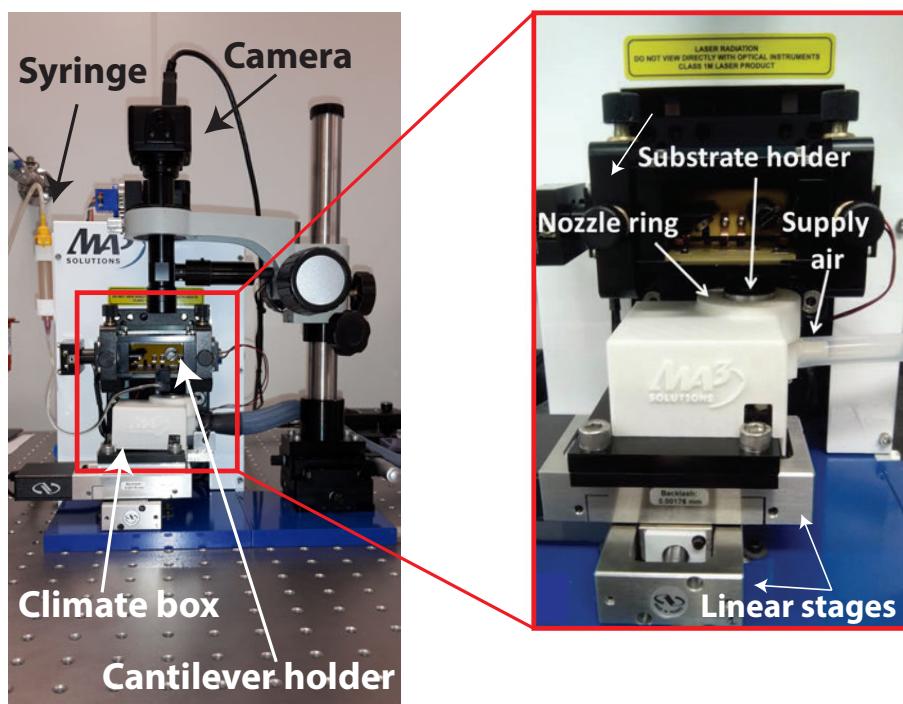


Figure A.3.: AFM system and climate box

A.0.4. Operation

To position the cantilever close to the substrate an automated substrate approach is available. Using the piezo stage for the fine movement in Z direction and for the coarse movement a stepper motor. The piezo stage is connected to the substrate and the stepper motor to the cantilever holder. The piezo stage is moved upwards by 10 μm and when no cantilever deflection

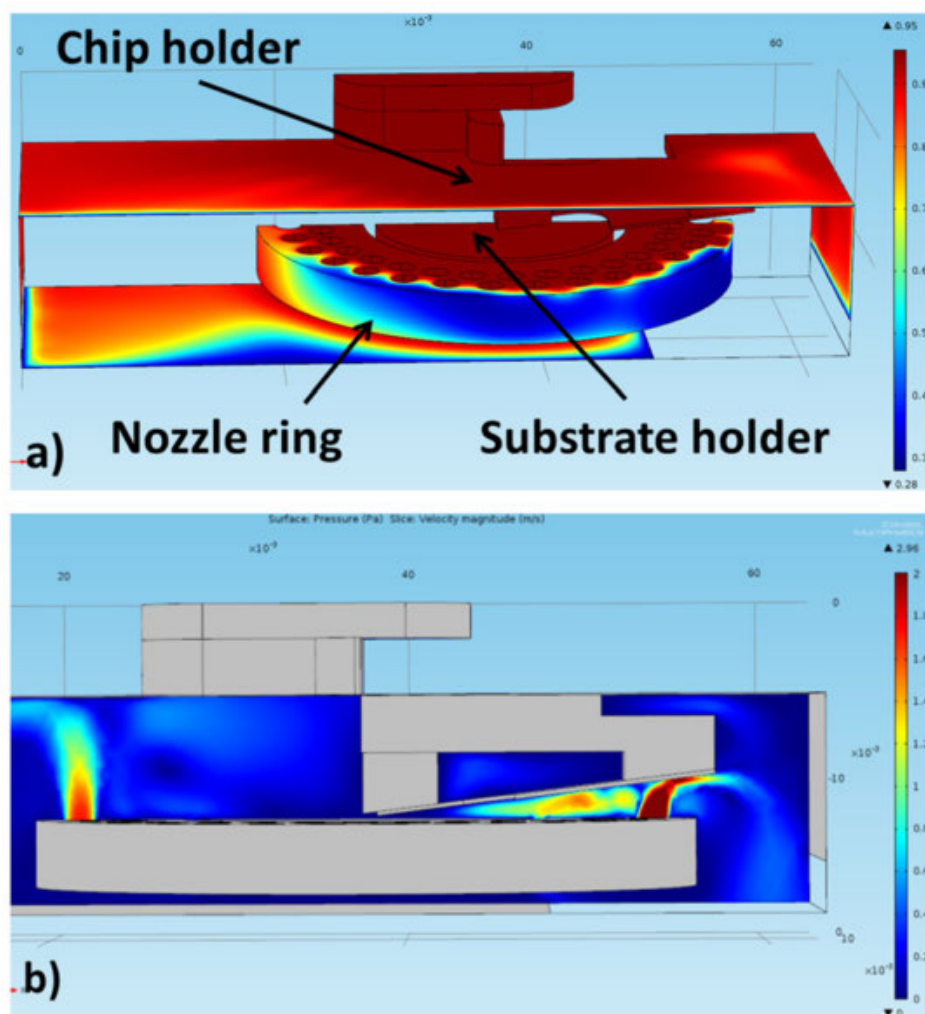


Figure A.4.: (a) Humidity profile at 95 %RH supply air, showing uniform humidity profile inside the nozzle ring where the substrate is located. (b) Cross-section view of the air velocity profile, indicating low air speeds around microfluidic chip and substrate

is detected the piezo stage moves down again and subsequently a coarse movement of $10\ \mu\text{m}$ with the stepper motor is executed. This process is repeated until a cantilever deflection is detected. Finally the tip of the cantilever will be hanging $5\ \mu\text{m}$ above the substrate. Now the system can be used for force measurements or dispensing.

For the X-Y movement two linear stages (Newport smc100) are mounted on top of each other. The stages have a range of 25 mm and can be positioned within $1\ \mu\text{m}$ accuracy. After the coarse movement a piezo stage is used for the fine movement for positioning sub-micron accuracy. The piezo stage has a range of $50\ \mu\text{m}$ in X and Y direction.

Several parameters can be controlled (see figure A.5) for example: the approaching speed, contact time and applied pressure. For automatic dispensing of an array, the coordinates and the settings of the desired dispense action are given to the program via an Excel file. The program automatically executes every step. Grids of 10×10 droplets on a area of $50 \times 50\ \mu\text{m}$ have been shown.

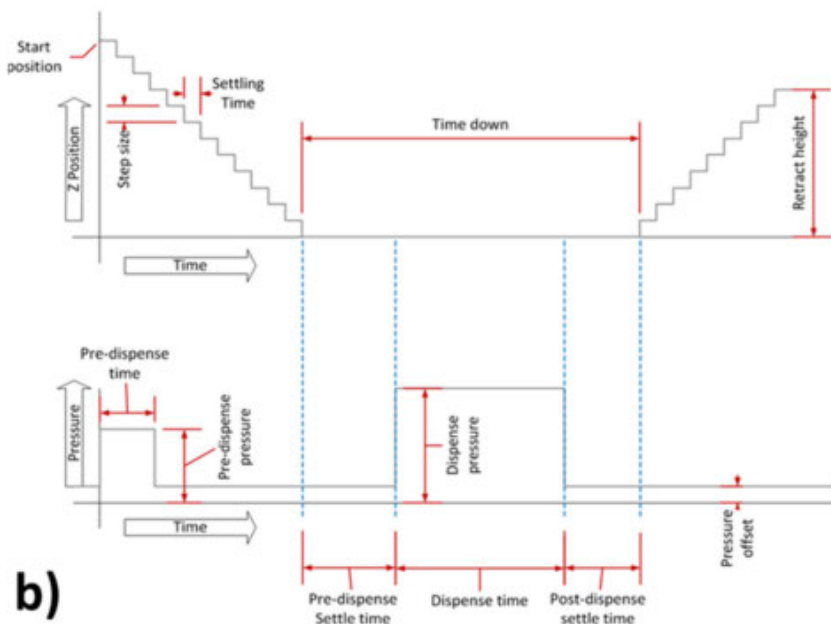
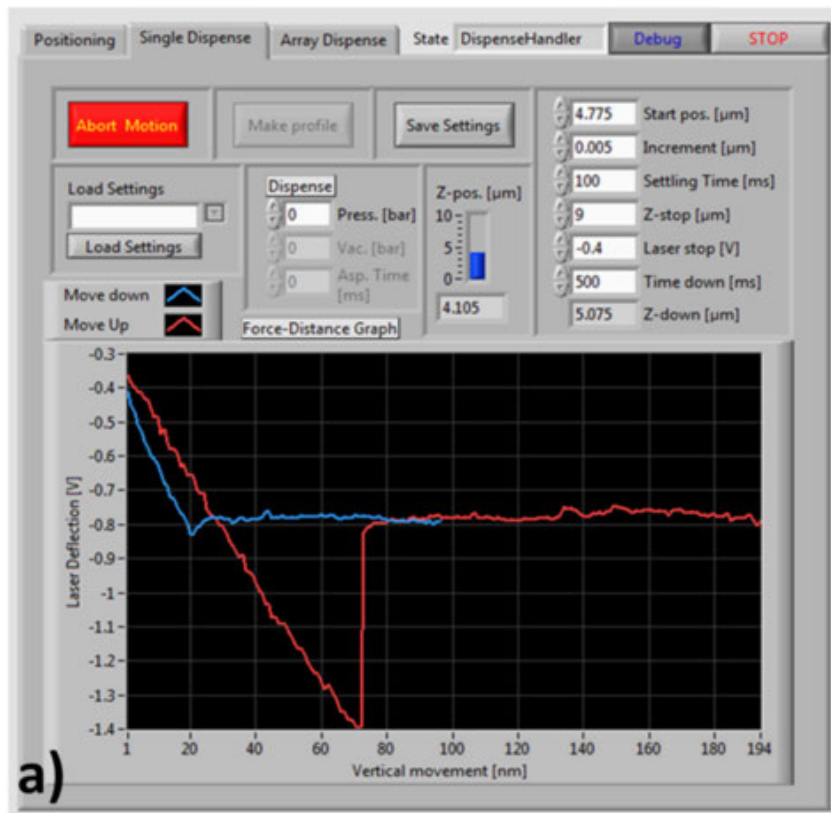


Figure A.5.: (a)Dispensing software, with a force distance curve (b) Controllable parameters, with the Z-positioning in the top panel and pressure settings in the bottom panel

A.0.5. Specifications

External dispenser

Pressure range 0.85 bars under pressure to 5.0 bar overpressure; 0.01 bar resolution

Settling time at dispenser out <100 ms

Climate control

Temperature range Ambient to 40°C ±0.5

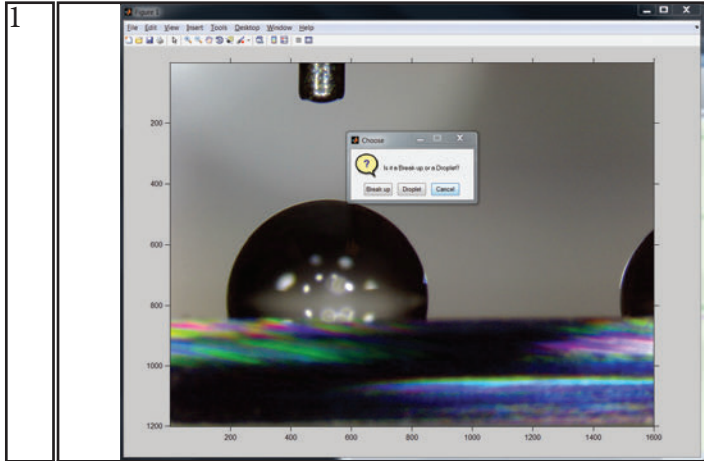
Humidity range 30% – 90% RH ±5% non condensing 90% – 100% RH ±5% condensation

Substrate alignment

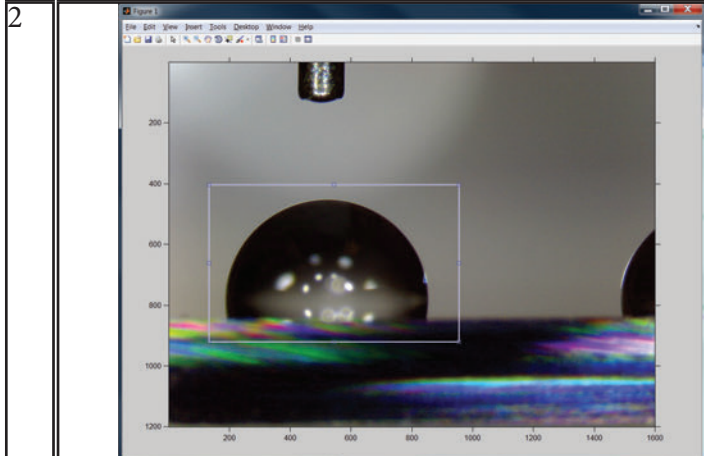
Alignment accuracy Between chip positions on the same substrate: <1 µm Between different chips: <2 µm

Figure A.6.: Specifications of the microfluidic platform

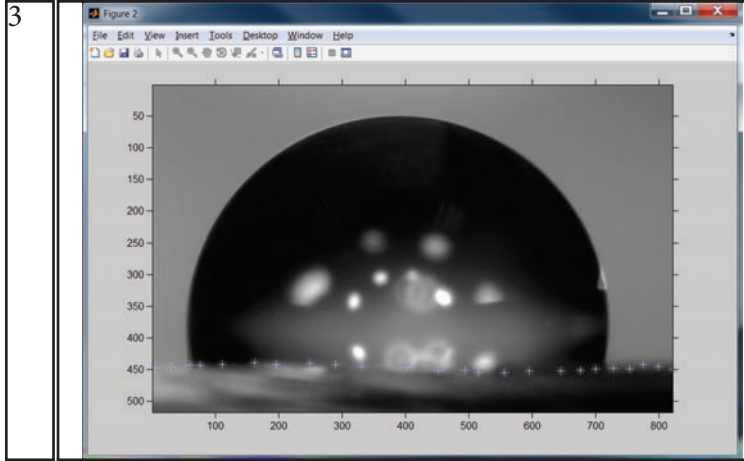
B — Software steps



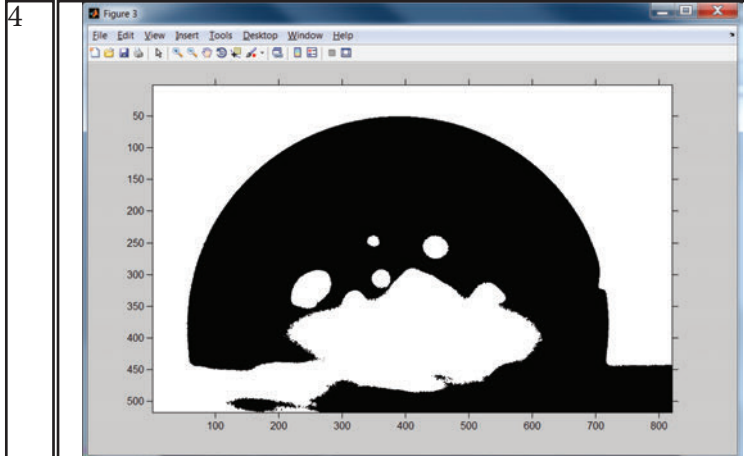
will ask if it is a droplet or a breakup situation.



To reduce the processing time the droplet has to be selected then press enter.

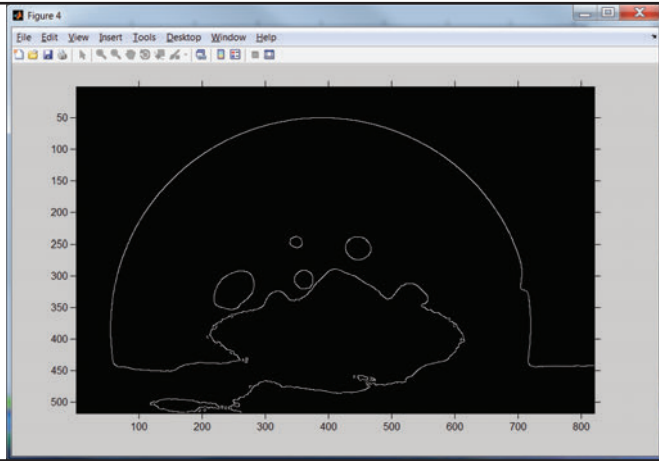


to detect therefore a user input is required. By clicking



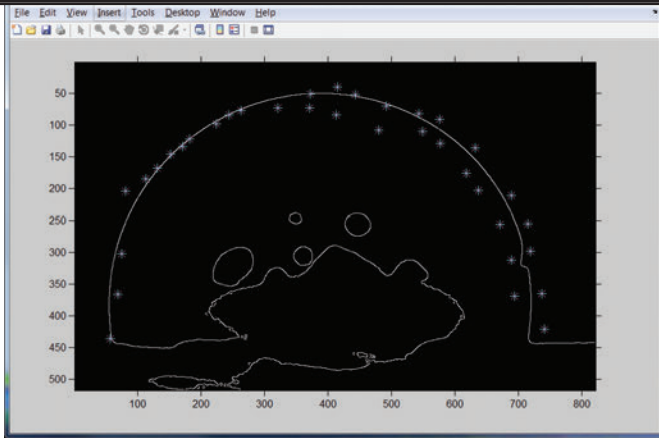
Now a black and white image is created.

5



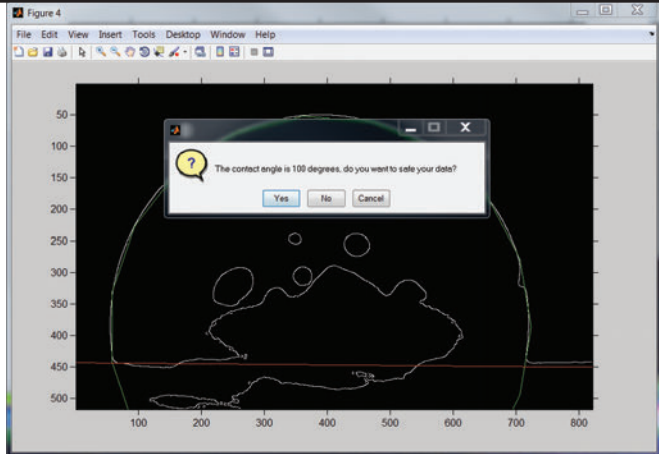
Matlab will detect the edges and a line image is created.

6



Another user input is required. By clicking close to the edge of the droplet it is assured that the detected edge is used.

7



Matlab will fit a circle to the edge of the droplet and calculates the contact angle of the droplet and the substrate. Now also an option to save the data appears.

C — Visualization of capillary condensation

C.1 Methods and materials

To confirm the contact angle in sub-micron scale and gain information about the liquid bridge formation an experiment is conducted using an ESEM (FEI Nova NanoSEM). The SEM is operated at low vacuum mode, the pressure in the chamber can go up to 200 Pa. Low vacuum is reached by introducing water molecules from a bubbler. The bubbler assures that there are enough water molecules available to condense.

Two samples are prepared, one using a hollow cantilever AFM tip (SmartTip Probe Solutions) and two, a tungsten wire with sharp tip. Both samples are fixed using carbon tape to a glass slide. To make the glass slide conducting it is sputter coated with gold/palladium (Au/Pd). The approach of the AFM chip is done by mounting a vacuum holder to a stage (see figure C.1). When the tip is fixed to the substrate the vacuum is switched off and the holder is retracted. The tip of cantilever is touching the glass and the rest of the chip is on the double sided tape.

The tungsten wire is cut with a wire cutter. While cutting the wire is pulled to make the sharp tip. The wire is bend so the tip is touching the substrate and a bended piece is fixed to the double side carbon tape.

Cooling can help to force the water to condense. For cooling a Peltier element can be used. A Peltier element uses the Seebeck effect to convert a voltage into a temperature difference. The performance is tested by mounting the element to a aluminum block with thermal paste. The aluminum acts as heat sink. Using a lab voltage source the voltage on the element is varied from 0 to 12 Volt. The temperature is measured with a thermo couple.

C.2 Discussion

The AFM cantilever was imaged using the ESEM (see figure C.2). The image is taken at 200 Pa, the pressure was increased with an air stream via a bubbler. Unfortunately no capillary condensation is observed. Probably the cantilever was too far away from the substrate. As it was not possible to image the substrate and the cantilever together. Also the tip of the cantilever can be observed suggesting that no substrate is close by.

To exclude the fact that the AFM cantilever was far away, experiments with the tungsten wire are conducted (see figure C.3). The tungsten wire is in contact with the substrate. In contact examples have shown capillary condensation in previous researches. Unfortunately no capillary condensation is observed with the tungsten wire example. It is possible that not enough water molecules were available to condense and that the pressure was too low and therefore it is more energy favorable for water to stay in gaseous phase. In the literature values of 6.4 tor or 850 Pa are reported.

To force the water to condense the temperature can be brought down. A Peltier element can be used for cooling there is a good relation between applied voltage and temperature (see figure

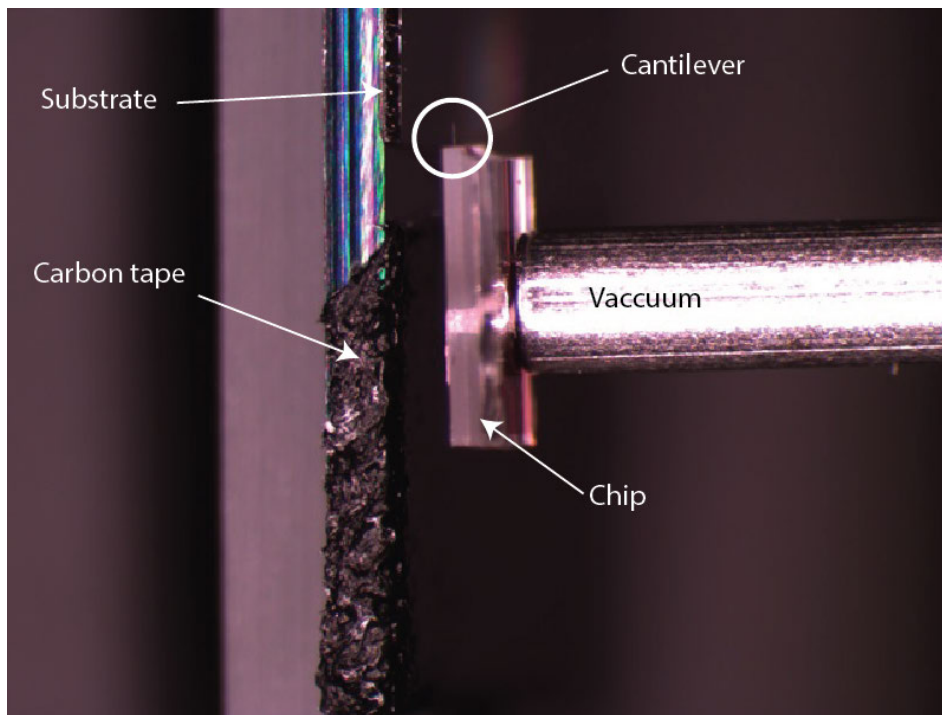


Figure C.1.: Mounting the chip on the carbon tape

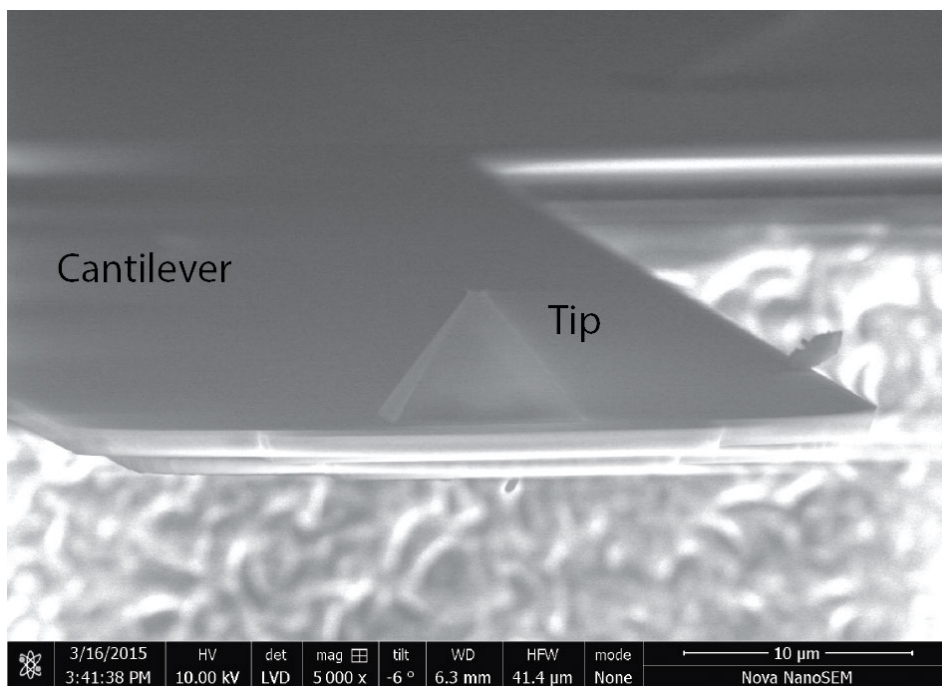


Figure C.2.: Smartip imaged with Novanano SEM

C.4). With increasing voltage a decrease in temperature is observed. The minimum constant temperature reached is -7°C . The voltage needed is 8.5 V and the estimated power to keep this temperature is 28.9 W. During the experiment the heat sink reached a temperature around 35°C .

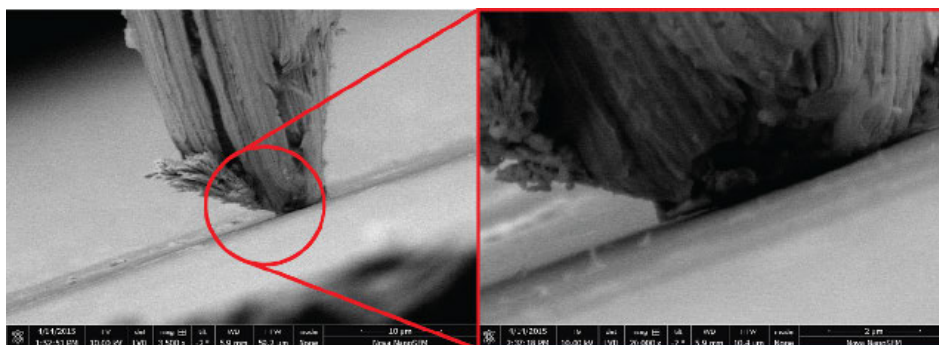


Figure C.3.: Tungsten wire on glass substrate

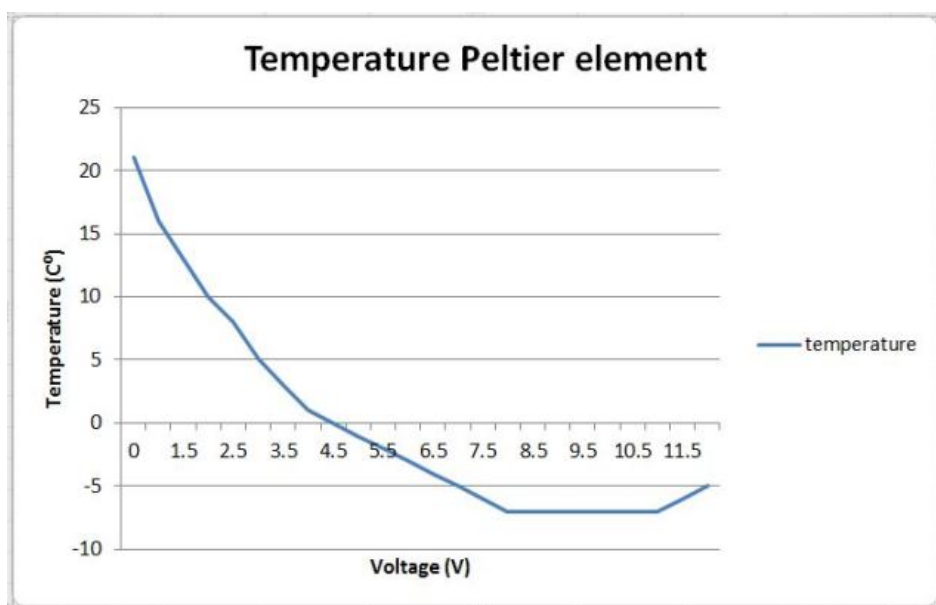
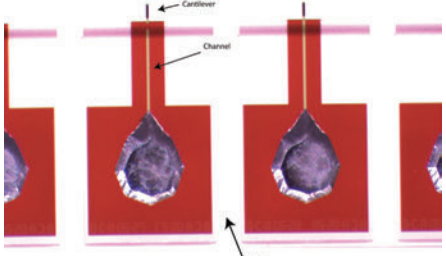
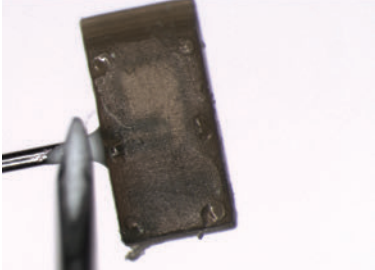
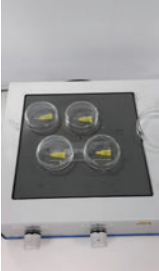
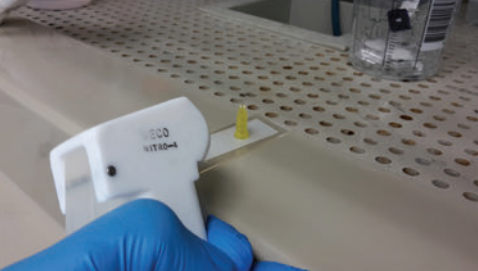
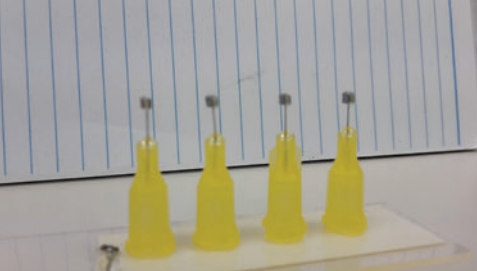
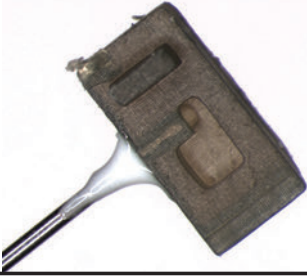
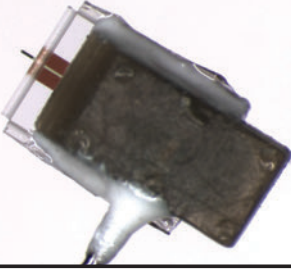
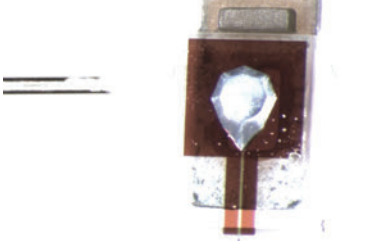
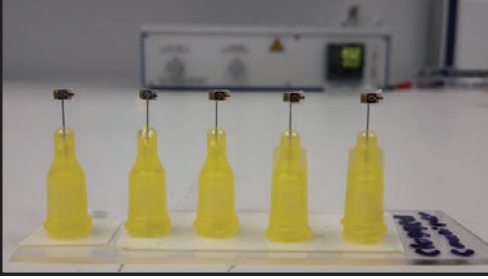
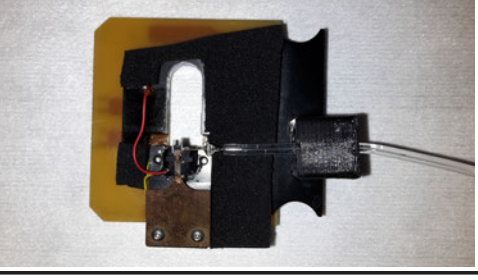
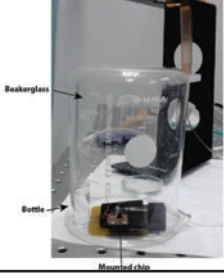


Figure C.4.: Results from Peltier element measurement

D — Gluing steps

| | | | |
|---|---|--|---|
| 1 |  |  | <p>Place a small piece of double sided tape under the corner of the chip. Remove chip from array using scalpel. Place scalpel in the notch between chips and apply little pressure.</p> |
| 2 |  |  | <p>Use 32 Ga syringe tip. Insert stainless tube in the side of the interface. Hold the interface at the side using tweezers.</p> |
| 3 |  |  | <p>Glue, high viscosity, temperature curing epoxy. Loctite hysol 9492. Mix glue, white resin with grey harder ratio 2:1 on a microscope glass. For mixing a syringe needle is used.</p> |
| 4 |  |  | <p>Mount chip on holder. Use a syringe needle or a scalpel to apply glue to the stainless tube and the interface.</p> |
| 5 |  | | <p>Cure the glued interface for 10 minutes at 80 degrees Celsius. Cover interfaces with a Petridish to prevent heat loss.</p> |
| 6 |  |  | <p>Clean the interfaces using compressed air or nitrogen. After cleaning store the glued interfaces on a microscope glass using double sided tape.</p> |

| | | | |
|----|---|---|--|
| 6 |  |  | <p>Result after first step of gluing. Mount syringe tip on the holder and apply glue in a continuous line around the hole as thin as possible. Use tweezers to mount the chip. Prevent sliding of the chip to avert clogging. Cure the chip 80 degrees 10 minutes.</p> |
| 7 |  |  | <p>Seal the edges between the interface and the chip. Apply as little glue as possible in the front to prevent laser blockage.</p> |
| 8 |  |  | <p>Individual result and array of results of glued chips. Store chips on microscope glass with double sided tape. Cover the chips with a plastic beaker to prevent dirt on the chips</p> |
| 9 |  | | <p>Before using the fluidic chip, use a wire cutter to remove stainless tube from the housing.</p> |
| 10 |  | | <p>Insert the chip in the holder and attach the Tygon tubing.</p> |
| 11 |  | | <p>Store an in use cantilever at high humidity to prevent clogging. High humidity is created under a beaker-glass by an open bottle of water.</p> |

E — Cantilever details

| Cantilever | Dimensions |
|------------------------------|-------------------|
| Length | 206 ± 10 |
| Width | 36 ± 1 |
| Wall thickness | 0.598 ± 0.03 |
| Channel | |
| Length | 201 ± 10 |
| Width | 30 ± 2 |
| Height | 1 ± 0.05 |
| Additional parameters | |
| Hole to hole | 1760 ± 2 |
| Stiffness | 3 N/m |

F — Volume data

| Droplet | contact time (s) | Volume (fl) | Breakup height (nm) |
|----------------|-------------------------|--------------------|----------------------------|
| 1 | 0.05 | 0.60 | 2000 |
| 2 | 0.05 | 0.34 | 1650 |
| 3 | 0.05 | 0.34 | 1650 |
| 4 | 0.05 | 0.40 | 1750 |
| 5 | 0.5 | 0.40 | 1750 |
| 6 | 0.5 | 0.44 | 1800 |
| 7 | 0.5 | 0.37 | 1700 |
| 8 | 0.5 | 0.40 | 1750 |
| 9 | 5 | 0.60 | 2000 |
| 10 | 5 | 0.56 | 1950 |
| 11 | 5 | 0.40 | 1750 |
| 12 | 5 | 0.40 | 1750 |
| 13 | 10 | 0.56 | 1950 |
| 14 | 10 | 0.70 | 2100 |
| 15 | 10 | 0.60 | 2000 |
| 16 | 10 | 0.48 | 1850 |

Figure F.1.: Breakup data from 4x4 array with varying contact time

| Droplet | contact time (s) | Volume (fl) | Breakup height (nm) |
|---------|------------------|-------------|---------------------|
| 1 | 0.02 | 0.34 | 1650 |
| 2 | 0.02 | 0.34 | 1650 |
| 3 | 0.02 | 0.44 | 1800 |
| 4 | 0.02 | 0.40 | 1750 |
| 5 | 0.02 | 0.37 | 1700 |
| 6 | 0.02 | 0.34 | 1650 |
| 7 | 0.05 | 0.40 | 1750 |
| 8 | 0.05 | 0.34 | 1650 |
| 9 | 0.05 | 0.44 | 1800 |
| 10 | 0.05 | 0.44 | 1800 |
| 11 | 0.05 | 0.34 | 1650 |
| 12 | 0.05 | 0.44 | 1800 |
| 13 | 0.5 | 0.34 | 1650 |
| 14 | 0.5 | 0.40 | 1750 |
| 15 | 0.5 | 0.40 | 1750 |
| 16 | 0.5 | 0.37 | 1700 |
| 17 | 0.5 | 0.34 | 1650 |
| 18 | 0.5 | 0.31 | 1600 |
| 19 | 5 | 0.48 | 1850 |
| 20 | 5 | 0.40 | 1750 |
| 21 | 5 | 0.44 | 1800 |
| 22 | 5 | 0.40 | 1750 |
| 23 | 5 | 0.52 | 1900 |
| 24 | 5 | 0.48 | 1850 |
| 25 | 10 | 0.60 | 2000 |
| 26 | 10 | 0.60 | 2000 |
| 27 | 10 | 0.48 | 1850 |
| 28 | 10 | 0.52 | 1900 |
| 29 | 10 | 0.56 | 1950 |
| 30 | 10 | 0.44 | 1800 |
| 31 | 15 | 0.52 | 1900 |
| 32 | 15 | 0.40 | 1750 |
| 33 | 15 | 0.44 | 1800 |
| 34 | 15 | 0.52 | 1900 |
| 35 | 15 | 0.56 | 1950 |

Figure F.2.: Breakup data from 35 array with varying contact time

| Droplet | Pressure (Bar) | Volume (fl) | Breakup height (nm) |
|----------------|-----------------------|--------------------|----------------------------|
| 1 | 0.05 | 0.23 | 1450 |
| 2 | 0.05 | 0.21 | 1400 |
| 3 | 0.05 | 0.18 | 1350 |
| 4 | 0.05 | 0.21 | 1400 |
| 5 | 0.1 | 0.28 | 1550 |
| 6 | 0.1 | 0.34 | 1650 |
| 7 | 0.1 | 0.40 | 1750 |
| 8 | 0.1 | 0.40 | 1750 |
| 9 | 0.15 | 0.80 | 2200 |
| 10 | 0.15 | 0.80 | 2200 |
| 11 | 0.15 | 0.65 | 2050 |
| 12 | 0.15 | 0.80 | 2200 |
| 13 | 0.2 | 0.86 | 2250 |
| 14 | 0.2 | 0.97 | 2350 |
| 15 | 0.2 | 1.04 | 2400 |
| 16 | 0.2 | 1.04 | 2400 |

Figure F.3.: Breakup data from 4x4 array with varying pressure

G — Force distance curves

Corresponding force distance curves to the measurement with varying pressure (see chapter 6.3.1). It is observed that several steps are needed to get snap off again. Therefore the retract height of 2500 nm is not enough for dispensing droplets.

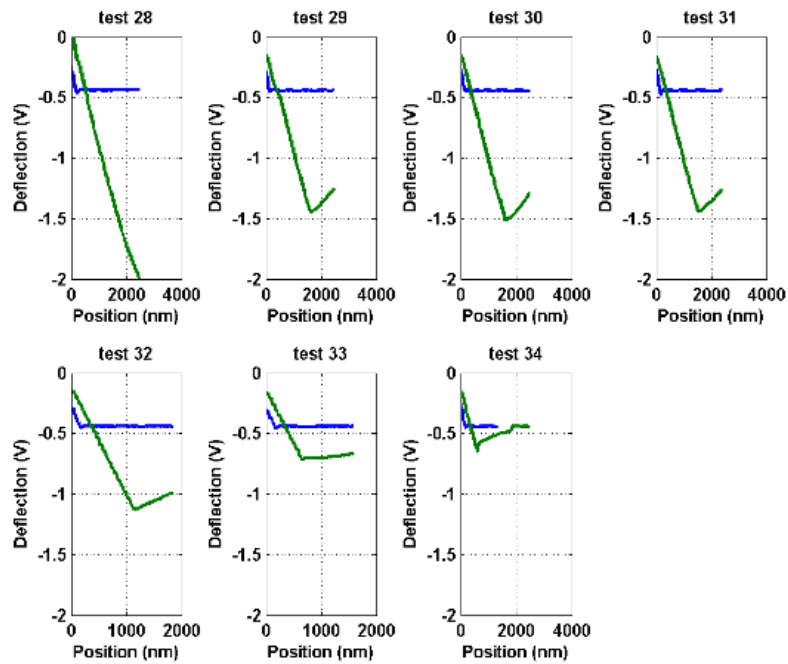


Figure G.1.: Test 28 2.4 bar to create droplet subsequently the distance distance curves for dispensing with 0.4 Bar. It is observed that the breakup height decreases with number of experiments indicating that in every step some liquid is dispensed but the retract height is to small for proper measurement

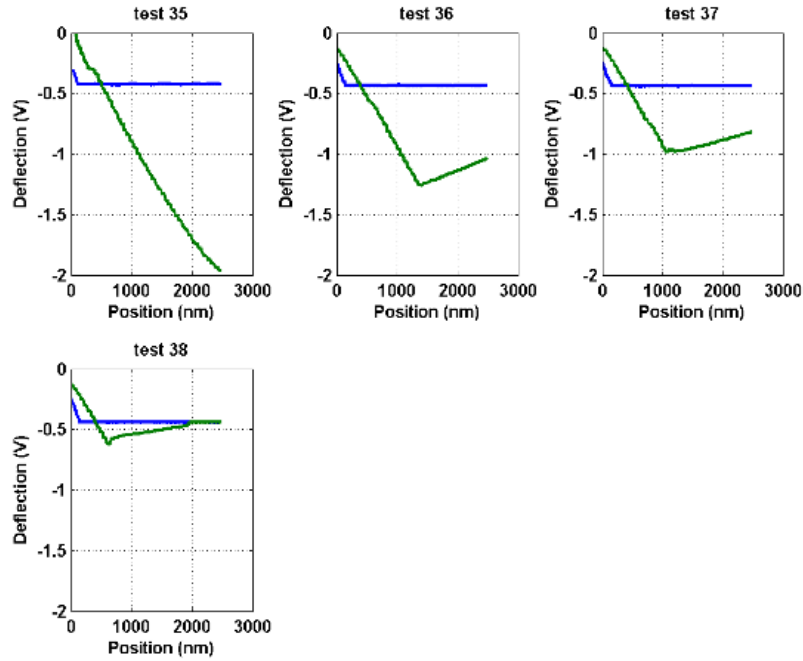


Figure G.2.: Test 35 2.4 bar to create droplet subsequently the distance distance curves for dispensing without pressure. It is observed that the breakup height decreases with number of experiments indicating that in every step some liquid is dispensed but the retract height is to small for proper measurement

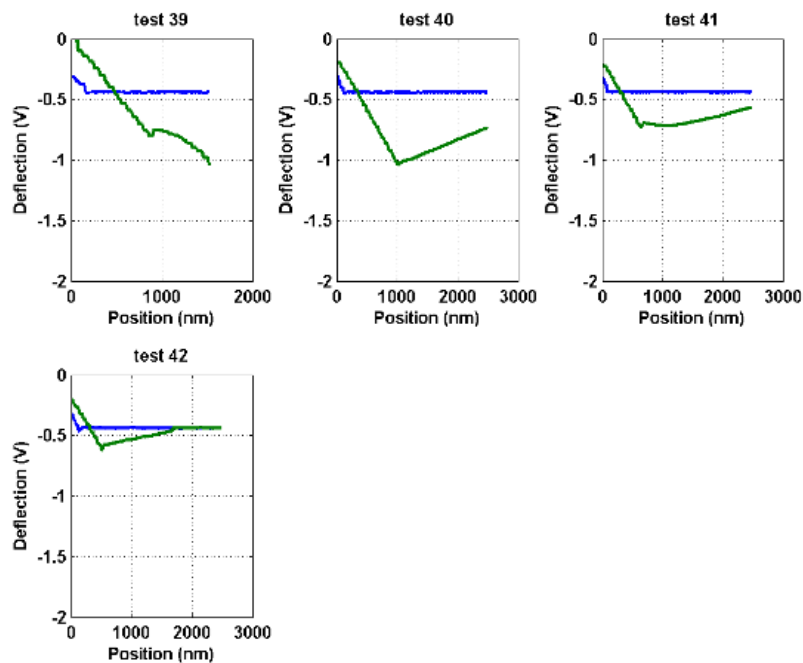


Figure G.3.: Test 39 2.4 bar to create droplet subsequently the distance distance curves for dispensing without pressure with a step size of 20 nm. It is observed that the breakup height decreases with number of experiments indicating that in every step some liquid is dispensed but the retract height is to small for proper measurement

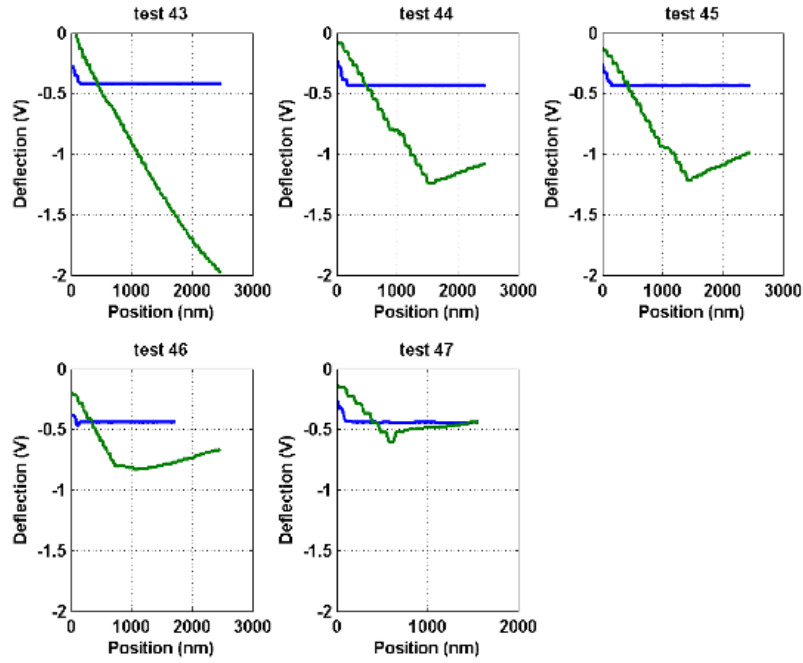


Figure G.4.: Test 43 2.4 bar to create droplet subsequently the distance distance curves for dispensing without pressure with a step size of 30 nm. It is observed that the breakup height decreases with number of experiments indicating that in every step some liquid is dispensed but the retract height is to small for proper measurement

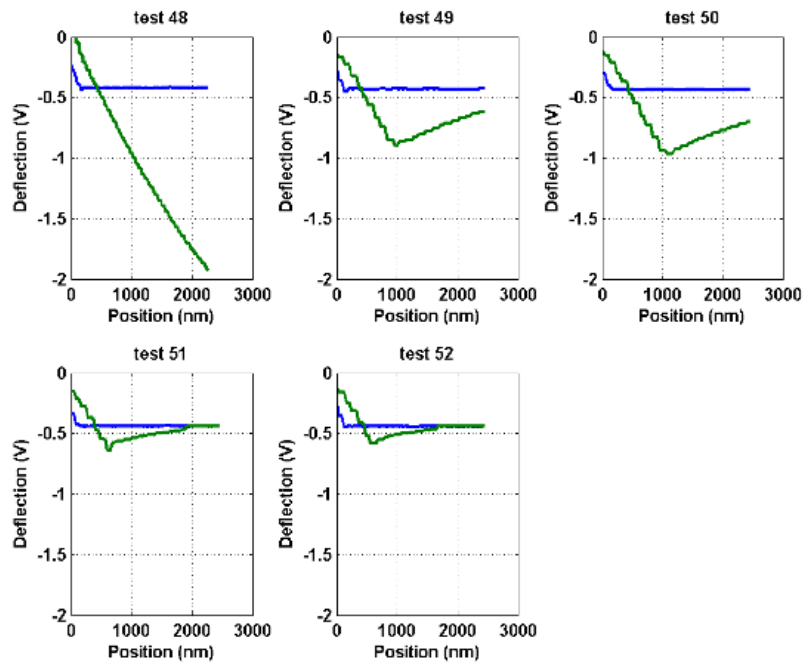


Figure G.5.: Test 48 2.4 bar to create droplet subsequently the distance distance curves for dispensing without pressure with a step size of 20 nm. It is observed that the breakup height decreases with number of experiments indicating that in every step some liquid is dispensed but the retract height is to small for proper measurement

H — Contact angle

```
1 function [base, Re, ca, path] = edge.detect()
2 % This function calculates the contact angle of a droplet from a picture
3 % It uses the pixel location to fit a circle to the detected edges.
4 %
5 % The function requires several user inputs displayed in the command
6 % window. The function gives as output the length of droplet base, the
7 % radius of the droplet, the contact angle of the droplet with the
8 % substrate and the path of the located file.
9 %
10 % In principal the more data points created the more accurate the contact
11 % angle can be determined but the longer it takes.
12 %
13 % Software made by Rick de Gruiter
14 % Project: Dosing of AFM droplets
15 % TU Delft, MNE
16 % Version 1.1
17 % Date: 19-3-15
18 %
19 % Make sure circ_fit is in the same folder
20 %
21 % opens a interactive dialog sreen to select the input string with the path
22 % where the file is located
23 [fn, pn] = uigetfile('*.jpg;*.tif;*.png;*.gif;*.bmp','Select the file to analyze');
24
25 path = [pn,fn];
26
27 % can be checked when the image edges cannot be detected
28 check.messy = false; % true undetectable edge – false detectable edge
29
30 % the file which needs to be readed
31 I = imread(path);
32
33 % show figure
34 figure(1)
35 imshow(I)
36
37 % to determine breakup or droplet
38 button = questdlg('Is it a Break up or a Droplet?','Choose','Break up',...
39     'Droplet','Cancel','Cancel');
40
41 if strcmp(button, 'Droplet') == 1
42 check.breakup = false; % true break up – false droplet
43 elseif strcmp(button, 'Break up') == 1
44     check.breakup = true;
45 else
46     error('Not enough inputs')
47 end
```

```

48
49 % select droplet to reduce processing time
50 disp('Select the droplet by dragging a window around the droplet.')
51 disp('Double click in window when finished.')
52 I2 = imcrop(I);
53 clc
54
55 % converts image to gray
56 gr = im2double(rgb2gray(I2));
57 figure(2)
58 imshow(gr)
59
60 % select substrate
61 disp('Select substrate by clicking on the edge of the substrate (at least two points).')
62 disp('Press enter when finished.')
63 [x_coordinates_subst, y_coordinates_subst, Pixel_vals1] = impixel;
64 clc
65
66 if check.messy
67 % define the edge by clicking
68 disp('Click on the droplet edge (at least three points).')
69 disp('Press enter when finished.')
70 [x_coordinates, y_coordinates, Pixel_vals] = impixel;
71 clc
72 coordinates = [x_coordinates,y_coordinates];
73
74 % best fit to the line
75 % determine the circle
76 [xc,yc,Re] = circfit(x_coordinates,y_coordinates);
77
78 else
79 % Make Image Black and White
80 BW = im2bw(gr, 0.3);
81 figure(3)
82 imshow(BW)
83
84 % edge detection
85 BW1 = edge(BW,'sobel');
86 BW2 = edge(BW,'canny');
87 figure(4)
88 imshow(BW2)
89
90
91 % define the edge by clicking
92 disp('Click in the surrounding of the droplet edge (at least three points).')
93 disp('Press enter when finished.')
94 [x_coordinates, y_coordinates, Pixel_vals] = impixel;
95 clc
96 coordinates = [x_coordinates,y_coordinates];
97
98 % detects white dots in the matrix
99 [Y(:,2),Y(:,1)] = find(BW2); % coordinates of the image
100
101 % predefining size for the for loop
102 x_coordinates_det=zeros(length(x_coordinates),1);
103 y_coordinates_det=zeros(length(x_coordinates),1);
104
105 % for the length of defined coordinates determine shortest distance
106 for n=1:length(x_coordinates)
107 X(:,1) = ones(size(Y,1),1)*x_coordinates(n);

```

```

108 X(:,2) = ones(size(Y,1),1)*y_coordinates(n);
109
110 [D] = pdist2(X,Y,'euclidean','smallest',1); % euclidean distance
111 [M,O] = min(D);
112
113 x_coordinates_det(n) = Y(O,1);
114 y_coordinates_det(n) = Y(O,2);
115
116 end
117 [xc,yc,Re] = circfit(x_coordinates_det,y_coordinates_det);
118 end
119
120 th = linspace(0,2*pi,20)';
121 % makes circle
122 xe = Re*cos(th)+xc; % x-coordinate
123 ye = Re*sin(th)+yc; % y-coordinate
124
125 % Determine substrate
126 substrate = polyfit(x_coordinates_subst, y_coordinates_subst, 1);
127 x_subst = 0:0.1:1500;
128 y_subst = substrate(1)*x_subst+substrate(2);
129
130 % plot substrate and circle in picture
131 figure(2)
132 hold on
133 plot(xe,ye,'g',x_subst,y_subst,'r')
134
135
136 %% calculate contact angle
137 % abc formula for detection intersection substrate with droplet
138 a = substrate(1)^2+1;
139 b = 2*(substrate(1)*substrate(2)-yc*substrate(1)-xc);
140 c = substrate(2)^2-2*substrate(2)*yc+yc^2+xc^2-Re^2;
141
142 x_int = [(-b+sqrt(b^2-4*a*c))/(2*a),(-b-sqrt(b^2-4*a*c))/(2*a)];
143 y_int = [substrate(1)*x_int(1)+substrate(2),substrate(1)*x_int(2)+substrate(2)];
144
145 base = sqrt((x_int(1)-x_int(2))^2+(y_int(1)-y_int(2))^2);
146
147 if check.breakup
148 if substrate(1)*xc+substrate(2)<yc
149 ca = 90+acosd(0.5*base/Re);
150 disp(['Contact angle is ', num2str(round(ca)) , ' degrees therefore hydrophobic' ])
151 elseif substrate(1)*xc+substrate(2)>yc
152 ca = 90-acosd(0.5*base/Re);
153 disp(['Contact angle is ', num2str(round(ca)) , ' degrees therefore hydrophylic' ])
154 elseif substrate(1)*xc+substrate(2)==yc
155 ca = 90;
156 disp(['Contact angle is ', num2str(round(ca)) , ' degrees therefore hydrophobic' ])
157 end
158
159 else
160 % droplet
161 % circle is on the other side therefore different formulas are needed
162 if substrate(1)*xc+substrate(2)>yc
163 ca = 90+acosd(0.5*base/Re);
164 disp(['Contact angle is ', num2str(round(ca)) , ' degrees therefore hydrophobic' ])
165 elseif substrate(1)*xc+substrate(2)<yc
166 ca = 90-acosd(0.5*base/Re);
167 disp(['Contact angle is ', num2str(round(ca)) , ' degrees therefore hydrophylic' ])

```

```

168 elseif substrate(1)*xc+substrate(2)==yc
169     ca = 90;
170     disp(['Contact angle is ', num2str(round(ca)) , ' degrees therefore hydrophobic' ])
171 end
172 end
173
174 button2 = questdlg(['The contact angle is ', num2str(round(ca)), ' degrees, do you want
175
176 if strcmp(button2, 'Yes')==1
177 name = inputdlg({'Savename'}, 'Savetitle', [1 50], {'Contact Angle Data'});
178 savetitle1=[pn, name{1,1}, '.txt'];
179 fid = fopen(savetitle1, 'a');
180 fprintf(fid, '%s', ['Contact angle is ', num2str(round(ca)) , ' degrees', 13 10]);
181 fclose('all');
182 end
183
184 clc
185 close all
186 end
187 % End of the M-file

```

I — Matlab code force distance curves

I.1 Read data from CSV

```
1 %%%%%%%%%%%%%%%%%%%%%%%%%%%%%%%%%%%%%%%%%%%%%%%%%%%%%%%%%%%%%%%%%%%%%%%%%%
2 % saves the data from csv to files which Matlab can read
3 % Rick de Gruiter
4 % dosing AFM droplets
5 % 26-March-15
6 % MNE
7 % version 2.0
8 % used for correcting data check before running whether it imports the
9 % right start position and step size
10 %
11 % Used for now software with number of data related to stepsize
12 %
13 % to put data in right format:
14 %   ctrl+a in folder where excel data is
15 %   right click rename to: 'test'
16 %   on folder, shift right click, open command window here
17 %   typ: 'ren *.xls *.csv' press enter
18 %   now data is converted from xls to csv
19 %   When data is from an array dispans remove 001Data.xls from folder
20 %%%%%%%%%%%%%%%%%%%%%%%%%%%%%%%%%%%%%%%%%%%%%%%%%%%%%%%%%%%%%%%%%%%%%%%%%%
21
22 %% initialization
23 clear all
24 close all
25 clc
26
27 % noe = 1; % number of experiments
28
29 %% make sure data is in csv file and got good following names
30
31 % get the path of the files, select last file (set to the desired folder)
32 % pn_i      = 'C:\Users\Rick\Documents\master jaar 2';
33 [fn, pn] = uigetfile('*.csv','Select files to open');
34
35 % determine number of experiments
36 disp('click on the last file in the folder')
37 fn = strrep(fn,'test ','');
38 fn = strrep(fn,') .csv','');
39 noe = str2double(fn); % gives the number of tests
40
41 [fn_s, pn_s] = uigetfile('*','Select save location',pn);
42 % read the files
```

```

43 tic
44 for n=1:noe
45
46     readfile = [pn, 'test (' , num2str(n), ').csv'];
47
48     % read the start position and step size
49     fid      = fopen(readfile);
50     C        = textscan(fid, '%s');
51     fclose(fid);
52
53     % depends if a profile is used for dispensing
54 %     start_pos = str2double(C{1,1}{28,1})*1e-6;
55 %     step_size = str2double(C{1,1}{29,1})*1e-9; % no profile
56
57     start_pos = str2double(C{1,1}{30,1})*1e-6;
58     step_size = str2double(C{1,1}{31,1})*1e-9; % with profile (array)
59
60     % read the data from csv file
61     M = csvread(readfile, 6, 0);
62     M2 = csvread(readfile, 6, 0, [6, 0, (length(M)-1)*3+5, 0]);
63
64     % implement placing data in the right place
65
66     % get approach curve data (mirror down)
67     mirror_down = zeros(1, (length(M2)/3));
68     for i=2:3:length(M2)
69         mirror_down((i-2)/3+1) = M2(i);
70     end
71
72     % get retract data (mirror up)
73     mirror_up = zeros(1, (length(M2)/3));
74     for i=3:3:length(M2)
75         mirror_up((i-3)/3+1) = M2(i);
76     end
77
78     % position using stepsize and length the position is determined
79     position = zeros(1, (length(M2)/3));
80     for i = 1:length(mirror_down)-1
81         position(1) = 0;
82         position(i+1) = position(i)+step_size;
83     end
84
85     %saving data
86     savefile = [pn_s, num2str(n), 'Force.distance.curve'];
87     save(savefile, 'mirror_down', 'mirror_up', 'position', 'start_pos', 'step_size')
88
89     clear('mirror_down', 'mirror_up', 'position', 'start_pos', 'step_size')
90 end
91
92
93 time = toc;
94 disp(['Time ', num2str(time), ' s'])
95 % end of m file

```

I.2 Force distance curves

```

1 %%%%%%%%%%%%%%%%%%%%%%%%%%%%%%%%%%%%%%%%%%%%%%%%%%%%%%%%%%%%%%%%%%%%%%%%%

```

```

2 %% gives a force distance curve obtained from measurement %
3 % !! First save data as matlab file using A_read_data_csv3
4 %
5 %
6 % Rick de Gruiter %
7 % 11-25-2014
8 % version 1.4
9 % added saving
10 % %%%%%%%%%%%%%%%%%%%%%%%%%%%%%%%%%%%%%%%%%%%%%%%%%%%%%%%%%%%%%%%%%%%%%%%%%%
11
12 %% initialization
13 clear all
14 close all
15 clc
16
17 pn.i = 'C:\Users\Rick\Documents\master jaar 2';
18
19 check.savebreakup = false;
20
21 tic
22 %% load data from previous saved files
23
24 % determine 1 or multiple figures
25 a=questdlg('Do you want to put the data in seperate figures');
26 if strcmp(a,'Yes')==1
27     check.multiple.figs = true;
28 elseif strcmp(a,'No')==1
29     check.multiple.figs = false;
30 else
31     error('Je moet wel yes of no kiezen')
32 end
33
34 %% select files to open it opens all the files above the selected
35 [fn, pn] = uigetfile('', 'Select files to open', pn.i);
36
37 fn = strrep(fn, 'Force.distance.curve', '');
38 fn = strrep(fn, '.mat', '');
39 noe = str2double(fn);
40
41 breakup=zeros(1,noe);
42 cont_time=zeros(1,noe);
43 % calculate breakup height
44 for n = 1:noe
45 loadfile = [pn, num2str(n), 'Force.distance.curve'];
46
47 load(loadfile)
48
49 %%
50 % position = 0:1e-9:(length(mirror_down)-1)*1e-9;
51 pos_down = find(mirror_down==min(mirror_down));
52 pos_up = find(mirror_up==min(mirror_up));
53 breakup(1,n) = position(pos_up(1,1))-position(pos_down(1,1));
54 cont_length = position(pos_up(1,1))+position(pos_down(1,1));
55 cont_time(1,n) = cont_length/step_size*10;
56 %% find first minimal value
57 for i = 1:length(mirror_down)-1
58 if mirror_down(i+1)>mirror_down(i)
59 pos(i)=position(i);
60 else
61 pos(i)=0;

```

```

62 end
63 end
64 ind = find(pos);
65
66 if isempty(ind)==1
67     ind(1)=1;
68 end
69
70 pos_down2 = pos(ind(1));
71
72 for i = 1:length(mirror_up)-1
73     if mirror_up(i+1)>mirror_up(i)
74         pos2(i)=position(i);
75     else
76         pos2(i)=0;
77     end
78 end
79 ind2 = find(pos2);
80
81
82 if isempty(ind2)==1
83     ind2(1)=1;
84 end
85
86 pos_up2 = pos2(ind2(1));
87
88 breakup2(1,n) = pos_up2-pos_down2;
89 %% post process
90
91 if check.multiple_figs
92     % nice figures
93     figure(n)
94     plot(position*1e9,mirror_down,'linewidth', 2)
95     hold on
96     plot(position*1e9,mirror_up,'r','linewidth', 2)
97     title(['Test ', num2str(n)], 'fontweight', 'bold', 'fontsize', 14)
98     ylabel('Light sensor signal, Deflection (V)', 'fontweight', 'bold', 'fontsize', 14)
99     xlabel('Position (nm)', 'fontweight', 'bold', 'fontsize', 14)
100    legend('Downward', 'Upwards')
101    set(gca, 'fontweight', 'bold', 'fontsize', 14)
102    grid on
103
104    disp(['Breakup height test ', num2str(n), ' is ', num2str(breakup(1,n)*1e9), ' nanomete
105    disp(['Breakup2 height test ', num2str(n), ' is ', num2str(breakup2(1,n)*1e9), ' nanomete
106
107    %% make figure with down and one with up
108    % improve lay out at end
109    else
110        figure(1)
111        hold on
112        v=plot(position*1e9,mirror_down);
113        set(v, 'Color', [0 n/noe 1-n/noe])
114        xlabel('Position (nm)', 'fontweight', 'bold', 'fontsize', 18)
115        ylabel('Light sensor signal, Deflection (V)', 'fontweight', 'bold', 'fontsize', 18)
116        title('Reproducibility', 'fontweight', 'bold', 'fontsize', 18)
117        grid on
118
119        figure(1)
120        hold on
121        r=plot(position*1e9,mirror_up);

```

```

122 set(r, 'Color', [1-n/noe 0 0])
123 xlabel('Position (nm)', 'fontweight', 'bold', 'fontsize', 18)
124 ylabel('Light sensor signal, Deflection (V)', 'fontweight', 'bold', 'fontsize', 18)
125 title('Reproducibility', 'fontweight', 'bold', 'fontsize', 18)
126 set(gca, 'fontweight', 'bold', 'fontsize', 14)
127 grid on
128
129 % shift in x and y
130 figure(3)
131 [z,b] = min(mirror_down);
132 r1=plot((position-position(b(1,1)))*1e9, mirror_down-mean(mirror_down(end-10:end)));
133 hold on
134 r2=plot((position-position(b(1,1)))*1e9, mirror_up-mean(mirror_up(end-10:end)));
135 ylabel('Light sensor signal, Deflection (V)', 'FontSize', 12)
136 xlabel('Relative position (nm)', 'FontSize', 12)
137 set(r1, 'Color', [0 n/noe 1-n/noe])
138 set(r2, 'Color', [1-n/noe n/noe n/noe])
139 grid on
140
141 disp(['Breakup height test ', num2str(n), ' is ', num2str(breakup(1,n)*1e9), ' nanomete.
142 disp(['Breakup2 height test ', num2str(n), ' is ', num2str(breakup2(1,n)*1e9), ' nanomete
143
144 end
145
146 end
147
148 if check.multiple_figs
149
150 else
151     figure(1)
152     legend('First experiment')
153
154 % saving figure?
155     a = questdlg('Do you want to save the figure');
156     if strcmp(a, 'Yes')==1
157         check.savefigure = true;
158     else
159         check.savefigure = false;
160     end
161
162 if check.savefigure
163     figure(1)
164     saveas(gcf, [pn, '\result.png'])
165 end
166
167 %     figure(2)
168 %     legend('First experiment')
169 end
170
171
172 if check.savebreakup
173     savefile = 'C:\Users\Rick\Desktop\breakup';
174     save(savefile, 'breakup')
175 end
176
177 check_break = round((breakup-breakup2)*1e9)';
178
179 time_stop    = toc;
180
181 disp(['Elapsed time is ', num2str(time_stop), ' seconds.'])

```

I.3 Save breakup height

```

1  %%%%%%%%%%%%%%%%%%%%%%%%%%%%%%%%%%%%%%%%%%%%%%%%%%%%%%%%%%%%%%%%%%%%%%%%%
2  % calculates break up height with 2 different methods
3  % first method minimal values
4  % second method first minimal value
5  % !! First save data as matlab file using A.read.data.csv3
6  %
7  % save as m file
8  % Rick de Gruiter
9  % dosing AFM
10 % mne
11 % version 1.0
12 % June 1st 2015
13 %%%%%%%%%%%%%%%%%%%%%%%%%%%%%%%%%%%%%%%%%%%%%%%%%%%%%%%%%%%%%%%%%%%%%%%%%
14
15 %% initialization
16 clear all
17 close all
18 clc
19
20
21 count = 1;
22 % pn_i = 'C:\Users\Rick\Documents\master jaar 2\15-6-3 rh vs bh';
23 %% load previous saved m-file
24 [fn, pn] = uigetfile('', 'Open files');
25
26 fn = strrep(fn, 'Force.distance.curve', '');
27 fn = strrep(fn, '.mat', '');
28 noe = str2double(fn);
29
30 breakup = zeros(noe, 2);
31 breakup2 = zeros(noe, 2);
32
33 % for loop to load multiple files in folder all above files are loaded
34 for n=1:noe
35
36 loadfile = [pn, num2str(n), 'Force.distance.curve'];
37 load(loadfile)
38
39 %% first method find overall minimal value
40 position = 0:1e-9:(length(mirror_down)-1)*1e-9;
41 pos_down = find(mirror_down==min(mirror_down));
42 pos_up = find(mirror_up==min(mirror_up));
43 breakup(n, 1) = position(pos_up(1, 1)) - position(pos_down(1, 1));
44
45 %% second method find first minimal value
46 for i = 10:length(mirror_down)-1
47 if mirror_down(i+1) > mirror_down(i)
48 pos(i) = position(i);
49 else
50 pos(i) = 0;
51 end
52 end
53 ind = find(pos);

```

```

54 pos_down2 = pos(ind(1));
55
56 for i = 50:length(mirror_up)-1
57 if mirror_up(i+1)>mirror_up(i)
58 pos2(i)=position(i);
59 else
60 pos2(i)=0;
61 end
62 end
63 ind2 = find(pos2);
64 pos_up2 = pos2(ind2(1));
65
66 breakup2(n,1) = pos_up2-pos_down2;
67
68 if count == noe
69 disp(breakup2*1e9)
70 end
71
72 breakup2(n,2)=count;
73 breakup(n,2)=count;
74
75 count = count+1;
76
77
78 end
79
80 a = questdlg('save break up?');
81 if strcmp(a, 'Yes') == 1;
82     save([pn,'breakup2'],'breakup2','breakup')
83 else
84     disp('klaar')
85 end
86
87 % end of mfile

```

I.4 Breakup height with dispensing

```

1 %%%%%%%%%%%%%%%%%%%%%%%%%%%%%%%%%%%%%%%%%%%%%%%%%%%%%%%%%%%%%%%%%%%%%%%%%
2 % calculates break up height from the derivative of the retract curve
3 % To use the break up height, right click in the work space and save as
4 % !! First save data as matlab file using A.read_data_csv3
5 %
6 % Rick de Gruiter
7 % dosing AFM
8 % mne
9 % version 1.0
10 % June 1st 2015
11 %%%%%%%%%%%%%%%%%%%%%%%%%%%%%%%%%%%%%%%%%%%%%%%%%%%%%%%%%%%%%%%%%%%%%%%%%
12
13 %% initialization
14 clear all
15 close all
16 clc
17
18
19 count = 1;
20 % pn_i = 'C:\Users\Rick\Documents\master jaar 2';

```

```

21 %% load previous saved m-file
22 [fn, pn] = uigetfile('','Open files');
23
24
25 fn = strrep(fn,'Force.distance.curve','');
26 fn = strrep(fn,'.mat','');
27 noe = str2double(fn);
28 %
29 % breakup = zeros(noe,2);
30 % breakup2 = zeros(noe,2);
31
32 % noe=37;
33 % for loop to load multiple files in folder all above files are loaded
34 for n=1:noe
35 % pn = 'C:\Users\Rick\Documents\master jaar 2\2015-08-03\Data array 4\';
36 loadfile = [pn, num2str(n), 'Force.distance.curve'];
37 load(loadfile)
38
39 % calculate the deravative
40 for i=1:length(mirror.up)-1
41 d_up(i) = (mirror.up(i)-mirror.up(i+1))/step_size;
42 d_up(length(mirror.up))=0;
43 end
44
45 % b= d_up*1e-7.*mirror.up;
46 figure(n)
47 plot(position*1e9,d_up*1e-7,'linewidth',2)
48 hold on
49 plot(position*1e9,mirror.up+abs(mean(mirror.up(end-20:end))), 'r', 'linewidth',2)
50 % plot(b+abs(mean(mirror.up(end-20:end))), 'b')
51
52 ylabel('Light sensor signal, Deflection (V)','fontweight','bold','FontSize',12)
53 xlabel('Relative position (nm)','fontweight','bold','FontSize',12)
54 set(gca,'fontweight','bold','fontsize',12)
55 [ar a]=min(d_up);
56 oncontact = position(find(d_up<0,1,'first'))*1e9;
57 offcontact = position(a)*1e9;
58
59 breakup(n) =offcontact-oncontact;
60
61 clear d_up
62
63 end

```

I.5 Calculate volume

```

1 %% calculate the volume of a liquid bridge during breakup
2 % calculate the breakup height first using D.breakupheight2.withbathtub
3 % or C.breakup.height
4
5 % Be sure the right contact angle is used
6 %
7 % Rick de Gruiter
8 % february
9 % version 1.1
10 % dosing afm droplets MNE
11

```

```

12 %initialization
13 clear all
14 close all
15 clc
16
17 % pn.i = 'C:\Users\Rick\Documents\master jaar 2';
18 [fn, pn] = uigetfile('', 'Open files');
19 loadfile = [pn, fn];
20 load(loadfile)
21 %
22 h_in = breakup*1e-9;
23 % h_in = [4000]*1e-9
24 %% parameters
25
26 theta_d = 41; % receding contact angle water(deg)
27 % theta_d = 50.5; % receding angle hydrophobic surface deg
28 % theta_d = 30.5; % receding angle diethyl
29 V_b      = zeros(1,length(h_in));
30
31 for i = 1:length(h_in)
32
33 h = h_in(i);
34
35 %% calculated parameters
36 theta = theta_d*pi/180;
37 r      = h/(cos(theta)); % curvature
38 a1     = r;              % center x
39 b1     = h;              % center y
40 a2     = -a1;
41 b2     = b1;
42
43 %% variables
44 start1 = pi;
45 end1   = 1.5*pi-theta;
46
47 start2 = -0.5*pi+theta;
48 end2   = 0;
49
50 t1 = start1:0.0001:end1;
51 t2 = start2:0.0001:end2;
52
53 %% formulas for plotting
54 x1 = a1+r*cos(t1);
55 y1 = b1+r*sin(t1);
56
57 x2 = a2+r*cos(t2);
58 y2 = b2+r*sin(t2);
59
60
61
62 %% formulas for volume from break_up_bridge
63 V_b(i) = (2*pi*h^3)/cos(theta)^2 - (pi*h^3)/3 - (pi*h^3*(1 - cos(theta)^2)...
64         ^ (1/2))/cos(theta)^2 - (pi*h^2*asinh(h*(-cos(theta)^2/h^2)^(1/2)))/...
65         (cos(theta)^2*(-cos(theta)^2/h^2)^(1/2));
66
67 %% volume cone
68 coord = 2*r*sin(0.5*(0.5*pi-theta));
69 base   = sqrt(coord^2-h^2);
70 A_base = pi*base^2;
71 V_cone = 1/3*A_base*h;

```

```

72
73
74
75 %% post process
76 disp(['The volume of the liquid bridge is ', num2str(V_b(i)*1e18), ' fL'])
77
78 % figure(1)
79 % hold on
80 % v1 = plot(x1*1e6,y1*1e6);
81 % v2 = plot(x2*1e6,y2*1e6);
82 % % axis([-1,6,-1,6])
83 % set(v1, 'Color', [i/6 1-i/6 0],'linewidth',2)
84 % set(v2, 'Color', [i/6 1-i/6 0],'linewidth',2)
85 % xlabel('x position \mum','FontSize',12)
86 % ylabel('y position \mum','FontSize',12)
87 % title(['Assumed shape of the liquid bridge (contact angle ', num2str(theta_d), '^{\circ}
88 % grid on
89
90 figure(1)
91 bar(V_b*1e18)
92 title('Droplet volumes with increasing pressure','fontweight', 'bold', 'FontSize',22)
93 ylabel('Volume (fL)','fontweight', 'bold', 'FontSize',22)
94 xlabel('Droplet','fontweight', 'bold', 'FontSize',22)
95 % ylim([0,0.5])
96 set(gca,'fontweight', 'bold', 'FontSize',22)
97 end
98
99 %% end o m file

```

J — Stiffness

```
1 %% Stiffness and eigenfrequency beam
2 % Rick de Gruiter
3 % 2-apr-15
4 % dosing AFM droplets
5 % MNE
6 % version 1.1
7
8 clear all
9 close all
10 clc
11
12 %% parameters
13 % silicon nitrate
14 E = 310e9; % Youngs modulus silicon Pa
15 rho = 3100; % density silicon kg m-3
16
17 % silicon
18 % E = 179e9; % Youngs modulus silicon Pa
19 % rho = 2330; % density silicon kg m-3
20
21 % water
22 rho_w = 0:1:2000; % kg m-3
23
24
25 % veeco
26 % l = 132e-6; % m
27 % b = 41.1e-6; % m
28 % h = 3.6e-6; % m
29 % Wn_meas = 338e3; % Hz
30
31 % smarttip
32 l = 216e-6;
33 b = 35e-6;
34 h = 2086e-9;
35 Wn_meas = 466.2e3;
36 w_p = 1.96*1e-6;
37
38 % hollow channel
39 l_c = 211e-6;
40 b_c = 28e-6;
41 h_c = 950e-9;
42
43 % compare paper AFM stiffness comparison
44 % l = 398e-6; % m
45 % b = 33e-6; % m
46 % h = 3.6e-6; % m
47 % Wn_meas = 19.93e3; % Hz
```

```

48
49 a1 = 1.875;      % ()
50 a2 = 4.694;      % ()
51
52 F = 1;          % N
53 %% constants calculated
54 I = (b*h^3)/12-((b_c*h_c^3)/12); % m4
55 A = b*h;        % m2
56
57 V_t = l*b*h;
58 V_l = l_c*b_c*h_c;
59
60 vol_pil = pi*(w_p/2)^2*h_c;
61
62 %% variables
63 % rho liquid
64 m = (0:0.1:10)*1e-12; % added mass nanogram
65 %% formulas solid
66 Wn_Rad = a1^2*sqrt(E*I/(rho*(V_t-V_l)*l^3));
67 Wn_Rad2 = a2^2*sqrt(E*I/(rho*(V_t-V_l)*l^3));
68
69 Wn_kHz = Wn_Rad/(2*pi)/1000;
70 Wn2_kHz = Wn_Rad2/(2*pi)/1000;
71
72 defl = F*l^3/(3*E*I)*1e6;
73
74 for i=1:length(rho_w)
75 %% formulas filled
76 Wn_Rad_f = a1^2*sqrt(E*I/((rho*(V_t-V_l)+rho_w(i)*V_l)*l^3));
77 Wn_Rad2_f = a2^2*sqrt(E*I/((rho*(V_t-V_l)+rho_w(i)*V_l)*l^3));
78
79 D_Wn_Rad_f = a1^2*sqrt(E*I/((rho*(V_t-V_l))*l^3))-a1^2*sqrt(E*I/((rho*(V_t-V_l)+rho_w(i)*V_l)*l^3));
80
81 Wn_kHz_f(i) = Wn_Rad_f/(2*pi)/1000;
82 Wn2_kHz_f(i) = Wn_Rad2_f/(2*pi)/1000;
83
84 D_Wn_kHz_f(i) = D_Wn_Rad_f/(2*pi)/1000;
85 end
86
87 for i=1:length(m)
88 D_Wn_Rad_f_mass = a1^2*sqrt(E*I/((rho*(V_t-V_l))*l^3))-a1^2*sqrt(E*I/((rho*(V_t-V_l)+m(i)*V_l)*l^3));
89 D_Wn_kHz_f_mass(i) = D_Wn_Rad_f_mass/(2*pi)/1000;
90 end
91 %% stiffness calculation from eigenfrequency
92
93 % k comsol = 47.429 N/m
94 % k Cleveland
95 k_cl = 2*b*(pi*l*Wn_meas)^3*sqrt(rho^3/E);
96
97 figure
98 subplot(1,3,1)
99 plot(rho_w,Wn_kHz_f, 'linewidth', 2)
100 grid on
101 hold on
102 plot([1000 1000],[74,Wn_kHz_f(1000)],'r','linewidth', 2)
103 plot([0 1000],[Wn_kHz_f(1000) Wn_kHz_f(1000)],'r','linewidth', 2)
104 xlabel('Density (kg/m^3)', 'fontweight', 'bold', 'fontsize', 12)
105 ylabel('Eigenfrequency (kHz)', 'fontweight', 'bold', 'fontsize', 12)
106 title('Frequency versus added density', 'fontweight', 'bold', 'fontsize', 12)
107 set(gca, 'fontweight', 'bold', 'fontsize', 12)

```

```

108
109 subplot(1,3,2)
110 plot(rho_w,D_Wn_kHz_f, 'linewidth', 2)
111 grid on
112 hold on
113 plot([1000 1000],[0,D_Wn_kHz_f(1000)],'r','linewidth', 2)
114 plot([0 1000],[D_Wn_kHz_f(1000) D_Wn_kHz_f(1000)],'r','linewidth', 2)
115 xlabel('Density (kg/m^3)', 'fontweight', 'bold','fontsize', 12)
116 ylabel('Eigenfrequency shift (\DeltakHz)', 'fontweight', 'bold','fontsize', 12)
117 title('Frequency shift versus added density','fontweight', 'bold','fontsize', 12)
118 set(gca, 'fontweight', 'bold', 'fontsize', 12)
119
120 %% find desired values
121 md=find(round(D_Wn_kHz_f_mass*10)==25);
122
123 subplot(1,3,3)
124 hold on
125 plot(D_Wn_kHz_f_mass,m*1e12, 'linewidth', 2)
126 plot([2.5 2.5],[0 m(md)*1e12], 'r', 'linewidth', 2)
127 plot([0 2.5],[m(md)*1e12 m(md)*1e12], 'r', 'linewidth', 2)
128 grid on
129 ylabel('Added mass (ng)', 'fontweight', 'bold','fontsize', 12)
130 xlabel('Eigenfrequency shift (\DeltakHz)', 'fontweight', 'bold','fontsize', 12)
131 title('Added mass versus frequency shift','fontweight', 'bold','fontsize', 12)
132 set(gca, 'fontweight', 'bold', 'fontsize', 12)

```

J.1 Frequency sweep

```

1 %% plot frequency vs amlitude
2 % frequency sweep veeco probe
3 % with to much functionallity
4 % Rick de Gruiter
5 % 19-3-15
6
7 %% initizialization
8 clear all
9 close all
10 clc
11
12 %% read data from excel
13
14 % load data from excel
15 b=questdlg('Load from Excel?');
16
17 if strcmp(b, 'Yes')==1
18 [fn, pn] = uigetfile('.xls', 'Select file to open', 'C:\Users\Rick\Dropbox\Dosing-AFM-FP\1
19
20 %%
21     if fn==0
22         error('Not enough input parameters')
23     else
24         filename = [pn fn];
25         freq = xlsread(filename, 'a2:a1000');
26         amp = xlsread(filename, 'b2:b1000');
27     end
28 %%
29

```

```

30 % load presaved data
31 elseif strcmp(b, 'No')==1
32     [fn, pn] = uigetfile;
33
34 %%
35     if fn==0
36         error('je moeder, klik hier dan niet op')
37     else
38         filename = [pn fn];
39         load(filename)
40     end
41 %%
42
43 else
44     error('Not enough input parameters')
45 end
46
47 %% find eigenfrequency
48 [max_amp, Wn_pos_meas] = max(amp);
49 Wn_meas = freq(Wn_pos_meas);
50
51 %% post process
52 figure
53 plot(freq, amp, 'linewidth', 2)
54 grid on
55 xlabel('Frequency kHz', 'fontweight', 'bold', 'fontsize', 10)
56 ylabel('Amplitude V', 'fontweight', 'bold', 'fontsize', 10)
57 title('Frequency sweep of the Veeco probe', 'fontweight', 'bold', 'fontsize', 10)
58 set(gca, 'fontweight', 'bold', 'fontsize', 10)
59
60 %% insert text box at eigenfrequency
61 annotation('textbox', [0.5, 0.5, 0.35, 0.1], ...
62           'String', ['Eigenfrequency ', num2str(Wn_meas), ' kHz']...
63           'FontSize', 10, 'fontweight', 'bold', 'linestyle', 'none');
64
65 if strcmp(b, 'Yes')==1
66     a=questdlg('Save Data?');
67     if strcmp(a, 'Yes')==1
68         savefile=inputdlg({'Save name'});
69         save(savefile{1,1}, 'freq', 'amp')
70     else
71         errordlg('Nou dan niet he')
72     end
73 end

```

J.2 Frequency shift

```

1 %% make figures for the frequency shift
2 % Rick de Gruiter
3 % 18-May-15
4 % Version 1.0
5 % Dosing AFM droplets
6
7 %% Initialization
8 clear all
9 close all
10 clc

```

```

11
12 a = 'Yes';
13 count = 0;
14
15 while strcmp(a, 'Yes') == 1
16 %% load data
17 if count == 0
18     [fn, pn] = uigetfile;
19 else
20     [fn, pn] = uigetfile(loadfile);
21 end
22 loadfile = [pn fn];
23
24 load(loadfile)
25
26 %% post process
27 if count ~= 2
28 figure(1)
29 hold on
30 r = plot(freq, amp);
31 set(r, 'color', [count, 0, 1-count], 'linewidth', 2)
32
33 a = questdlg('Open another file?');
34
35 count = count+1;
36
37 else
38 figure(1)
39 hold on
40 r = plot(freq, amp);
41 set(r, 'color', [2-count, count-1, 2-count], 'linewidth', 2)
42
43 a = questdlg('Open another file?');
44
45 count = count+1;
46 end
47
48 end
49
50 figure(1)
51 grid on
52 xlabel('Frequency (kHz)', 'fontsize', 12)
53 ylabel('Amplitude (V)', 'fontsize', 12)
54 title('Eigenfrequency of the Smarttip probe', 'fontweight', 'bold')
55 % legend('Empty', 'Filled')
56
57 % end of mfile

```

K — Relative humidity

```
1 %% based on time retrieve RH and breakup height
2 % read filenames
3 % relate based on time the relative humidity to the number of experiment
4 % a delay of 15 seconds is added
5 % make sure format of log file is corrrerc see Get.Rh file
6 % Rick de Gruiter
7 % dosing AFM
8 % MNE
9 % version 1.1
10 % added delay
11 % June 7 2015
12
13 clear all
14 close all
15 clc
16
17 % get log file
18 [fn, pn] = uigetfile('*.csv','select csv file');
19 loadfile = [pn, fn];
20 % loadfile = 'C:\Users\Rick\Dropbox\Dosing-AFM-FP\15-5-29 rh vs t\2015-05-29.csv';
21
22 [time_h, time_m, time_s, RH, temp] = Get_RH(loadfile); % read log file
23
24 tic
25 [fn, pn] = uigetfile('*.xls');
26 loadlocation = pn;
27
28 % loadlocation = 'C:\Users\Rick\Dropbox\Dosing-AFM-FP\15-6-3 rh vs bh\RH98 T23\Data arr
29
30 excel_names = dir(loadlocation);
31
32 %% reserve memory
33 time_e_h = zeros(length(excel_names)-3,1);
34 time_e_m = zeros(length(excel_names)-3,1);
35 time_e_s = zeros(length(excel_names)-3,1);
36 test_no = zeros(length(excel_names)-3,1);
37 result = zeros(length(excel_names)-3,3);
38
39 % read data
40 for i = 3:length(excel_names)
41     base = excel_names(i,1);
42
43     name = base.name;
44
45     % test numbr
46     test_no(i-2) = str2double(name(1:2));
47
```

```

48 % time experiment performed
49 time_e_h(i-2) = str2double(name(15:16));
50 time_e_m(i-2) = str2double(name(18:19));
51 time_e_s(i-2) = str2double(name(21:22));
52
53 % work around to get use single numbers
54 if isnan(test_no(i-2))
55     test_no(i-2) = str2double(name(1:1));
56
57     time_e_h(i-2) = str2double(name(14:15));
58     time_e_m(i-2) = str2double(name(17:18));
59     time_e_s(i-2) = str2double(name(20:21));
60 end
61
62 delay = 15;
63
64 time_e_s(i-2) = time_e_s(i-2)-delay;
65
66 if time_e_s(i-2)<0
67     time_e_s(i-2) = 60+time_e_s(i-2);
68     time_e_m(i-2) = time_e_m(i-2)-1;
69 end
70
71 if time_e_m(i-2)<0
72     time_e_m(i-2) = 60+time_e_m(i-2);
73     time_e_h(i-2) = time_e_h(i-2)-1;
74 end
75
76 % find coresponding data in log file
77 for j = 1:length(time_s)
78     if time_h(j) == time_e_h(i-2) && time_m(j) == time_e_m(i-2)...
79         && time_s(j) == time_e_s(i-2)
80         result(i-2,1) = test_no(i-2);
81         result(i-2,2) = RH(j);
82         result(i-2,3) = temp(j);
83     end
84 end
85
86 end
87
88
89
90
91 total=[test_no, time_e_h, time_e_m, time_e_s ];
92
93 % end of m file

```

```

1 function [time_h, time_m, time_s, RH, RH_set, temp, temp_set] = Get_RH(loadfile)
2 %UNTITLED4 Summary of this function goes here
3 % Detailed explanation goes here
4
5 %% read log data climate controller
6 % Relate climate to break up height
7 % time stamp of dispense data
8 % logged climate data
9 %
10 % Data is saved as text file
11 % Read titles in a map
12 %

```

```

13 % Rick de Gruiter
14 % Dosing AFM
15 % MNE
16 % version 1.0
17 % 4 -6-2015
18 %
19 % Select all in log paste in excel save as excel and as csv remove error
20 % message
21
22
23
24
25 %% Get text file
26
27
28 % loadfile = 'C:\Users\Rick\Dropbox\Dosing-AFM-FP\15-6-3 rh vs bh\2015-06-03.csv';
29
30 %% read text file
31 T1 = readtable(loadfile); % for time
32 [l_T1, w_T1] = size(T1);
33
34 temp_set = zeros(l_T1,1);
35 temp      = zeros(l_T1,1);
36 RH_set    = zeros(l_T1,1);
37 RH        = zeros(l_T1,1);
38 time_s    = zeros(l_T1,1);
39 time_m    = zeros(l_T1,1);
40 time_h    = zeros(l_T1,1);
41
42 for i=1:l_T1
43 a = T1{i,1};
44 b = a{1,1};
45
46 time_h(i) = str2double(b(1:2));
47 time_m(i) = str2double(b(4:5));
48 time_s(i) = str2double(b(7:8));
49
50 temp_set(i) = str2double(b(95:99));
51 temp(i)     = str2double(b(55:59));
52 RH_set(i)   = str2double(b(105:109));
53 RH(i)       = str2double(b(65:69));
54 end
55
56 %% read the excel names
57
58 end

```

Bibliography

- [1] Gilson, “Gilson solution at work for you,” 2013.
- [2] D. B. Wallace, W. R. Cox, D. J. Hayes, A. Pique, and D. Chrisey, “Direct write using inkjet techniques,” *Direct-Write technologies for rapid prototyping applications-sensors, electronics, and integrated power sources*, pp. 177–227, 2002.
- [3] A. J. Sloane, J. L. Duff, N. L. Wilson, P. S. Gandhi, C. J. Hill, F. G. Hopwood, P. E. Smith, M. L. Thomas, R. A. Cole, N. H. Packer, *et al.*, “High throughput peptide mass fingerprinting and protein macroarray analysis using chemical printing strategies,” *Molecular & Cellular Proteomics*, vol. 1, no. 7, pp. 490–499, 2002.
- [4] M. E. Kuil, J. P. Abrahams, and J. Marijnissen, “Nano-dispensing by electrospray for biotechnology,” *Biotechnology journal*, vol. 1, no. 9, pp. 969–975, 2006.
- [5] G. K. Binnig, “Atomic force microscope and method for imaging surfaces with atomic resolution,” Feb. 9 1988. US Patent 4,724,318.
- [6] G. Binnig, C. F. Quate, and C. Gerber, “Atomic force microscope,” *Physical review letters*, vol. 56, no. 9, p. 930, 1986.
- [7] Veeco, “Multimode SPM Instruction Manual,” 2004.
- [8] Q. Zhong, D. Inniss, K. Kjoller, and V. Elings, “Fractured polymer/silica fiber surface studied by tapping mode atomic force microscopy,” *Surface Science Letters*, vol. 290, no. 1, pp. L688–L692, 1993.
- [9] C. Prater, P. Maivald, K. Kjoller, and M. Heaton, “Tappingmode imaging applications and technology,” *Digital Instruments Nanonotes, Santa Barbara, California, USA*, 1995.
- [10] B. Cappella and G. Dietler, “Force-distance curves by atomic force microscopy,” *Surface science reports*, vol. 34, no. 1, pp. 1–104, 1999.
- [11] M. K. Ghatkesar, H. H. P. Garza, F. Heuck, and U. Staufer, “Scanning probe microscope-based fluid dispensing,” *Micromachines*, vol. 5, no. 4, pp. 954–1001, 2014.
- [12] A. Fang, E. Dujardin, and T. Ondarçuhu, “Control of droplet size in liquid nanodispensing,” *Nano letters*, vol. 6, no. 10, pp. 2368–2374, 2006.
- [13] R. D. Piner, J. Zhu, F. Xu, S. Hong, and C. A. Mirkin, ““ dip-pen” nanolithography,” *science*, vol. 283, no. 5402, pp. 661–663, 1999.
- [14] T. Leichle, M. Lishchynska, F. Mathieu, J.-B. Pourciel, D. Saya, and L. Nicu, “A microcantilever-based picoliter droplet dispenser with integrated force sensors and electroassisted deposition means,” *Microelectromechanical Systems, Journal of*, vol. 17, no. 5, pp. 1239–1253, 2008.

- [15] D. S. Ginger, H. Zhang, and C. A. Mirkin, “The evolution of dip-pen nanolithography,” *Angewandte Chemie International Edition*, vol. 43, no. 1, pp. 30–45, 2004.
- [16] K. Salaita, Y. Wang, and C. A. Mirkin, “Applications of dip-pen nanolithography,” *Nature Nanotechnology*, vol. 2, no. 3, pp. 145–155, 2007.
- [17] T. V. Tsulaia, N. L. Prokopishyn, A. Yao, N. V. Carsrud, M. C. Carou, D. B. Brown, B. R. Davis, and J. Yannariello-Brown, “Glass needle-mediated microinjection of macromolecules and transgenes into primary human mesenchymal stem cells,” *Journal of biomedical science*, vol. 10, no. 3, pp. 328–336, 2003.
- [18] B. R. Davis, J. Yannariello-Brown, N. L. Prokopishyn, Z. Luo, M. R. Smith, J. Wang, N. V. Carsrud, and D. B. Brown, “Glass needle-mediated microinjection of macromolecules and transgenes into primary human blood stem/progenitor cells,” *Blood*, vol. 95, no. 2, pp. 437–444, 2000.
- [19] I. Obataya, C. Nakamura, S. Han, N. Nakamura, and J. Miyake, “Nanoscale operation of a living cell using an atomic force microscope with a nanoneedle,” *Nano letters*, vol. 5, no. 1, pp. 27–30, 2005.
- [20] A. Meister, M. Gabi, P. Behr, P. Studer, J. Voros, P. Niedermann, J. Bitterli, J. Polesel-Maris, M. Liley, H. Heinzelmann, *et al.*, “Fluidfm: combining atomic force microscopy and nanofluidics in a universal liquid delivery system for single cell applications and beyond,” *Nano letters*, vol. 9, no. 6, pp. 2501–2507, 2009.
- [21] J. P. Giraldo-Vela, W. Kang, R. L. McNaughton, X. Zhang, B. M. Wile, A. Tsourkas, G. Bao, and H. D. Espinosa, “Single-cell detection of mrna expression using nanofountain-probe electroporated molecular beacons,” *Small*, vol. 11, no. 20, pp. 2386–2391, 2015.
- [22] O. Guillaume-Gentil, E. Potthoff, D. Ossola, C. M. Franz, T. Zambelli, and J. A. Vorholt, “Force-controlled manipulation of single cells: from afm to fluidfm,” *Trends in biotechnology*, vol. 32, no. 7, pp. 381–388, 2014.
- [23] H. Uehara, T. Osada, and A. Ikai, “Quantitative measurement of mrna at different loci within an individual living cell,” *Ultramicroscopy*, vol. 100, no. 3, pp. 197–201, 2004.
- [24] M. Schena, D. Shalon, R. Heller, A. Chai, P. O. Brown, and R. W. Davis, “Parallel human genome analysis: microarray-based expression monitoring of 1000 genes,” *Proceedings of the National Academy of Sciences*, vol. 93, no. 20, pp. 10614–10619, 1996.
- [25] H. P. Rang, *Drug discovery and development*. Churchill Livingstone Elsevier, 2006.
- [26] H. H. Perez Garza, E. W. Kievit, G. F. Schneider, and U. Staufer, “Controlled, reversible, and nondestructive generation of uniaxial extreme strains (ϵ 10%) in graphene,” *Nano letters*, vol. 14, no. 7, pp. 4107–4113, 2014.
- [27] E. Pérez, E. Schäffer, and U. Steiner, “Spreading dynamics of polydimethylsiloxane drops: Crossover from laplace to van der waals spreading,” *Journal of colloid and interface science*, vol. 234, no. 1, pp. 178–193, 2001.
- [28] S. Sugiura, K. Hattori, and T. Kanamori, “Microfluidic serial dilution cell-based assay for analyzing drug dose response over a wide concentration range,” *Analytical chemistry*, vol. 82, no. 19, pp. 8278–8282, 2010.

- [29] D. Mark, P. Weber, S. Lutz, M. Focke, R. Zengerle, and F. von Stetten, "Aliquoting on the centrifugal microfluidic platform based on centrifugo-pneumatic valves," *Microfluidics and Nanofluidics*, vol. 10, no. 6, pp. 1279–1288, 2011.
- [30] C. L. Hansen, *Microfluidic technologies for structural biology*. PhD thesis, California Institute of Technology, 2004.
- [31] T. V. Murthy, D. Kroncke, and P. D. Bonin, "Adding precise nanoliter volume capabilities to liquid-handling automation for compound screening experimentation," *Journal of the Association for Laboratory Automation*, vol. 16, no. 3, pp. 221–228, 2011.
- [32] C. Haber, M. Boillat, and B. v. d. Schoot, "Precise nanoliter fluid handling system with integrated high-speed flow sensor," *Assay and drug development technologies*, vol. 3, no. 2, pp. 203–212, 2005.
- [33] M. Yamada and M. Seki, "Nanoliter-sized liquid dispenser array for multiple biochemical analysis in microfluidic devices," *Analytical chemistry*, vol. 76, no. 4, pp. 895–899, 2004.
- [34] K. Kaisei, N. Satoh, K. Kobayashi, K. Matsushige, and H. Yamada, "Nanoscale liquid droplet deposition using the ultrasmall aperture on a dynamic mode afm tip," *Nanotechnology*, vol. 22, no. 17, p. 175301, 2011.
- [35] M. Härth and D. W. Schubert, "Simple approach for spreading dynamics of polymeric fluids," *Macromolecular Chemistry and Physics*, vol. 213, no. 6, pp. 654–665, 2012.
- [36] P. Krishnakumar, "Wetting and spreading phenomena," 2010.
- [37] Elveflow, "Syringe pumps and microfluidics," 2015.
- [38] Elveflow, "Microfluidic flow control systems: Pressure controllers with a flow meter," 2015.
- [39] J. Kirby, Brian, *Micro and Nanoscale Fluid Mechanics*. New York: Cambridge, 2010.
- [40] Elveflow, "Compliance of a microfluidic tubing," 2015.
- [41] Wikibooks, "Microfluidics/hydraulic resistance and capacity," 2015.
- [42] J. Lee, W. Shen, K. Payer, T. P. Burg, and S. R. Manalis, "Toward attogram mass measurements in solution with suspended nanochannel resonators," *Nano letters*, vol. 10, no. 7, pp. 2537–2542, 2010.
- [43] T. P. Burg, M. Godin, S. M. Knudsen, W. Shen, G. Carlson, J. S. Foster, K. Babcock, and S. R. Manalis, "Weighing of biomolecules, single cells and single nanoparticles in fluid," *Nature*, vol. 446, no. 7139, pp. 1066–1069, 2007.
- [44] M. K. Ghatkesar, H. H. P. Garza, and U. Staufer, "Hollow afm cantilever pipette," *Micro-electronic Engineering*, vol. 124, pp. 22–25, 2014.
- [45] Y. Yuan and T. R. Lee, "Contact angle and wetting properties," in *Surface science techniques*, pp. 3–34, Springer, 2013.
- [46] D. Kwok and A. Neumann, "Contact angle measurement and contact angle interpretation," *Advances in colloid and interface science*, vol. 81, no. 3, pp. 167–249, 1999.
- [47] J. T. Korhonen, T. Huhtamaki, O. Ikkala, and R. H. Ras, "Reliable measurement of the receding contact angle," *Langmuir*, vol. 29, no. 12, pp. 3858–3863, 2013.

- [48] J. Stewart, *Calculus: early transcendentals*. Cengage Learning, 2015.
- [49] M. K. Chaudhury and G. M. Whitesides, “How to make water run uphill,” *Science*, vol. 256, no. 5063, pp. 1539–1541, 1992.
- [50] K. Osborne, *Determining the Contact Angle of a Droplet on a Substrate*. PhD thesis, Worcester Polytechnic Institute, 2008.
- [51] M. Nosonovsky and B. Bhushan, “Capillary adhesion and nanoscale properties of water,” in *Scanning Probe Microscopy in Nanoscience and Nanotechnology 2*, pp. 551–571, Springer, 2011.
- [52] R. Jones, H. M. Pollock, J. A. Cleaver, and C. S. Hodges, “Adhesion forces between glass and silicon surfaces in air studied by afm: Effects of relative humidity, particle size, roughness, and surface treatment,” *Langmuir*, vol. 18, no. 21, pp. 8045–8055, 2002.
- [53] H.-J. Butt and M. Kappl, “Normal capillary forces,” *Advances in colloid and interface science*, vol. 146, no. 1, pp. 48–60, 2009.
- [54] A. J. Harrison, D. S. Corti, and S. P. Beaudoin, “Capillary forces in nanoparticle adhesion: A review of afm methods,” *Particulate Science and Technology*, no. just-accepted, 2015.
- [55] S. H. Yang, M. Nosonovsky, H. Zhang, and K.-H. Chung, “Nanoscale water capillary bridges under deeply negative pressure,” *Chemical Physics Letters*, vol. 451, no. 1, pp. 88–92, 2008.
- [56] E. Herbert and F. Caupin, “The limit of metastability of water under tension: theories and experiments,” *Journal of Physics: Condensed Matter*, vol. 17, no. 45, p. S3597, 2005.
- [57] X. Xiao and L. Qian, “Investigation of humidity-dependent capillary force,” *Langmuir*, vol. 16, no. 21, pp. 8153–8158, 2000.
- [58] M. Farshchi-Tabrizi, M. Kappl, Y. Cheng, J. Gutmann, and H.-J. Butt, “On the adhesion between fine particles and nanocontacts: an atomic force microscope study,” *Langmuir*, vol. 22, no. 5, pp. 2171–2184, 2006.
- [59] B. L. Weeks, M. W. Vaughn, and J. J. DeYoreo, “Direct imaging of meniscus formation in atomic force microscopy using environmental scanning electron microscopy,” *Langmuir*, vol. 21, no. 18, pp. 8096–8098, 2005.
- [60] J. W. van Honschoten, N. Brunets, and N. R. Tas, “Capillarity at the nanoscale,” *Chemical Society Reviews*, vol. 39, no. 3, pp. 1096–1114, 2010.
- [61] B. L. Weeks and J. J. DeYoreo, “Dynamic meniscus growth at a scanning probe tip in contact with a gold substrate,” *The Journal of Physical Chemistry B*, vol. 110, no. 21, pp. 10231–10233, 2006.
- [62] E. Bonaccorso, D. S. Golovko, P. Bonanno, R. Raiteri, T. Haschke, W. Wiechert, and H.-J. Butt, “Atomic force microscope cantilevers used as sensors for monitoring microdrop evaporation,” in *Applied Scanning Probe Methods XI*, pp. 17–38, Springer, 2009.
- [63] S. S. Rao and F. F. Yap, *Mechanical vibrations*, vol. 4. Addison-Wesley Reading, 1995.
- [64] N. Burnham, X. Chen, C. Hodges, G. Matei, E. Thoreson, C. Roberts, M. Davies, and S. Tendler, “Comparison of calibration methods for atomic-force microscopy cantilevers,” *Nanotechnology*, vol. 14, no. 1, p. 1, 2003.

- [65] J. Cleveland, S. Manne, D. Bocek, and P. Hansma, “A nondestructive method for determining the spring constant of cantilevers for scanning force microscopy,” *Review of Scientific Instruments*, vol. 64, no. 2, pp. 403–405, 1993.
- [66] C. Ru, L. Chen, B. Shao, W. Rong, and L. Sun, “A hysteresis compensation method of piezoelectric actuator: Model, identification and control,” *Control Engineering Practice*, vol. 17, no. 9, pp. 1107–1114, 2009.
- [67] R. van Oorschot, H. H. P. Garza, R. J. Derks, U. Staufer, and M. K. Ghatkesar, “A microfluidic afm cantilever based dispensing and aspiration platform,” *EPJ Techniques and Instrumentation*, vol. 2, no. 1, pp. 1–11, 2015.
- [68] Mareco, “Mareco prototyping materials,” 2012.
- [69] A. Workshop, “Afm workshop,” 2012.
- [70] S. Aldrich, “Sigma aldrich,” 2015.
- [71] L. Fabié and T. Ondarçuhu, “Writing with liquid using a nanodispenser: spreading dynamics at the sub-micron scale,” *Soft Matter*, vol. 8, no. 18, pp. 4995–5001, 2012.
- [72] C. Wohlfarth, “Viscosity of diethyl carbonate,” in *Supplement to IV/18*, pp. 151–153, Springer, 2009.